Basal Constriction:
Shaping the Vertebrate Brain

by

Ellie Graham Graeden

B.S. Microbiology
Oregon State University, 2002

SUBMITTED TO THE DEPARTMENT OF BIOLOGY
IN PARTIAL FULFILLMENT OF THE REQUIREMENTS FOR THE DEGREE OF

DOCTOR OF PHILOSOPHY IN BIOLOGY
AT THE
MASSACHUSETTS INSTITUTE OF TECHNOLOGY

SEPTEMBER 2010
[February 2011]

Signature of Author: _____

Department of Biology, MIT
September 2010

Certified by: _____

Hazel L. Sive
Member, Whitehead Institute for Biomedical Research
Professor of Biology, MIT
Associate Dean, School of Science
Thesis Supervisor

Accepted by: _____

Tania A. Baker
E. C. Whitehead Professor of Biology, MIT
Investigator, Howard Hughes Medical Institute
Co-chairperson, Graduate Committee

Basal Constriction:
Shaping the Vertebrate Brain

by

Ellie Graham Graeden

Submitted to the Department of Biology
on 10 September 2010 in Partial Fulfillment of the Requirements
for the Degree of Doctor of Philosophy in Biology

ABSTRACT

Organs are primarily formed from epithelia, polarized sheets of cells with an apical surface facing a lumen and basal surface resting on the underlying extracellular matrix. Cells within a sheet are joined by junctions, and changes in cell shape and size drive epithelial bending and folding during morphogenesis. These shape changes include constriction and expansion of the cell surfaces, elongation or shortening of the apical-basal length, or cell spreading. In this thesis, I present the first description of basal constriction, a process by which cells narrow on their basal surfaces to bend the neuroepithelium. Specifically, I describe morphogenesis of a major conserved bend in the vertebrate neural tube, the midbrain-hindbrain boundary constriction (MHBC). The MHBC forms between 17 and 24 hours post fertilization in zebrafish, concomitant with, but independent of ventricle inflation. Cells shorten to 75% the length of the surrounding cells prior to basal constriction, during which a band of 3-4 cells becomes wedge-shaped. Subsequently, these cells apically expand by twice the width of the surrounding cells. Basal constriction is laminin-dependent, with actin enriched at the basolateral surface of the constricted cells. Wnt5 is highly expressed specifically at the MHBC prior to and during basal constriction and is required for this process. Focal adhesion kinase (FAK) is activated by phosphorylation at the MHBC and is required for basal constriction. FAK activation at the MHBC is dependent upon Wnt5 function. Loss of basal constriction in Wnt5 and FAK loss-of-function embryos can be rescued by inhibiting Gsk3β. These data suggest a novel pathway in which Wnt5 activates FAK in conjunction with the inhibition of Gsk3β to drive basal constriction at the MHBC. This study is the first to describe basal constriction during epithelial morphogenesis and provides mechanistic insights into a newly described cell shape change required for normal brain development.

Thesis Supervisor: Hazel L. Sive
Title: Member, Whitehead Institute for Biomedical Research
Professor of Biology, MIT
Associate Dean, School of Science

BIOGRAPHICAL NOTE

Ellie Graeden was introduced to research in the laboratory of Dr. Phil Youderian at the University of Idaho, studying antibiotic resistance in *Myxoccocus xanthus* and *Salmonella typhimurium*. She earned her B.S. in microbiology at Oregon State University where she worked with Dr. Stephen Giovannoni analyzing the phylogeny of novel marine communities. After teaching at a Swiss boarding school, she returned to research in the laboratory of Dr. George Sprague at the University of Oregon where she characterized protein-protein interactions in the filamentous growth pathway of *Saccharomyces cerevisiea*. Her doctoral work in the Sive laboratory at MIT was supported by an NSF Pre-doctoral Fellowship.

ACKNOWLEDGMENTS

I offer many thanks to my advisor, Hazel Sive, for her support not only of my research, but of my intellectual development; to members of the Sive lab, particularly Jen Gutzman and Amanda Dickinson, for their help, support, and mentorship, and to Olivier Paugois for taking such good care of my fish; to Frank Solomon for his kind support of me, my research, and of the BioREFS program; to the members of the BioREFS, particularly Lourdes Aleman for helping me get it going and Calvin Jan and Shankar Sundar for keeping me going; to Brute Squad – 100% BS; to Kurt Weiss for reminding me that sometimes it is more important to go play in the sun; to Sarah Bagby for her unfailing and dear friendship; to Bec Gianotti and Gin Rich for laughter and perspective; to Julie Mumford who is both friend and family; to my grandparents, parents and brother, who are both family and friends; to my son, Finn, who I am just getting to know; and, finally, to my husband, Ryan, who makes anything possible.

TABLE OF CONTENTS

1. Introduction: Cellular Mechanisms of Epithelial Morphogenesis 7

2. Formation of the zebrafish midbrain-hindbrain boundary constriction requires laminin-dependent basal constriction 43

3. Basal constriction at the midbrain-hindbrain boundary constriction is regulated by Wnt5, FAK and Gsk3β 83

4. Future Directions 149

5. Appendix 1: The role of microtubules in basal constriction 161

1

Introduction:

Cellular mechanisms of epithelial morphogenesis

CONTRIBUTIONS

This chapter and its figures were drafted solely by me.

ABSTRACT

Epithelial morphogenesis is a pivotal process by which the developing embryonic body plan and forming organs are shaped. Changes in cell shape and length that bend epithelia include cell shortening, elongation, and cell spreading or flattening. In addition, cells can undergo apical and basal constriction, which bend a cell sheet in opposite directions. I describe the epithelial organization upon which these cell shape and length changes depend and discuss the mechanisms driving these changes. I then discuss possible mechanisms by which epithelial cell shortening and elongation could be regulated, in the context of cuboidal or columnar epithelia and during cell spreading. Apical constriction is well-established, and I review the current state of the field. Basal constriction is little-studied, but my analysis of embryos suggests that this is a widespread mechanism of cell sheet bending. Identification of basal constriction and mechanisms underlying this process form the basis of this thesis.

INTRODUCTION

During animal development, epithelial tissue is shaped by bending, folding, elongation and growth to form the organs that compose the embryo. An epithelium is defined as a tissue composed of linked cells of three basic types: squamous, cuboidal, or columnar. The basic structure and development of the epithelium are highly conserved across species and tissues. Cells within epithelia can change shape to become apically or basally constricted, which bends the cell sheet. Here, I address the cell shape and length changes that drive epithelial morphogenesis during development with particular emphasis on gastrulation (formation of the germ layers in the embryo) and organogenesis.

Organization of epithelia

The hallmark of an epithelium is its apical and basal polarity (Bryant and Mostov, 2008). The apical surface faces the outside of the embryo or the lumen of an organ, as in the lung, stomach, and brain. The basal surface is bound to an underlying stabilizing substrate, the extracellular matrix, which connects the epithelia to other tissues (Schock and Perrimon, 2002). The cell membrane composing the apical and basal domains of each cell differ in function, types of proteins localized or bound to them, and in lipid composition (Schuck and Simons, 2004; van Meer and Simons, 1988). The lateral domains of neighboring cells are joined via junctions, highly regulated protein complexes that link the cells within the epithelia through the interaction of membrane-bound proteins at the cell surface (Schock and Perrimon, 2002). Each type of lateral junction has distinct functions. Apico-lateral junctions include tight junctions, adherens junctions, and gap junctions (Giepmans and van Ijzendoorn, 2009). Adherens junctions link the actin and microtubule cytoskeletons of neighboring cells and function as a membrane barrier, separating the apical and basal membrane domains by preventing

movement of membrane-bound proteins between the domains (Perez-Moreno et al., 2003). Tight and gap junctions serve opposite purposes, respectively preventing and allowing diffusion of molecules between cells (Giepmans and van Ijzendoorn, 2009). Tight junctions are additionally responsible for preventing movement of domain-specific lipids between apical and basolateral domains (van Meer and Simons, 1988). In the basolateral membrane, desmosomes connect neighboring cells through binding with intermediate filaments (Giepmans and van Ijzendoorn, 2009). At the basal cell surface, integral membrane proteins, often within focal adhesions, bind the membrane to the underlying extracellular matrix, a complex network of proteoglycans necessary for structural integrity and signaling (Hynes, 2009; Parsons, 2003) (Fig. 1).

Cell shape changes within epithelia

Cells within epithelia are constrained by their neighbors. This allows local changes in shape of even a few cells to drive the formation of bends and folds in regions of the tissue as a whole (Pilot and Lecuit, 2005). Changes in cell shape may be in width at either or both poles or in length. In a cuboidal or columnar epithelium, constriction of cell width at one pole will form either a conical or wedge-shaped cell. If the force of the constriction is circumferential, then the cell forms a cone, like the tip of a pencil (Fig. 2A to B). This often occurs in conjunction with cell elongation (Lee and Harland, 2007; Sawyer et al., 2010) (Fig. 2A to D to B). If the force of the constriction is lateral instead of circumferential, the cell will form a wedge with flat sides that meet at an edge like a piece of pie (Fig. 2A to C). This has been shown to occur in conjunction with cell shortening (Gutzman et al., 2008) (Fig. 2A to E to C). Changes in cell length, sometimes referred to as cell height, describe an elongation or shortening of the distance between the apical and basal cell surfaces (Fristrom, 1988) (Fig. 2A to D, A to E). Cell elongation can also describe lateral cell extension, in which both the apical and basal surfaces

simultaneously expand, as occurs during flattening or spreading (Solnica-Krezel, 2006) (Fig. 2A to F)

Conventionally, it is assumed that there is minimal change in cell volume with changes of cell shape or length. This was analyzed explicitly in the fiber cells of the adult vertebrate lens where it was determined that cell length increased significantly more than the cell volume (15-fold versus 4-fold) (Bassnett, 2005). Where it has been analyzed during development, this has been corroborated. For example, during transition from cuboidal to columnar epithelia, there was no observed change in cell volume in the developing wing imaginal disc in *Drosophila* (Widmann and Dahmann, 2009). Therefore, the discussion here will focus on mechanisms of cell shape and length changes independent of cell volume.

Together, these cell shape changes drive the epithelial morphogenesis required for organogenesis and shaping the body plan in developing embryos.

CELL LENGTH CHANGE

Cell elongation and cell shortening are often coupled with apical and basal constrictions during morphogenesis of cuboidal or columnar epithelia, but are also required for cell spreading during embryonic epiboly, or the extension of the enveloping layer over the yolk during gastrulation early in development (Lee et al., 2007; Pilot and Lecuit, 2005; Solnica-Krezel, 2006). Apical constriction is most often paired with cell elongation, whereas cell shortening has been associated with basal constriction. For example, cells nearly double in length concomitant with apical constriction during neural tube closure in *Xenopus* (Lee et al., 2007). Cell elongation paired with apical constriction has also been described in bottle cells during *Xenopus* gastrulation (Lee and Harland, 2007) and wing imaginal disc development in *Drosophila* (Schlichting and Dahmann, 2008; Widmann and Dahmann, 2009). Both cell elongation and shortening are

necessary for cell intercalation and deep cell rearrangements in *Xenopus* gastrulation (Keller, 1980), and cell elongation drives sheet spreading during both *Drosophila* dorsal closure and zebrafish epiboly (Koppen et al., 2006).

Cell length changes have long been associated with microtubules, and this appears to be tightly related to their organization in these cells (Burnside, 1971; Byers and Porter, 1964; Chisholm and Hardin, 2005; Karfunkel, 1972; Piatigorsky et al., 1973; Solnica-Krezel, 2005). In mesenchymal cells, polarized microtubules are organized in radial arrays, anchored by their minus-ends at the centrosome or microtubule organizing center (MTOC) near the nucleus with their plus-ends extending to the cell cortex (Bartolini and Gundersen, 2006). In epithelial cells, microtubules become organized in non-centrosomal arrays with their minus ends anchored at the apical surface and their plus-ends anchored at the basal cell surface (Bellett et al., 2009; Reilein and Nelson, 2005; Reilein et al., 2005). Microtubules are nucleated from their minus-ends and grow from their plus-ends; microtubule shrinking is termed catastrophe and occurs from the plus-end at random (Wade, 2009). As epithelial cells become polarized, the plus-ends are captured by dynein and stabilized by Eb1 and APC at the cell cortex to form both non-centrosomal microtubule networks at the cortex as well as parallel apical-basal arrays running the length of the cell (Bartolini and Gundersen, 2006; Bellett et al., 2009; Byers and Porter, 1964; Lee and Harland, 2007; Reilein and Nelson, 2005; Shaw et al., 2007; Wen et al., 2004). Dynein and kinesin are force-generating microtubule-associated motors (Hirokawa et al., 2009; Kardon and Vale, 2009). In the case of cell elongation in the lens of the sunfish, sliding of parallel microtubule arrays mediated by dynein results in rapid cell elongation (Dearry and Burnside, 1986; Troutt and Burnside, 1988). Kinesin has been shown to mediate microtubule sliding with enough force to deform membranes (Jolly et al., 2010). Together, these data suggest a possible model of cell length change in which apico-basally oriented microtubules are captured and

stabilized at the cell cortex by plus-end-binding proteins. Once captured, the apical and basal cell surfaces are either pushed away or pulled toward each other by the force generated by dynein- or kinesin-mediated sliding. Alternatively, or in conjunction with this process, the cortical network could function to reshape the membrane and remodel the junctions to accommodate the change in cell length (Bellett et al., 2009).

The actomyosin cytoskeleton is also required for cell length changes. Cell flattening or spreading drives large-scale epithelial sheet migrations such as during zebrafish epiboly and *Drosophila* dorsal closure (Koppen et al., 2006; Pope and Harris, 2008). Both of these processes require accumulation of actin and non-muscle myosin at the leading edge of the advancing sheet to drive elongation of cells necessary to extend the sheet (Koppen et al., 2006; Pope and Harris, 2008; Solnica-Krezel, 2005). In the case of amnioserosa, one set of cells remodeled during *Drosophila* dorsal closure, columnar epithelial cells flatten to form a squamous epithelium. This process requires microtubule rotation driven by the actin cytoskeleton as myosin helps remodel the cell-cell junctions (Pope and Harris, 2008). Similarly, *C. elegans* epidermal elongation along the anterior-posterior axis requires Rho-mediated actomyosin contraction (Chisholm and Hardin, 2005). Rho signaling upstream of the myosin regulatory light chain is also required for cell flattening in *Drosophila* wing disc epithelia (Widmann and Dahmann, 2009).

Cell intercalation is the process by which cells in apposing sheets extend membrane protrusions between cells in the other sheet. Cell elongation and movement into the sheet forms a new, longer epithelium (Pilot and Lecuit, 2005). This process is termed convergent extension (Keller, 2002). Myosin regulation of the actin cytoskeleton appears to be a conserved driver of this process as it is required for both vertebrate and *Drosophila* gastrulation as well as neurulation and neural tube elongation (Nikolaidou and Barrett, 2004; Rolo et al., 2009).

Signaling in cell length change

The upstream regulation of cell length change varies significantly between developmental systems. Hedgehog (Hh) and Decapentaplegic (Dpp) drive cell shortening in both the wing and eye imaginal discs in *Drosophila* (Schlichting and Dahmann, 2008). This signaling was shown to be upstream of myosin during ingression in the eye imaginal disc (Escudero et al., 2007). In *Xenopus*, the transcription factor, Pitx1, regulates Shroom3 in the developing gut (Chung et al., 2010). Shroom3, in turn, is required for cell elongation during neural tube closure (Lee et al., 2007). Shroom3 expression during mouse lens placode invagination is dependent on Pax6, a known downstream component of Wnt signaling (Kim et al., 2001; Osumi et al., 1997; Plageman et al., 2010). This suggests a pathway in which early, localized expression of Pitx1 regulates Wnt-dependent Shroom3 to drive cell shortening. The planar cell polarity branch of Wnt signaling regulates convergent extension in *Xenopus*, zebrafish, mice, *Drosophila*, and ascidians, to name a few (Qian et al., 2007; Torban et al., 2004). Given the link between cell length and shape changes, it is also possible that the signaling pathways known to regulate cell shape change may be required to regulate the concomitant cell length changes.

APICAL CONSTRICTION

Apical constriction, the constriction of the apical surface of an epithelial cell, bends the epithelium toward an apical lumen or drives invagination, in-pocketing, of the tissue. Apical constriction was described as early as in 1902, and it has been studied extensively since (Sawyer et al., 2010). It is required for a wide range of developmental processes. Gastrulation requires apical constriction to invaginate the tissue. Apical constriction has been studied during this process in many organisms including sea urchins, *Drosophila*, *Caenorhabditis elegans* (*C. elegans*), and *Xenopus*. Apical

constriction is also required to close an opening in the epithelium such as during dorsal closure in *Drosophila* or wound healing in *Xenopus*. During organogenesis, apical constriction has been studied during neural tube closure and gut formation in *Xenopus* and hingepoint formation in chick, among others (Chung et al., 2010; Lee and Harland, 2007; Sawyer et al., 2010). While there are distinctions between the mechanisms that drive apical constriction in each context, there is significant conservation.

Mechanisms of apical constriction

The process of apical constriction requires contraction of the actomyosin cytoskeleton at the apical cell surface. Actin within epithelia is localized both to a circumferential band linking the apically-localized adherens junctions of neighboring cells, and to a cortical meshwork of highly branched F-actin. Immediately prior to apical constriction, actin is enriched at the apical surface (Anstrom, 1992). This is concomitant with apical recruitment of non-muscle myosin II (hereafter, myosin), a motor protein required for actin contraction (Pilot and Lecuit, 2005). In most cases, once actin and myosin are recruited apically, Rho (a small GTPase) triggers contraction (Sawyer et al., 2010).

For many years, the mechanism of contraction during apical constriction has been described by the purse-string model. The apical actin band links adherens junctions in neighboring cells and transmits tension between them. In this model, myosin contracts the actin bands, driving apical constriction in a group of cells within the tissue (Baker and Schroeder, 1967; Burnside, 1971; Hildebrand, 2005; Karfunkel, 1972). However, recent studies suggest that this may not be the most likely mechanism. During wounding in *Xenopus*, actin is apically enriched in the cells surrounding the wound. If intercellular tension were responsible for pulling the tissue together around the wound, breaking the actin cable would be expected to result in recoil. Davidson et al. tested this

hypothesis and found no evidence of recoil (Davidson et al., 2002). The purse-string model would also suggest that a square wound would become rounded at the corners as healing progressed and the cells were pulled together. Instead, the authors found that the square shape was retained, and a triangle-shaped wound healed first into at Y-shape before closing. The authors conclude that actin-mediated tension between the cells is insufficient to drive migration during wound healing; such a mechanism may also be insufficient to drive apical constriction in a group of epithelial cells during development.

Martin et al. recently suggested an alternative model of apical constriction (Martin et al., 2009). During gastrulation in *Drosophila*, cells at the midline apically constrict to form an invagination at the ventral furrow. Analysis of time lapse imaging during the invagination showed a series of pulsed contractions each of which pulled the membranes closer to constrict the apical surface. Remarkably, the points of myosin responsible for these contractions co-localized not with the adherens junctions, but with the cortical actin between the junctions. Cortical actin, unlike the apical band of actin linking the adherens junctions, is composed almost entirely of highly branched actin (Weed and Parsons, 2001). Arp2/3 is an actin-related protein that functions to both nucleate and facilitate branching of actin at the cell cortex (Mullins et al., 1998). In *C. elegans* gastrulation, Arp2/3 is required for apical constriction of the two endodermal cells that initiate internalization (Roh-Johnson and Goldstein, 2009). These data suggest a model in which cortical actin, rather than the apical band of actin at adherens junctions, may be specifically required for apical constriction.

While the role and regulation of actin in apical constriction has been well parsed, microtubules have also been identified as necessary in some contexts. Formation of bottle cells by apical constriction during *Xenopus* gastrulation requires intact microtubules (Lee and Harland, 2007). Apical localization of γ-tubulin and stabilization of microtubules is required for apical constriction during *Xenopus* neural tube closure

(Lee et al., 2007; Suzuki et al.). Microtubules could either be required for trafficking of components necessary for the apical constriction or could be dynamically involved in the constriction itself. However, in both of these cases, apical constriction occurs subsequent to cell elongation. Microtubules may instead be required for the change in cell length and not the apical constriction itself, as discussed in the section on cell length change.

Basal expansion

Apical constriction is often accompanied by basal expansion, though this latter process has not been studied independently. *Xenopus* bottle cells are defined as having "dramatically constricted apical sides and enlarged basolateral areas" (Sawyer et al., 2010), and cells at the ventral furrow in *Drosophila* are described as undergoing basal expansion after apical constriction (Sweeton et al., 1991).

The most obvious cellular change during basal expansion is an increase in basal membrane. Such an expansion could be driven by biogenesis of new membrane, transcytosis of the shrinking apical membrane to the basal surface, or transition in identity from apical to basal or basolateral membrane. Differential rates of biogenesis could expand the basal surface. However, where it has been described, basal expansion appears to occur rapidly following apical constriction (Sweeton et al., 1991). Membrane biogenesis is closely tied to lipid metabolism (Nohturfft and Zhang, 2009), but the rate of biogenesis may not be rapid enough to drive the membrane expansion. An alternative hypothesis is based on data suggesting that endocytosis and transcytosis can result in the deposition of membrane from one region of the cell to another. This is a Rab-dependent mechanism by which specific cell regions can gain surface area (Pelissier et al., 2003). The hypothesis is particularly appealing given an observation that Rab5- and dynamin-mediated endocytosis is required for apical constriction during bottle cell formation in *Xenopus* (Lee and Harland, 2007). Labeled apical membrane did not appear to re-

integrate in bulk on the expanded basal surface, but this may have been due to a lack of resolution and not a reflection of the mechanism. Another possible mechanism of basal expansion is that apical membrane could shift in identity to basal or basolateral. In *Drosophila*, downregulation of either apical or basolateral polarity determinants causes an expansion of the opposite domain type (Kaplan et al., 2009). This could drive basal expansion by reducing the amount of apical membrane in the cell and increasing the amount of basal membrane. If coordinated with apical constriction and basal expansion, this would allow the basal membrane to increase in direct response to a decrease in apical membrane without the need for membrane biogenesis or transport. This remains an open area of study in the context of epithelial cell shape change.

Signaling in apical constriction

The upstream signals that regulate apical constriction vary much more than the physical mechanism of the cell shape change and can differ not only between organisms but between tissues within an organism. For example, in *Drosophila*, Hedgehog and Bmp signaling signal to form the eye morphogenetic furrow, which requires apical constriction (Schlichting and Dahmann, 2008), while Twist and Snail downstream of Dorsal regulate apical constriction during ventral furrow formation (Martin et al., 2009; Sawyer et al., 2010). In sea urchin gastrulation, Wnt/Frizzled, Fgf, and calcium signaling have all been implicated (Croce et al., 2006; Nakajima and Burke, 1996; Rottinger et al., 2008), while non-canonical-Wnt signaling regulates zebrafish gastrulation (Ulrich et al., 2005). Apical constriction during *Xenopus* bottle cell formation appears to be regulated by non-canonical-Wnt signaling (Choi and Sokol, 2009), while canonical-Wnt signaling regulates apical constriction upstream of Rho and myosin in the *Drosophila* wing imaginal disc (Zimmerman et al., 2010). It is likely that some of these pathways regulate tissue identity while others regulate the physical aspects of the cell shape changes

themselves. Closer analysis including temporally-specific activation or inhibition of signaling may bring to light more conservation in regulating these processes than is currently evident.

BASAL CONSTRICTION

Basal constriction, the constriction of the basal surface of an epithelial cell, is a process by which an epithelial sheet can bend away from an apical lumen or evaginate to form an out-pocketing of the epithelia. Such constriction requires the remodeling of the cell surface bound to the underlying extracellular matrix and expands the apical surface of the tissue. This process, unlike apical constriction, has not been studied in detail, and, in fact, has only been described as a mechanism of development in a few contexts. Basal constriction was first demonstrated in a squamous cell line in culture (Auersperg et al., 1973) (Fig. 3A). A decade later, this type of cell shape change was speculated to be a possible mechanism of epithelial morphogenesis, but this was not shown experimentally (Fristrom, 1988). Although apical constriction and apico-basal lengthening drive invagination during *Drosophila* ventral furrow formation, Leptin and Grunewald also noted "narrowing" of the basal cell surface in cells adjacent to the invagination though this has not been further explored (Leptin and Grunewald, 1990) (Figure 3B). The regulation of basal constriction was first studied explicitly as a necessary step in formation of the midbrain-hindbrain boundary constriction (MHBC) in zebrafish as part of this thesis (Fig. 3C). This was followed by a study showing basal constriction to be required during morphogenesis of the optic cup in *Medaka* (Martinez-Morales et al., 2009).

Despite the paucity of examples described in the literature, my own analysis of data from previous studies suggests that this may be a much more common mechanism of epithelial morphogenesis than previously considered. Apical constriction initiates

ectodermal invagination during sea urchin invagination; reminiscent of the observations of ventral furrow formation in *Drosophila* mentioned above, cells with a basal-constriction-like morphology lie on either side of the invagination (Sweeton et al., 1991). Early during mouse neurulation, electron microscopy and the observation of actin enrichment at the basal cell surfaces also suggest basal constriction (Sadler et al., 1982), while in the eye imaginal disc of *Drosophila*, cells appear to constrict basally during tissue ingression (Corrigall et al., 2007)(Fig. 3D). In addition to these examples of epithelial folding, basal constriction appears to occur during evagination of the salivary gland in *Drosophila* (Fristrom, 1988). A recent study of the evaginating *Hydra* bud shows cells at the tip of the evagination that appear to be both basally constricted and apically expanded (Philipp et al., 2009) (Fig. 3E). While further experiments will be required to confirm whether these cell shape changes share other characteristics of basal constriction, these observations from the literature indicate that basal constriction may be a conserved process that warrants greater attention.

Signaling in basal constriction

What signals initiate basal constriction? I considered both Wnt and focal adhesion kinase (FAK) signaling in regulating this process.

The Wnt signaling pathway is generally considered to include two branches: the canonical, whose activation results in transcriptional activation of downstream target genes, and the non-canonical, the activation of which generally results in cytoskeletal regulation (van Amerongen and Nusse, 2009) (Fig. 4). The canonical pathway, required for tissue specification during zebrafish MHBC development, is activated by binding of an extracellular Wnt ligand to its receptor, Frizzled. This activation is tied to the activity of a co-receptor, LRP (Verkaar and Zaman, 2010) and results in the inhibition of a destruction complex including Gsk3β, APC, CK-1, Axin and MACF1 by Dishevelled

(Salinas, 2007). In the absence of Wnt ligand, Gsk3β and CK1 phosphorylate cytoplasmic β-catenin, targeting it for degradation. Inhibition of this complex in the presence of Wnt ligand prevents this phosphorylation, which allows β-catenin to activate transcription of downstream targets through binding to TCF/LEF transcription factors in the nucleus (Salinas, 2007). Interestingly, Gsk3β and APC have also recently been shown to regulate the microtubule cytoskeleton in response to Wnt signaling, suggesting that these components may also play roles outside the traditional canonical pathway (Zumbrunn et al, 2009; Salinas, 2009).

The non-canonical Wnt signaling pathway is similarly activated by Wnt binding to Frizzled receptors, though in this pathway, Ror often acts as a co-receptor, and the pathway can also be activated by binding to alternate receptors such as Ryk (van Amerongen and Nusse, 2010). The signal is transmitted through Dishevelled, an adapter protein that binds to the receptor, sometimes in conjunction with Daam1. The small GTPases Rho or Rac and Jnk are then activated, promoting cytoskeletal rearrangements (Schlessinger et al, 2009). Alternatively, binding of non-canonical Wnt ligands to their receptors can result in activation of calcium signaling or the non-receptor tyrosine kinase, Src, although these pathways are less well understood (van Amerongen and Nusse, 2010). Non-canonical Wnt signaling has been shown to regulate cell shape changes, particularly during convergent extension (Qian, 2007; Torban, 2004).

FAK is of particular interest in considering the regulation of basal constriction, as this process is likely to require active regulation of adhesion between the basal cell surface and the underlying basement membrane. This protein is a well-known regulator of focal adhesions, but has also been shown to play a role in several signaling pathways (Parsons, 2003) (Fig. 5). Among others, FAK has been shown to signal upstream of Akt and PI3K in the inhibition of Gsk3β (Huang 2006; Huang 2009), and in signaling pathways with Src and the small GTPases, Rho, Rac, and Jnk to regulate the cytoskeleton

(Parsons, 2003; Igishi 1999). However, the specific role of FAK in these pathways is not well understood.

A NOTE ABOUT REGION-SPECIFIC MORPHOGENESIS

As described above, epithelial morphogenesis is often driven by changes in cell size and shape. These changes in cell size or shape must occur not only at a specific time during development, but at a specific position in the epithelia. Thus, these changes require components to drive or execute the physical process itself as well as signals to position and initiate the process. In determining what components are necessary for a given cell size or shape change, it is useful to consider how components necessary for execution and initiation differ.

In order for a component to be involved in executing a cell shape change, it must be present at the right time and place and required for the process. This means it must be expressed and localized to the region during the cell shape change, but may also be present elsewhere in the tissue at the same time. For example, actin is required for apical constriction, and thus, must be expressed and localized to the apical surface of the cells undergoing the cell shape change, but it is also present in epithelial cells not undergoing the cell shape change (Pilot and Lecuit, 2005). In addition, the component must be required for the process, which can be tested by loss of function analysis. Taking the same example, to establish that actin is required for apical constriction, its depolymerization must prevent the process.

For a component to be characterized as positioning and/or initiating a cell shape change, it must similarly be required for the process. However, its expression and localization must be specific *only* to the time and place that the process is occurring. For example, during gastrulation, apical constriction occurs in one specific region of the tissue to drive invagination, although the entire tissue is composed of epithelial cells that

might also be competent to constrict apically (Martin et al, 2009). The signal necessary to position or initiate the cell shape change must be localized specifically and only to the cells that constrict apically. The defining characteristic of a localizing or initiating signal is that it will drive the cell shape change in any cells that are competent. This suggests that an initiating signal expressed or localized in an expanded region of tissue would increase the total number of cells undergoing the cell shape change.

CONCLUSION

In this thesis, I establish basal constriction as a mechanism of epithelial morphogenesis at the midbrain-hindbrain boundary constriction in zebrafish and begin to address the components required both to execute and initiate this process.

FIGURE LEGENDS

Fig. 1 Schematic of an epithelial cell

The apical and basolateral cell membrane domains are separated by tight junctions, adherens junctions, and gap junctions at the apical cell surface with desmosomes at the basolateral surface. Membrane-bound proteins at the basal surface, sometimes localized to focal adhesions, bind the underlying extracellular matrix. Actin is localized to the cell cortex, links the adherens junctions, and forms stress fibers at focal adhesions. Microtubules are oriented apico-basally.

Fig. 2 Epithelial cell shape and length changes during morphogenesis

(A) A columnar epithelial cell is depicted though these processes could also be initiated from cells of other types. (B) Circumferential constriction of one cell membrane will result in a cone-shaped cell. (C) Symmetrical lateral constriction will result in a wedge-shaped cell. (D) Cell elongation as along the apico-basal axis is depicted. This is often coupled with circumferential constriction (Lee et al., 2007; Widmann and Dahmann, 2009). (E) Cell shortening along apico-basal axis is depicted. This has been shown to occur concomitant with basal constriction (Gutzman et al., 2008). (F) Cell spreading can be described as cell shortening along the apico-basal axis or as lateral elongation and results in a flattened epithelial cell.

Fig. 3 Examples of basal constriction from the literature

Camera lucida drawings taken from the literature show examples of basal constriction either as published or from my own analysis. Red cells appear basally constricted. (A) Squamous cell carcinoma in 3D culture (Auersperg et al., 1973). (B) Ventral furrow as forms during *Drosophila* gastrulation (Leptin and Grunewald, 1990). (C) Zebrafish

midbrain-hindbrain boundary constriction (Gutzman et al., 2008). (D) *Drosophila* eye imaginal disc (Corrigall et al., 2007). (E) Tentacle bud in *Hydra* (Philipp et al., 2009).

Fig. 4 Overview of Wnt signaling

The canonical and non-canonical Wnt signaling pathways promote transcriptional activation and regulation of the cytoskeleton respectively. Wnt5 is shown as one example of a non-canonical Wnt signaling component that may be involved basal constriction at the MHBC. Figure adapted from (van Amerongen and Nusse, 2010).

Fig. 5 Focal Adhesion Kinase as a signaling regulator

Shown are two pathways in which focal adhesion kinase (FAK) acts as a signaling regulator (Huang 2006; Huang, 2009; Igishi, 1999; Parsons, 2003).

FIGURE 1

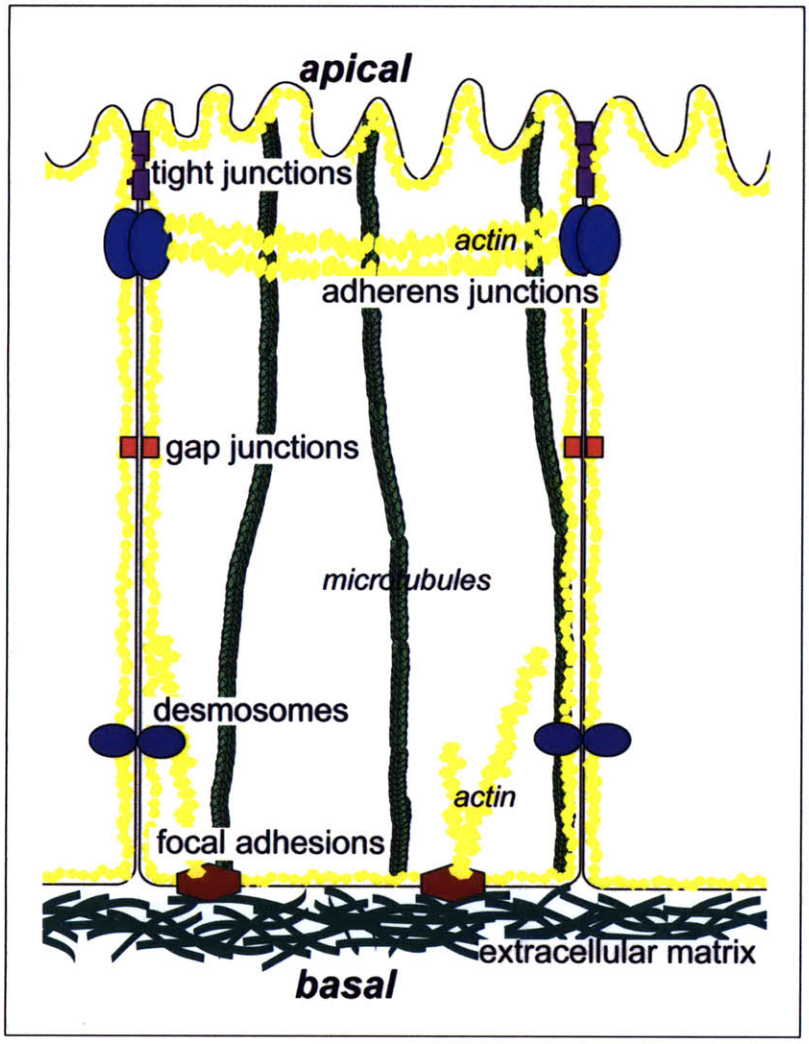
apical
tight junctions
actin
adherens junctions
gap junctions
microtubules
desmosomes
actin
focal adhesions
extracellular matrix
basal

FIGURE 2

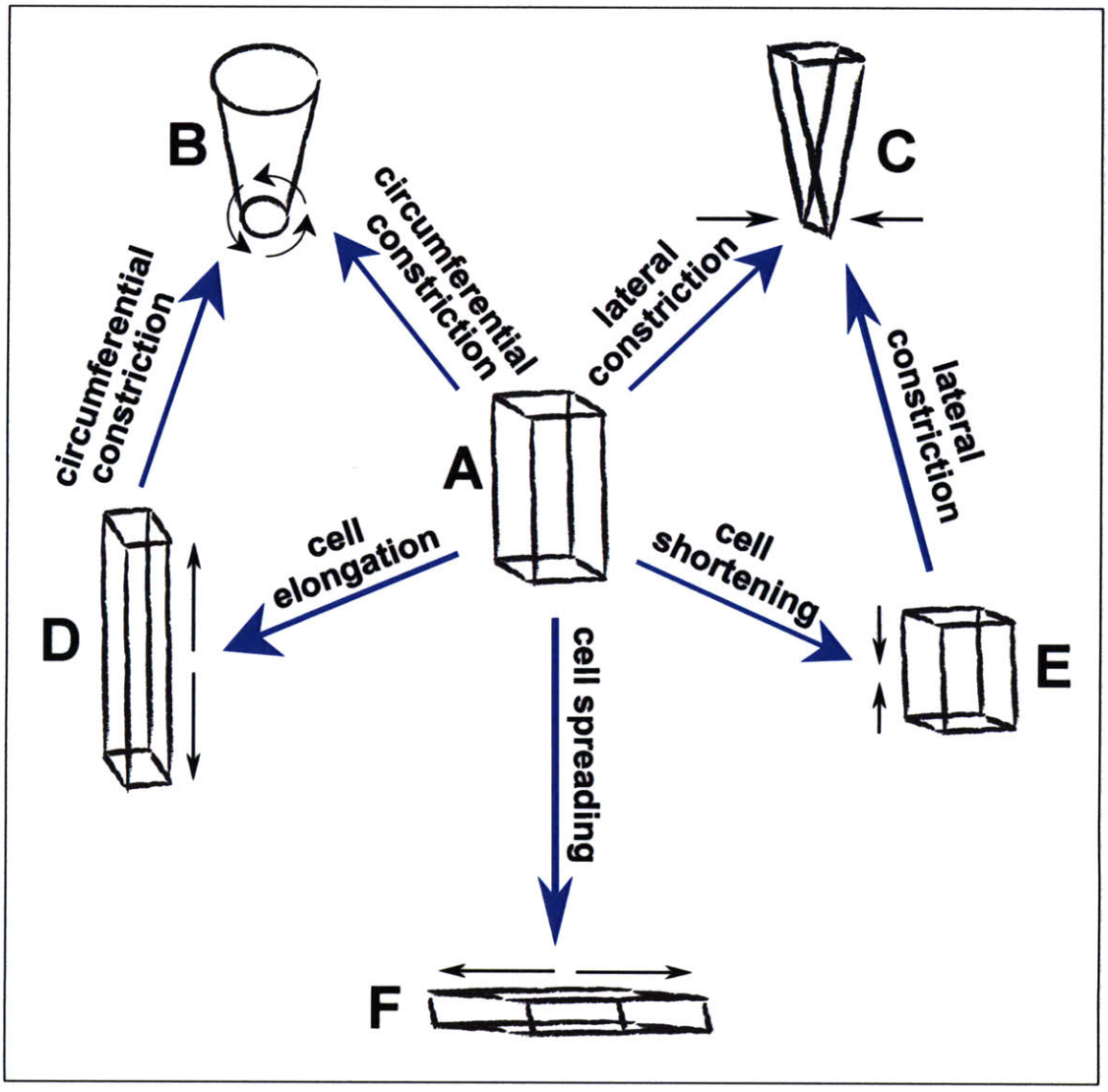
B
C
A
D
E
F
circumferential constriction
circumferential constriction
lateral constriction
lateral constriction
cell elongation
cell shortening
cell spreading

FIGURE 3

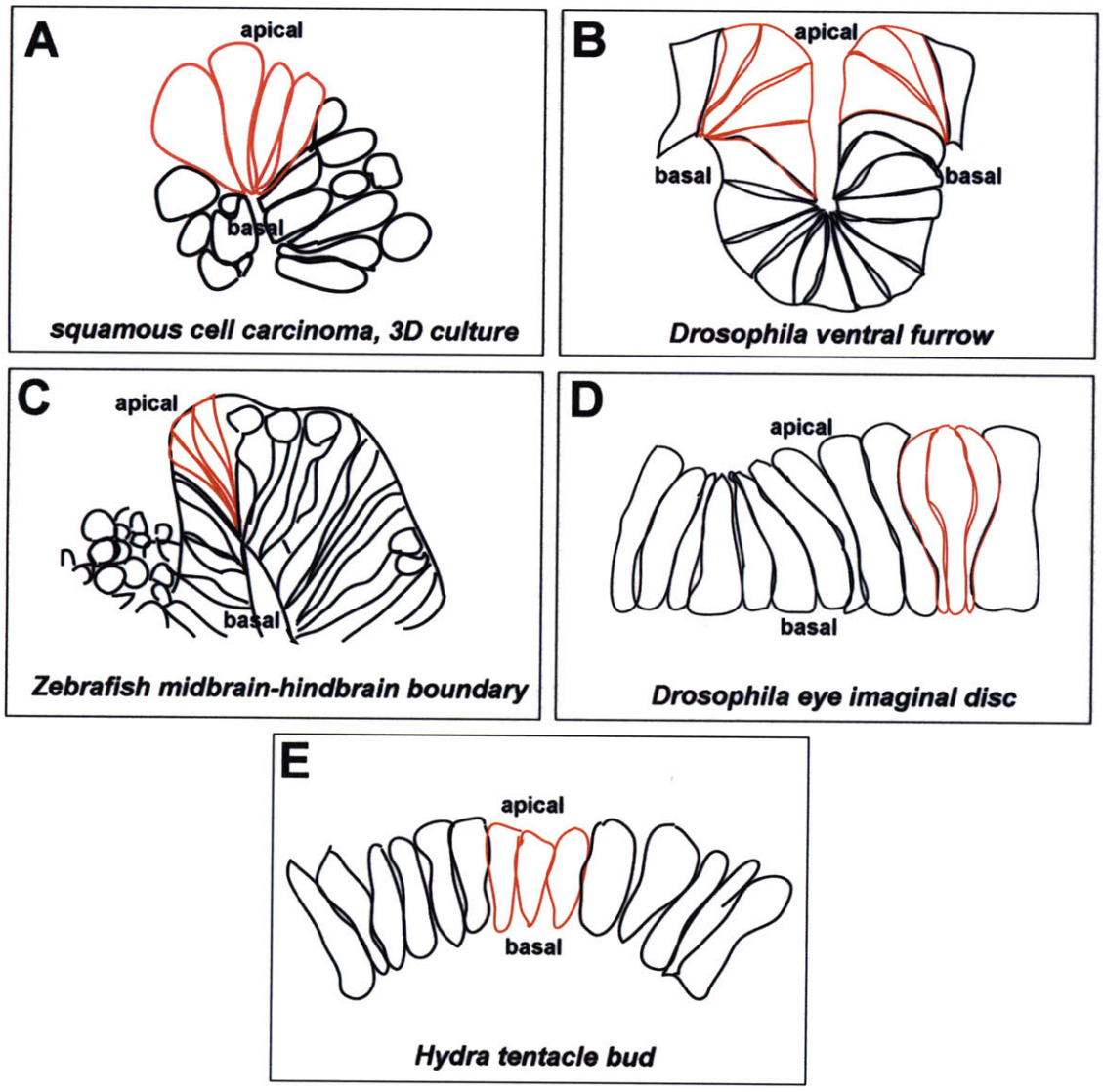
A
apical
basal
squamous cell carcinoma, 3D culture
B
apical
basal
basal
Drosophila ventral furrow
C
apical
basal
Zebrafish midbrain-hindbrain boundary
D
apical
basal
Drosophila eye imaginal disc
E
apical
basal
Hydra tentacle bud

FIGURE 4

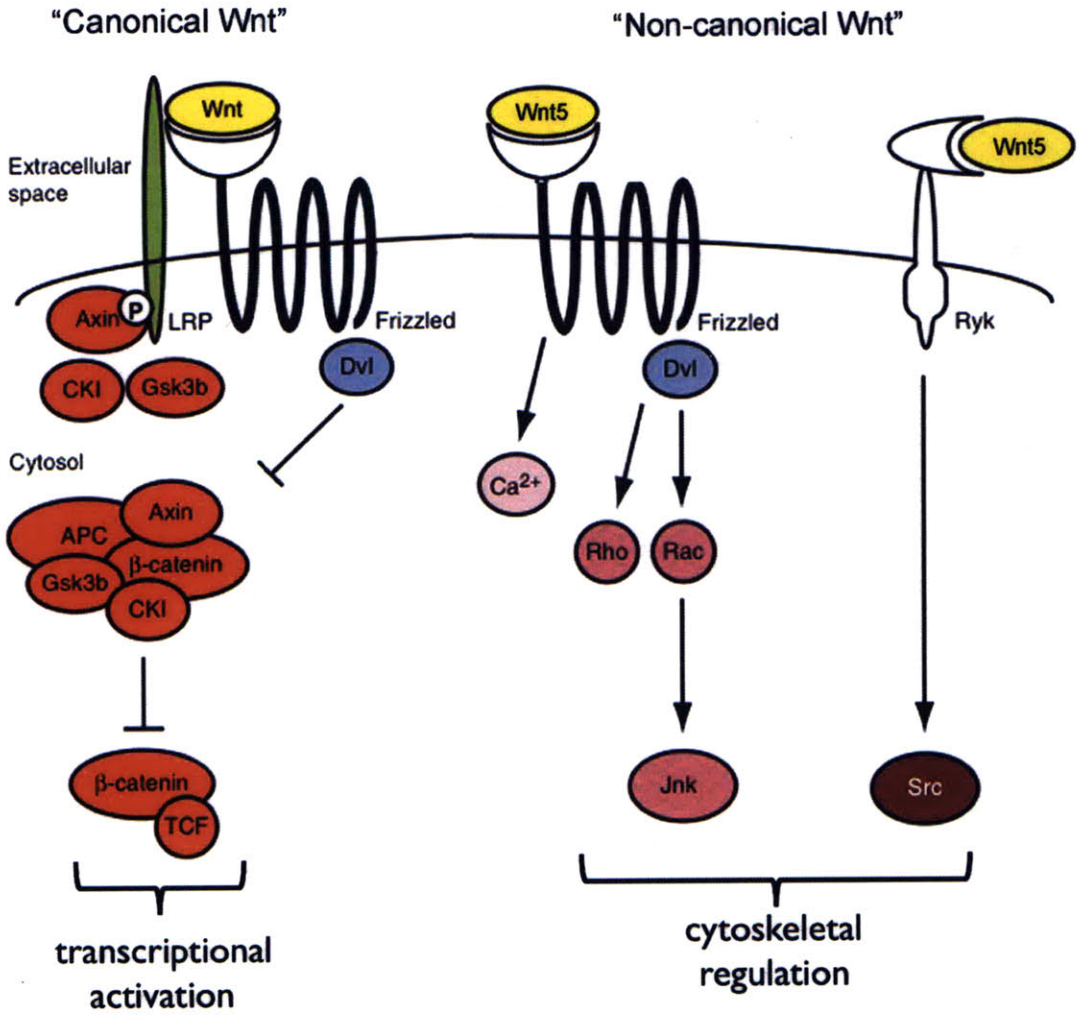
"Canonical Wnt"
"Non-canonical Wnt"
Wnt
Wnt5
Wnt5
Extracellular space
Axin
P
LRP
Frizzled
Frizzled
Ryk
Dvl
Dvl
CKI
Gsk3b
Cytosol
Ca2+
Axin
APC
β-catenin
Gsk3b
CKI
Rho
Rac
β-catenin
TCF
Jnk
Src
transcriptional activation
cytoskeletal regulation

FIGURE 5

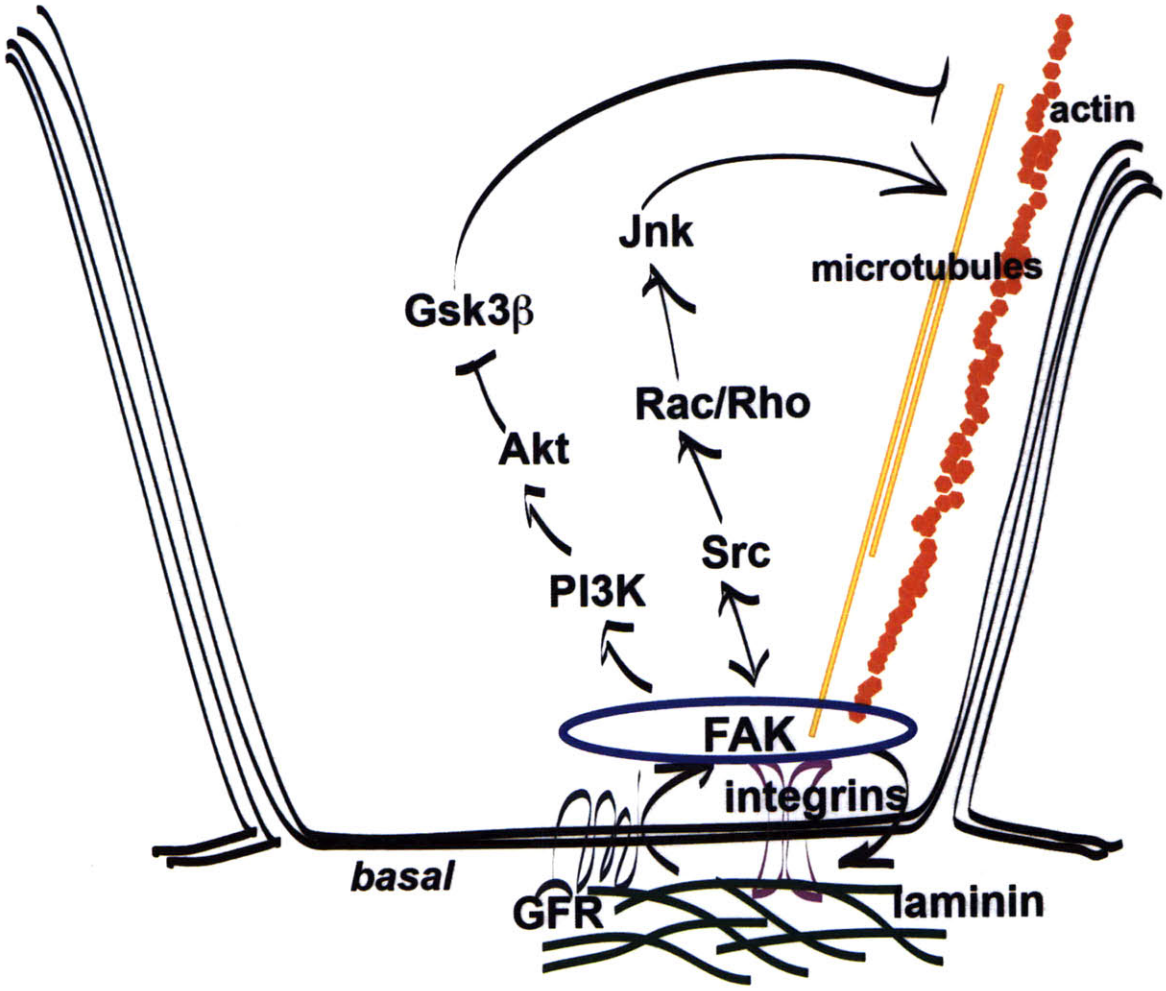
actin
Jnk
microtubules
Gsk3β
Rac/Rho
Akt
Src
PI3K
FAK
integrins
basal
GFR
laminin

REFERENCES

Anstrom, J. A. (1992). Microfilaments, cell shape changes, and the formation of primary mesenchyme in sea urchin embryos. *J Exp Zool* **264**, 312-22.

Auersperg, N., Erber, H. and Worth, A. (1973). Histologic variation among poorly differentiated invasive carcinomas of the human uterine cervix. *J Natl Cancer Inst* **51**, 1461-77.

Baker, P. C. and Schroeder, T. E. (1967). Cytoplasmic filaments and morphogenetic movement in the amphibian neural tube. *Dev Biol* **15**, 432-50.

Bartolini, F. and Gundersen, G. G. (2006). Generation of noncentrosomal microtubule arrays. *J Cell Sci* **119**, 4155-63.

Bassnett, S. (2005). Three-dimensional reconstruction of cells in the living lens: the relationship between cell length and volume. *Exp Eye Res* **81**, 716-23.

Bellett, G., Carter, J. M., Keynton, J., Goldspink, D., James, C., Moss, D. K. and Mogensen, M. M. (2009). Microtubule plus-end and minus-end capture at adherens junctions is involved in the assembly of apico-basal arrays in polarised epithelial cells. *Cell Motil Cytoskeleton* **66**, 893-908.

Brand, M., Heisenberg, C. P., Jiang, Y. J., Beuchle, D., Lun, K., Furutani-Seiki, M., Granato, M., Haffter, P., Hammerschmidt, M., Kane, D. A. et al. (1996). Mutations in zebrafish genes affecting the formation of the boundary between midbrain and hindbrain. *Development* **123**, 179-90.

Bryant, D. M. and Mostov, K. E. (2008). From cells to organs: building polarized tissue. *Nat Rev Mol Cell Biol* **9**, 887-901.

Buckles, G. R., Thorpe, C. J., Ramel, M. C. and Lekven, A. C. (2004). Combinatorial Wnt control of zebrafish midbrain-hindbrain boundary formation. *Mech Dev* **121**, 437-47.

Burnside, B. (1971). Microtubules and microfilaments in newt neuralation. *Dev Biol* **26**, 416-41.

Byers, B. and Porter, K. R. (1964). Oriented Microtubules in Elongating Cells of the Developing Lens Rudiment after Induction. *Proc Natl Acad Sci U S A* **52**, 1091-9.

Chisholm, A. D. and Hardin, J. (2005). Epidermal morphogenesis. *WormBook*, 1-22.

Choi, S. C. and Sokol, S. Y. (2009). The involvement of lethal giant larvae and Wnt signaling in bottle cell formation in Xenopus embryos. *Dev Biol* **336**, 68-75.

Chung, M. I., Nascone-Yoder, N. M., Grover, S. A., Drysdale, T. A. and Wallingford, J. B. (2010). Direct activation of Shroom3 transcription by Pitx proteins drives epithelial morphogenesis in the developing gut. *Development* **137**, 1339-49.

Corrigall, D., Walther, R. F., Rodriguez, L., Fichelson, P. and Pichaud, F. (2007). Hedgehog signaling is a principal inducer of Myosin-II-driven cell ingression in Drosophila epithelia. *Dev Cell* **13**, 730-42.

Croce, J., Duloquin, L., Lhomond, G., McClay, D. R. and Gache, C. (2006). Frizzled5/8 is required in secondary mesenchyme cells to initiate archenteron invagination during sea urchin development. *Development* **133**, 547-57.

Davidson, L. A., Ezin, A. M. and Keller, R. (2002). Embryonic wound healing by apical contraction and ingression in Xenopus laevis. *Cell Motil Cytoskeleton* **53**, 163-76.

Dearry, A. and Burnside, B. (1986). Dopaminergic regulation of cone retinomotor movement in isolated teleost retinas: I. Induction of cone contraction is mediated by D2 receptors. *J Neurochem* **46**, 1006-21.

Escudero, L. M., Bischoff, M. and Freeman, M. (2007). Myosin II regulates complex cellular arrangement and epithelial architecture in Drosophila. *Dev Cell* **13**, 717-29.

Fristrom, D. (1988). The cellular basis of epithelial morphogenesis. A review. *Tissue Cell* **20**, 645-90.

Giepmans, B. N. and van Ijzendoorn, S. C. (2009). Epithelial cell-cell junctions and plasma membrane domains. *Biochim Biophys Acta* **1788**, 820-31.

Gutzman, J. H., Graeden, E. G., Lowery, L. A., Holley, H. S. and Sive, H. (2008). Formation of the zebrafish midbrain-hindbrain boundary constriction requires laminin-dependent basal constriction. *Mech Dev* **125**, 974-83.

Hildebrand, J. D. (2005). Shroom regulates epithelial cell shape via the apical positioning of an actomyosin network. *J Cell Sci* **118**, 5191-203.

Hirokawa, N., Noda, Y., Tanaka, Y. and Niwa, S. (2009). Kinesin superfamily motor proteins and intracellular transport. *Nat Rev Mol Cell Biol* **10**, 682-96.

Hynes, R. O. (2009). The extracellular matrix: not just pretty fibrils. *Science* **326**, 1216-9.

Jolly, A. L., Kim, H., Srinivasan, D., Lakonishok, M., Larson, A. G. and Gelfand, V. I. (2010). Kinesin-1 heavy chain mediates microtubule sliding to drive changes in cell shape. *Proc Natl Acad Sci U S A* **107**, 12151-6.

Joyner, A. L. (1996). Engrailed, Wnt and Pax genes regulate midbrain--hindbrain development. *Trends Genet* **12**, 15-20.

Kaplan, N. A., Liu, X. and Tolwinski, N. S. (2009). Epithelial polarity: interactions between junctions and apical-basal machinery. *Genetics* **183**, 897-904.

Kardon, J. R. and Vale, R. D. (2009). Regulators of the cytoplasmic dynein motor. *Nat Rev Mol Cell Biol* **10**, 854-65.

Karfunkel, P. (1972). The activity of microtubules and microfilaments in neurulation in the chick. *J Exp Zool* **181**, 289-301.

Keller, R. (2002). Shaping the vertebrate body plan by polarized embryonic cell movements. *Science* **298**, 1950-4.

Keller, R. E. (1980). The cellular basis of epiboly: an SEM study of deep-cell rearrangement during gastrulation in Xenopus laevis. *J Embryol Exp Morphol* **60**, 201-34.

Kim, A. S., Anderson, S. A., Rubenstein, J. L., Lowenstein, D. H. and Pleasure, S. J. (2001). Pax-6 regulates expression of SFRP-2 and Wnt-7b in the developing CNS. *J Neurosci* **21**, RC132.

Koppen, M., Fernandez, B. G., Carvalho, L., Jacinto, A. and Heisenberg, C. P. (2006). Coordinated cell-shape changes control epithelial movement in zebrafish and Drosophila. *Development* **133**, 2671-81.

Lee, C., Scherr, H. M. and Wallingford, J. B. (2007). Shroom family proteins regulate gamma-tubulin distribution and microtubule architecture during epithelial cell shape change. *Development* **134**, 1431-41.

Lee, J. Y. and Harland, R. M. (2007). Actomyosin contractility and microtubules drive apical constriction in Xenopus bottle cells. *Dev Biol* **311**, 40-52.

Leptin, M. and Grunewald, B. (1990). Cell shape changes during gastrulation in Drosophila. *Development* **110**, 73-84.

Lun, K. and Brand, M. (1998). A series of no isthmus (noi) alleles of the zebrafish pax2.1 gene reveals multiple signaling events in development of the midbrain-hindbrain boundary. *Development* **125**, 3049-62.

Martin, A. C., Kaschube, M. and Wieschaus, E. F. (2009). Pulsed contractions of an actin-myosin network drive apical constriction. *Nature* **457**, 495-9.

Martinez-Morales, J. R., Rembold, M., Greger, K., Simpson, J. C., Brown, K. E., Quiring, R., Pepperkok, R., Martin-Bermudo, M. D., Himmelbauer, H. and Wittbrodt, J. (2009). ojoplano-mediated basal constriction is essential for optic cup morphogenesis. *Development* **136**, 2165-75.

Mullins, R. D., Heuser, J. A. and Pollard, T. D. (1998). The interaction of Arp2/3 complex with actin: nucleation, high affinity pointed end capping, and formation of branching networks of filaments. *Proc Natl Acad Sci U S A* **95**, 6181-6.

Nakajima, Y. and Burke, R. D. (1996). The initial phase of gastrulation in sea urchins is accompanied by the formation of bottle cells. *Dev Biol* **179**, 436-46.

Nikolaidou, K. K. and Barrett, K. (2004). A Rho GTPase signaling pathway is used reiteratively in epithelial folding and potentially selects the outcome of Rho activation. *Curr Biol* **14**, 1822-6.

Nohturfft, A. and Zhang, S. C. (2009). Coordination of lipid metabolism in membrane biogenesis. *Annu Rev Cell Dev Biol* **25**, 539-66.

Osumi, N., Hirota, A., Ohuchi, H., Nakafuku, M., Iimura, T., Kuratani, S., Fujiwara, M., Noji, S. and Eto, K. (1997). Pax-6 is involved in the specification of hindbrain motor neuron subtype. *Development* **124**, 2961-72.

Parsons, J. T. (2003). Focal adhesion kinase: the first ten years. *J Cell Sci* **116**, 1409-16.

Pelissier, A., Chauvin, J. P. and Lecuit, T. (2003). Trafficking through Rab11 endosomes is required for cellularization during Drosophila embryogenesis. *Curr Biol* **13**, 1848-57.

Perez-Moreno, M., Jamora, C. and Fuchs, E. (2003). Sticky business: orchestrating cellular signals at adherens junctions. *Cell* **112**, 535-48.

Philipp, I., Aufschnaiter, R., Ozbek, S., Pontasch, S., Jenewein, M., Watanabe, H., Rentzsch, F., Holstein, T. W. and Hobmayer, B. (2009). Wnt/beta-catenin and noncanonical Wnt signaling interact in tissue evagination in the simple eumetazoan Hydra. *Proc Natl Acad Sci U S A* **106**, 4290-5.

Piatigorsky, J., Rothschild, S. S. and Wollberg, M. (1973). Stimulation by insulin of cell elongation and microtubule assembly in embryonic chick-lens epithelia. *Proc Natl Acad Sci U S A* **70**, 1195-8.

Pilot, F. and Lecuit, T. (2005). Compartmentalized morphogenesis in epithelia: from cell to tissue shape. *Dev Dyn* **232**, 685-94.

Plageman, T. F., Jr., Chung, M. I., Lou, M., Smith, A. N., Hildebrand, J. D., Wallingford, J. B. and Lang, R. A. (2010). Pax6-dependent Shroom3 expression regulates apical constriction during lens placode invagination. *Development* **137**, 405-15.

Pope, K. L. and Harris, T. J. (2008). Control of cell flattening and junctional remodeling during squamous epithelial morphogenesis in Drosophila. *Development* **135**, 2227-38.

Puelles, L. and Martinez-de-la-Torre, M. (1987). Autoradiographic and Golgi study on the early development of n. isthmi principalis and adjacent grisea in the chick embryo: a tridimensional viewpoint. *Anat Embryol (Berl)* **176**, 19-34.

Qian, D., Jones, C., Rzadzinska, A., Mark, S., Zhang, X., Steel, K. P., Dai, X. and Chen, P. (2007). Wnt5a functions in planar cell polarity regulation in mice. *Dev Biol* **306**, 121-33.

Reifers, F., Bohli, H., Walsh, E. C., Crossley, P. H., Stainier, D. Y. and Brand, M. (1998). Fgf8 is mutated in zebrafish acerebellar (ace) mutants and is required for maintenance of midbrain-hindbrain boundary development and somitogenesis. *Development* **125**, 2381-95.

Reilein, A. and Nelson, W. J. (2005). APC is a component of an organizing template for cortical microtubule networks. *Nat Cell Biol* **7**, 463-73.

Reilein, A., Yamada, S. and Nelson, W. J. (2005). Self-organization of an acentrosomal microtubule network at the basal cortex of polarized epithelial cells. *J Cell Biol* **171**, 845-55.

Roh-Johnson, M. and Goldstein, B. (2009). In vivo roles for Arp2/3 in cortical actin organization during C. elegans gastrulation. *J Cell Sci* **122**, 3983-93.

Rolo, A., Skoglund, P. and Keller, R. (2009). Morphogenetic movements driving neural tube closure in Xenopus require myosin IIB. *Dev Biol* **327**, 327-38.

Rottinger, E., Saudemont, A., Duboc, V., Besnardeau, L., McClay, D. and Lepage, T. (2008). FGF signals guide migration of mesenchymal cells, control skeletal morphogenesis [corrected] and regulate gastrulation during sea urchin development. *Development* **135**, 353-65.

Sadler, T. W., Greenberg, D., Coughlin, P. and Lessard, J. L. (1982). Actin distribution patterns in the mouse neural tube during neurulation. *Science* **215**, 172-4.

Sato, T., Joyner, A. L. and Nakamura, H. (2004). How does Fgf signaling from the isthmic organizer induce midbrain and cerebellum development? *Dev Growth Differ* **46**, 487-94.

Sawyer, J. M., Harrell, J. R., Shemer, G., Sullivan-Brown, J., Roh-Johnson, M. and Goldstein, B. (2010). Apical constriction: a cell shape change that can drive morphogenesis. *Dev Biol* **341**, 5-19.

Schlichting, K. and Dahmann, C. (2008). Hedgehog and Dpp signaling induce cadherin Cad86C expression in the morphogenetic furrow during Drosophila eye development. *Mech Dev* **125**, 712-28.

Schock, F. and Perrimon, N. (2002). Molecular mechanisms of epithelial morphogenesis. *Annu Rev Cell Dev Biol* **18**, 463-93.

Schuck, S. and Simons, K. (2004). Polarized sorting in epithelial cells: raft clustering and the biogenesis of the apical membrane. *J Cell Sci* **117**, 5955-64.

Shaw, R. M., Fay, A. J., Puthenveedu, M. A., von Zastrow, M., Jan, Y. N. and Jan, L. Y. (2007). Microtubule plus-end-tracking proteins target gap junctions directly from the cell interior to adherens junctions. *Cell* **128**, 547-60.

Solnica-Krezel, L. (2005). Conserved patterns of cell movements during vertebrate gastrulation. *Curr Biol* **15**, R213-28.

Solnica-Krezel, L. (2006). Gastrulation in zebrafish -- all just about adhesion? *Curr Opin Genet Dev* **16**, 433-41.

Suzuki, M., Hara, Y., Takagi, C., Yamamoto, T. S. and Ueno, N. (2010). MID1 and MID2 are required for Xenopus neural tube closure through the regulation of microtubule organization. *Development* **137**, 2329-39.

Sweeton, D., Parks, S., Costa, M. and Wieschaus, E. (1991). Gastrulation in Drosophila: the formation of the ventral furrow and posterior midgut invaginations. *Development* **112**, 775-89.

Torban, E., Kor, C. and Gros, P. (2004). Van Gogh-like2 (Strabismus) and its role in planar cell polarity and convergent extension in vertebrates. *Trends Genet* **20**, 570-7.

Troutt, L. L. and Burnside, B. (1988). Microtubule polarity and distribution in teleost photoreceptors. *J Neurosci* **8**, 2371-80.

Ulrich, F., Krieg, M., Schotz, E. M., Link, V., Castanon, I., Schnabel, V., Taubenberger, A., Mueller, D., Puech, P. H. and Heisenberg, C. P. (2005). Wnt11 functions in gastrulation by controlling cell cohesion through Rab5c and E-cadherin. *Dev Cell* **9**, 555-64.

van Meer, G. and Simons, K. (1988). Lipid polarity and sorting in epithelial cells. *J Cell Biochem* **36**, 51-8.

Wade, R. H. (2009). On and around microtubules: an overview. *Mol Biotechnol* **43**, 177-91.

Weed, S. A. and Parsons, J. T. (2001). Cortactin: coupling membrane dynamics to cortical actin assembly. *Oncogene* **20**, 6418-34.

Wen, Y., Eng, C. H., Schmoranzer, J., Cabrera-Poch, N., Morris, E. J., Chen, M., Wallar, B. J., Alberts, A. S. and Gundersen, G. G. (2004). EB1 and APC bind to mDia to stabilize microtubules downstream of Rho and promote cell migration. *Nat Cell Biol* **6**, 820-30.

Widmann, T. J. and Dahmann, C. (2009). Wingless signaling and the control of cell shape in Drosophila wing imaginal discs. *Dev Biol* **334**, 161-73.

Zimmerman, S. G., Thorpe, L. M., Medrano, V. R., Mallozzi, C. A. and McCartney, B. M. (2010). Apical constriction and invagination downstream of the canonical Wnt signaling pathway require Rho1 and Myosin II. *Dev Biol* **340**, 54-66.

2

Formation of the zebrafish midbrain-hindbrain boundary constriction requires laminin-dependent basal constriction

CONTRIBUTIONS

This work was completed in equal collaboration with Jennifer Gutzman, with help from Laura A. Lowery and Heidi S. Holley. Laura A. Lowery first identified *sly* mutants as lacking a midbrain-hindbrain boundary. Jennifer Gutzman performed the brightfield imaging, antibody staining, and time-lapse confocal microscopy. I characterized basal constriction by live confocal imaging in both wild type and mutant embryos and performed quantification of the phenotypes. I collaborated with Jennifer Gutzman to write the paper. Thanks to Nancy Hopkins and Adam Amsterdam for the *gup*^{hi1113b} mutant line. This work has been published as:

Gutzman, J. H., Graeden, E. G., Lowery, L. A., Holley, H. S. and Sive, H. (2008). Formation of the zebrafish midbrain-hindbrain boundary constriction requires laminin-dependent basal constriction. *Mech Dev* **125**, 974-83.

ABSTRACT

The midbrain-hindbrain boundary (MHB) is a highly conserved fold in the vertebrate embryonic brain. We have termed the deepest point of this fold the MHB constriction (MHBC) and have begun to define the mechanisms by which it develops. In the zebrafish, the MHBC is formed soon after neural tube closure, concomitant with inflation of the brain ventricles. The MHBC is unusual, as it forms by bending the basal side of the neuroepithelium. At single cell resolution, we show that zebrafish MHBC formation involves two steps. The first is a shortening of MHB cells to approximately 75% of the length of surrounding cells. The second is basal constriction, and apical expansion, of a small group of cells that contribute to the MHBC. In the absence of inflated brain ventricles, basal constriction still occurs, indicating that the MHBC is not formed as a passive consequence of ventricle inflation. In laminin mutants, basal constriction does not occur, indicating a requirement for the basement membrane in this process. Apical expansion also fails to occur in laminin mutants, suggesting that apical expansion may be dependent on basal constriction. This study demonstrates laminin-dependent basal constriction as a previously undescribed molecular mechanism for brain morphogenesis.

INTRODUCTION

During development of the vertebrate brain, the neural tube assumes a complex structure that includes formation of the brain ventricles and the appearance of conserved folds and bends. These folds and bends delineate functional units of the brain and are likely to shape the brain such that it can pack into the skull. The midbrain-hindbrain boundary (MHB) is the site of one of the earliest bends in the developing brain. In the embryo, the MHB functions as an embryonic organizing center (Brand et al., 1996; Joyner, 1996; Puelles and Martinez-de-la-Torre, 1987; Sato et al., 2004) and later becomes the cerebellum and part of the tectum (Louvi et al., 2003). MHB tissue later becomes the cerebellum and forms part of the midbrain roof plate, or tectum (Louvi et al., 2003). Patterning of the MHB begins long before neural tube closure (Joyner, 1996). Subsequent to neural tube closure, and unlike the remainder of the brain, the tissue at the MHB remains apposed at the midline, shows lower levels of cell proliferation than surrounding neuroepithelium, and bends sharply to form the MHBC (Lowery and Sive, 2005). Loss of signaling factors that pattern the MHB results in failure to form the MHBC (Brand et al., 1996; Sato et al., 2004). However, it is likely that these genes are responsible for specifying the fate of the tissue and, thus, affect the MHBC indirectly.

The brain neuroepithelium has characteristic apico-basal polarity, with apical cell surfaces facing the ventricular lumen, and the basal lamina, surrounding the tube under the basal cell surfaces. While junctions connect the apical and lateral surfaces of epithelia, the basal surface of these cells is anchored on an extracellular matrix, the basal lamina. This polarity defines the axis of cell division within the epithelium (Fristrom, 1988), coordinates cell movements (Pilot and Lecuit, 2005), and provides spatial orientation for the larger structural modifications of the entire sheet during extension and bending or folding (Schock and Perrimon, 2002).

The basal lamina plays a critical role in epithelial morphogenesis (Miner and Yurchenco, 2004). One of the major proteins in the basal lamina is laminin, a heterotrimeric protein that interacts with integrins to mediate adhesion of the basal lamina to the cytoskeleton of the overlying cells (Miner and Yurchenco, 2004). Injection of a function-blocking laminin antibody inhibits salivary gland morphogenesis in mice and neural tube closure, somite development, and heart tube formation in chick (Patel et al., 2006; Zagris et al., 2004). Laminin is also critical during mouse embryo implantation and gastrulation (Miner et al., 2004) and, in zebrafish, is required for proper notochord formation and blood vessel formation (Parsons et al., 2002; Pollard et al., 2006; Scott and Stemple, 2005; Stemple, 2002). A role for laminin in brain morphogenesis has not been described.

Another contribution to epithelial morphogenesis is the fluid pressure found in organ lumens. For example, blood flow through the heart modifies the morphology of the atrial and ventricular lumens (Berdougo et al., 2003), and the flow of blood through the ventricles stimulates valve morphogenesis (Hove et al., 2003) while pressure overload can stimulate ventricle hypertrophy (Seidman and Seidman, 2001). During development of the eye in chick, folds of the ciliary body form due to the hydrostatic pressure and swelling of the vitreous humor (Bard and Ross, 1982a; Bard and Ross, 1982b). During development of the brain, the embryonic cerebrospinal fluid (eCSF) inflates the brain ventricular lumen, and one possible function for the eCSF is to generate pressure in the brain ventricles that contributes to brain morphogenesis (Desmond and Levitan, 2002; Lowery and Sive, 2005).

We have called the deepest point in the MHB the "midbrain-hindbrain boundary constriction" (MHBC). Here, we ask what processes are necessary for MHBC morphogenesis, using the zebrafish as a model. In the zebrafish, the MHBC forms between 17 and 24 hours post fertilization (hpf), concomitant with formation of the brain

ventricles. At this stage of development, the neuroepithelium is a pseudostratified-columnar epithelium where apical cell surfaces face the brain ventricle lumen, and basal cell surfaces, on the outside of the tube, abut the basement membrane. Interestingly, the MHBC forms by bending the basal side of the neuroepithelium. This is unusual since essentially all epithelial bends have been described at the apical surface via apical constriction. Basal constriction has rarely been discussed in the literature and has not previously been studied as an independent mechanism of organogenesis. The organization of the neuroepithelium and correlation with brain ventricle inflation led us to consider three factors that may drive MHBC morphogenesis: (1) fluid pressure on the inside of the neural tube as the brain ventricles inflate (Lowery and Sive, 2005), (2) changes in cell shape during bending, and (3) interactions of the basal side of the neuroepithelium with the basement membrane.

We show here that MHBC morphogenesis involves two processes, cell shortening at the MHB and basal constriction of the neuroepithelial cells at the MHBC. Basal constriction is dependent upon laminin function, but not upon inflation of the brain ventricles. These data indicate that the MHBC forms through changes in cell shape, dependent on the extracellular matrix, which have not previously been described during brain morphogenesis.

EXPERIMENTAL PROCEDURES

Fish lines and Maintenance

Zebrafish lines were maintained and stages determined as previously described (Kimmel et al., 1995; Westerfield, 1995). Strains used include wild-type AB, *sly*^{m86} (Schier et al., 1996), *gup*^{hi1113b} (Amsterdam et al., 2004), *nok*^{m227} (Malicki et al., 1996), and *snk*^{to273a} (Jiang et al., 1996).

Live imaging

Brain ventricle imaging was carried out as previously described (Lowery and Sive, 2005). For confocal imaging, single cell embryos were micro-injected with CAAX-eGFP mRNA (memGFP) (kindly provided by J. B. Green, Dana-Farber Cancer Institute Boston, MA) transcribed with the mMessage mMachine kit (Ambion). The embryos were mounted inverted in 0.7% agarose (Sigma) and imaged by fluorescent, laser-scanning confocal microscopy (Zeiss LSM510) or with spinning disk confocal microscopy (Perkin Elmer Ultraview RS). Time-lapse data was analyzed using Imaris (Bitplane).

Quantification of cell length and apical cell width

Slices for measurement were chosen based on the ability to outline the entire extent of a cell from the apical to basal surface of the neuroepithelium and by following the cell through a full Z-series. The length of three cells at the MHBC and four cells outside the MHBC were measured using Imaris (Bitplane) software, and the ratio between cell lengths at and outside the MHBC were calculated for each embryo and averaged. The width of two wedge shaped cells at the MHBC and three unconstricted cells outside the MHBC at 24 hpf in each embryo were measured using Imaris (Bitplane). The error bars in Fig. 2 indicate the standard deviation between the ratios found for each embryo.

Immunohistochemistry

Embryos were fixed in 4% paraformaldehyde and dehydrated in methanol. After rehydrating in PBT, embryos were permeabilized with 2.5 mg/ml proteinase K for 1 minute, and blocked in PBT, 0.1% Triton X, 1% BSA, and 1% NGS. Embryos were incubated overnight at room temperature in laminin antibody (laminin rabbit anti-mouse, Sigma L-9393, 1:150), washed, and incubated in secondary antibody, (goat anti-

rabbit IgG Alexa Flour 488, Invitrogen, 1:500) in combination with propidium iodide (PI) (Invitrogen, 1:1000). Embryos were flat mounted in glycerol, imaged using a Zeiss LSM510 laser-scanning confocal microscope, and images analyzed with LSM software (Zeiss) and Photoshop.

Actin staining

Embryos were fixed in 4% paraformaldehyde for 2 hrs at room temperature and washed in PBT. Embryos were incubated at 4 degrees C overnight in Alexa Fluor 488 phalloidin (Invitrogen A12379) 1:40 in PBT, washed overnight at 4 degrees C in PBT, mounted in glycerol, imaged using a Zeiss LSM510 laser-scanning confocal microscope and images analyzed with LSM software (Zeiss) and Photoshop.

RESULTS

Zebrafish MHBC morphogenesis occurs soon after neural tube closure

In the zebrafish, brain morphogenesis begins after neural tube closure at 17 hpf (Kimmel et al., 1995; Lowery and Sive, 2005). At this stage, a slight indentation, visible on the outside of the tube at the MHB anlage (Fig. 1A), corresponds to the basal side of the neuroepithelium. Beginning at 18 hpf, the opposing apical sides of the neuroepithelium separate along the midline and inflate to form the fore-, mid-, and hindbrain ventricles (Lowery and Sive, 2005). However, cells at the MHB remain closely apposed at the midline. At 21 hpf, after the midbrain and hindbrain ventricles have opened further, the indentation at the MHB outside the tube is more prominent, but still shallow (Fig. 1B). By 24 hpf, the MHB is bent acutely at the basal surface creating a sharp point on the outside of the tube (Fig. 1C). This was clearly visible in all wild type embryos by staining the outside of the neural tube with a laminin antibody (Fig. 1D). We have called this sharp point at the deepest point of this fold the midbrain-hindbrain boundary

constriction (MHBC). This constriction is highly conserved amongst the vertebrates (Rhinn and Brand, 2001).

A sharp MHBC forms in ventricle inflation mutants

In order to determine the mechanisms regulating MHBC morphogenesis, we asked whether brain ventricle inflation plays a role in this process. We hypothesized that pressure from the embryonic cerebrospinal fluid (eCSF) within the brain ventricles is required to form the MHBC, through a passive "pushing" mechanism (Lowery and Sive, 2005). Supporting this hypothesis, blood flow modifies heart chamber morphology and stimulates valve morphogenesis (Berdougo et al., 2003; Hove et al., 2003; Seidman and Seidman, 2001).

We analyzed MHBC morphogenesis in two zebrafish mutants lacking inflated brain ventricles, *snakehead* (*snk*), with a mutation in *atp1a1* encoding a Na^+K^+ ATPase (Lowery and Sive, 2005) and *nagie oko* (*nok*), a mutant allele of the MAGUK scaffolding protein, Mpp5 (Wei and Malicki, 2002). *snk* and *nok* embryos were imaged at 24 hpf to examine the overall outline of the neural tube and shape of the MHBC. The abnormal refractility in *snk* embryos prevented visualization of the MHBC by brightfield microscopy (Fig. 1E). However, laminin staining of all *snk* embryos analyzed revealed that the MHBC does define a sharp point, although the angle at the MHB is less acute than that of wild type embryos (Fig. 1F). In *nok* mutants laminin staining indicated that the MHBC also defined a sharp point in all embryos observed (Fig. 1G,H).

The acuteness of the MHBC in the tissue in both *snk* and *nok* is clearly reduced compared to wild type embryos. Thus, ventricle inflation may be required to push together the neuroepithelium to form an extremely acute angle, but it is not required to form a sharp point at the MHBC.

Laminin is required for MHBC formation

We also hypothesized that the basement membrane, which lies adjacent to the MHBC on the outside of the brain primordium, may play a role in its formation. Laminin is a major component of the basement membrane that interacts with integrins to mediate adhesion to the cytoskeleton of overlying cells (Miner and Yurchenco, 2004). A role for laminin has been demonstrated during mouse salivary gland branching, axon pathfinding in multiple organisms, and zebrafish notochord development (Bernfield et al., 1984; Garcia-Alonso et al., 1996; Karlstrom et al., 1996; Parsons et al., 2002; Paulus and Halloran, 2006). Laminin has not previously been implicated in brain morphogenesis in any system, although it has been shown to play a role in development of the eye, which is derived from neuroepithelium (Svoboda and O'Shea, 1987).

We tested the requirement for laminin by examining the MHBC in the *sleepy* mutant (*sly*^{m86}) that has a mutation in the *gamma1* laminin gene (*lamc1*) (Parsons et al., 2002) and in the *grumpy* mutant (*gup*^{hi1113b}), which has a viral insertion in the first intron of the laminin *beta1* gene (*lamb1*), (Amsterdam et al., 2004 and A. Amsterdam, personal communication). By brightfield imaging, *sly* mutants showed an initially normally shaped neural tube (Fig. 1I,J), but by 24 hpf, the MHBC remained a shallow indentation (Fig. 1K). Similar results were observed with *gup* mutants (data not shown). Consistent with brightfield imaging, at 24 hpf, a shallow MHBC was observed in *gup* mutant embryos stained with the laminin 1 antibody (Fig. 1L). This angle was consistently shallow in all embryos, observed either by brightfield imaging or by laminin 1 staining. We used the *gup*^{hi1113b} viral insertion mutants for laminin 1 antibody staining, because the laminin 1 antibody is not immunoreactive in the allele of *sly* used in this study (*sly*^{m86}), nor in the other *gup* allele previously described (*gup*^{m186}) (Parsons et al., 2002). Although the mechanism by which this antibody recognizes laminin 1 in *gup*^{hi1113} is not known, the viral insertion may result in a recognizable, but non-functional protein,

whereas point mutation alleles of *sly* ^{m86} and *gup* ^{m186} result in the introduction of a premature stop codon and likely severely truncated proteins (Parsons et al., 2002). These data showed that laminin function is essential for the sharp point normally seen at the MHBC and define a new role for laminin in brain morphogenesis.

Cells shorten and basally constrict at the MHBC

Bends or folds in epithelial sheets are driven by changes in cell length and formation of wedge-shaped cells, such as the cell shortening and apical constriction during neurulation in Xenopus, optic vesicle formation in mice, and ventral furrow invagination in *Drosophila* (Lee et al., 2007; Smith et al., 1994; Svoboda and O'Shea, 1987; Sweeton et al., 1991). We therefore hypothesized that wedge-shaped cells would be required to form the MHBC. However, based on the orientation of the MHBC, we hypothesized that such wedge-shaped cells would be basally, rather than apically, constricted.

In order to test this hypothesis, we analyzed cell shape at the MHBC in wild type embryos by expressing membrane-localized green fluorescent protein (memGFP) and imaging live embryos by laser-scanning confocal microscopy. At 17 hpf, cells in the midbrain, hindbrain, and MHB are uniform in length and are both spindle and columnar-shaped, with some rounded dividing cells visible (Fig. 2A,A′). In contrast, by 21 hpf, MHB cells are shorter in length (0.76 the apical-basal length) than those in either the midbrain or hindbrain (Fig. 2B,B′,J). Do these MHB cells shorten relative to surrounding cells, or do they fail to lengthen in concert with the rest of the neuroepithelium? By imaging wild type embryos, using spinning-disk confocal microscopy to generate a live time-lapse data series between 17 and 21 hpf, we showed that single cells at the MHB shorten relative to surrounding cells (Fig. 2D-I). While shortening appears to be graded along the MHB, the uneven nature of the

pseudostratified neuroepithelium makes quantification of subtle changes in cell length in regions flanking the future MHBC difficult to measure. In conclusion, a first step in MHBC formation is the shortening of cells at the MHB.

Subsequent to cell shortening, we found that, by 24 hpf, a group of cells at the MHBC had become wedge-shaped, with constriction at their basal surface (Fig. 2C,C′). Within a single plane (Z-section) three to four wedge-shaped cells meet at a sharp point to form the MHBC in wild type (Fig. 2C′,L). Basally constricted cells were defined as those with a clear wedge-shaped morphology such that their basal surface was constricted to a point. We found that the apical width of the wedge-shaped cells at the MHBC had expanded to 1.6 times that of cells outside the MHBC (outlined cells in Fig. 2C′, Fig. 2K). Interestingly, although the midline in the MHB does not separate, we found that the basally constricted MHBC cells were not apposed at the midline, but instead were oriented with their apical surfaces exposed to the midbrain ventricle lumen (Fig. 2C,C′). These data demonstrate that cells at the MHBC undergo basal constriction and apical expansion.

Basal constriction at the MHBC occurs without ventricle inflation, but requires laminin

Since the MHBC forms a sharp point in the ventricle inflation mutants, *snk* and *nok*, we asked whether basally constricted cells formed in these mutants. Confocal imaging indicated that cells at the MHBC in both mutants demonstrated basal constriction (Fig. 3A-C′). However, unlike wild type, the basally constricted cells in these mutants apparently did not show apical expansion, relative to adjacent cells in the same embryo (Fig. 3H). This may be because apical expansion requires that cells have an unconstrained apical surface, which occurs when wild type MHBC cells abut the midbrain lumen. Where the ventricles do not inflate and the midline of the brain

primordium does not separate, the mutant cells may be constrained in their ability to expand apically. Therefore, the reduced bend angle formed at the MHBC in *nok* and *snk* may be due to failure of the cells at the MHBC to expand apically, in response to ventricle inflation. These data show that the basal constriction in the MHBC can occur independent of brain ventricle inflation, and moreover, that basal constriction is independent of apical expansion.

In order to determine what aspect of MHBC formation is disrupted in laminin mutants, we analyzed *sly* embryos for changes in cell length and shape (Fig. 3D-F′). At 17 hpf, the cells at the MHB of *sly* mutants appeared similar to wild type (compare Fig. 2A′ with Fig. 3D′). By 21 hpf, cells at the MHBC in *sly* mutants were 0.76 the length of cells on either side, similar to wild type (Fig. 3E,E′,G). However, by 24 hpf, cells at the MHBC in *sly* mutants had not basally constricted (Fig. 3F′). Neither was apical expansion observed in the MHBC of these mutants (Fig. 3H). Based on somite number, and marker gene expression (Fig. 4), development of laminin mutant embryos was not retarded relative to wild type. These data show that laminin is necessary for basal constriction, defining a new role for this protein in morphogenesis. The data also show that basal constriction is required for formation of the sharp point at the MHBC and that cell shortening is insufficient for this process. Further, the absence of apical expansion in the laminin mutants indicates that this process may be dependent on basal constriction.

Together with results from the ventricle inflation mutants, the data show that apical expansion occurs only in the presence of, but is not required for, basal constriction, and suggest that basal constriction, and not apical expansion, is the active process driving MHBC morphogenesis.

Patterning gene expression and levels of proliferation and apoptosis are normal in laminin mutants at the MHB

MHB morphogenesis is dependent on the expression of early patterning genes in the Wnt and Fgf signaling pathways (Brand et al., 1996; Hidalgo-Sanchez et al., 2005). To determine if the MHB defects in *sly* mutants were caused by a loss of tissue specification, we assayed for expression of patterning markers in these mutants by *in situ* hybridization. *pax2a* and *krox20* were both expressed similarly in wild type and *sly* mutant embryos at 17, 20, and 24 hpf (Fig. 4A – F). *engrailed3* (*eng3*) expression is somewhat expanded at the MHB in *sly* mutants in comparison to wild type embryos (Fig. 4I – J). This is likely a result of tissue extension of the MHB region in these mutants caused by a failure of the tissue to fold at the MHBC.

We also tested whether proliferation or apoptosis was abnormal at the MHB in the *sly* mutants. As determined by staining of phospho-histone-3 (PH3), proliferation is not statistically different in wild type as compared to *sly* mutants (Fig.5 A – C). Levels of apoptosis, as assayed by TUNEL staining, were also unchanged in *sly* mutants in comparison to wild type embryos (Fig. 5D – F).

Other process involved in MHBC morphogenesis

What other processes might be involved in MHBC formation? One possibility is that differential cell proliferation or apoptosis contributes to the MHBC. We have investigated cell death and proliferation in the brain during MHBC development, and find no significant differences between wild type and *sly* or *gup* embryos in the MHB region (Fig. 6).

The role of the actin cytoskeleton during apical constriction is well established (Haigo et al., 2003; Pilot and Lecuit, 2005). Therefore, we hypothesized that actin may

also localize basally in cells that are undergoing basal constriction at the MHBC. We addressed this by analyzing fixed wild type and *sly* embryos, at 24hpf, for actin localization using phalloidin staining. In wild type embryos, actin localized basally and apparently, at highest intensity in the basally constricted cells at the MHBC (Fig. 6A,A'). In *sly* embryos, where cells are not constricted basally, actin lined the basal side of the neuroepithelium, but did not concentrate in any cells in this region (Fig. 6B,B'). Although these data suggest differences in actin localization in the MHBC region in wild type versus *sly* embryos, further experiments, in live embryos, are required to more accurately investigate actin dynamics and localization at the MHBC.

DISCUSSION

Model for MHBC morphogenesis

The model presented in Fig. 7 summarizes our data indicating that two steps are involved in formation of the MHBC in the embryonic brain. In the first step, cells of the MHB shorten relative to the surrounding cells. This is followed by laminin-dependent basal constriction and coordinate apical expansion of a small group of cells that contribute to the sharp bend of the MHBC. Basal constriction is an active process, and not a passive consequence of brain ventricle inflation or other aspects of brain morphogenesis, as it occurs in mutants lacking ventricle inflation. An active role for the basal side of the neuroepithelium is supported by failure of basal constriction in laminin mutants. Additionally, since apical expansion does not occur when the basement membrane is disrupted, information from the apical side of the neuroepithelium does not drive basal constriction, but rather basal constriction and apical expansion may occur coordinately.

The mechanisms underlying basal constriction are not known; however, our data show that laminin provides a crucial function. Laminin is a secreted protein and can act on both the cells from which it is secreted and those surrounding (Parsons et al., 2002). Since laminin lines the entire neural tube, it is unlikely to play an instructive role in MHBC formation. Rather, laminin is likely to modulate basal constriction through its interaction with integrins in the basal cell membrane and subsequent regulation of cytoskeletal function. Although a difference in actin localization at the MHBC region may be present between wild type and *sly* mutants, we do not know whether actin is directly involved in driving basal constriction in these cells.

One clear requirement for MHBC formation is its precise positioning in the brain. While Fgf and Wnt signaling pathways are necessary to form the MHBC (Brand et al., 1996; Sato et al., 2004), it is not clear whether these genes are solely responsible for specifying MHB fate, or whether they also play a more direct role in MHBC morphogenesis. Laminin acts downstream of MHB specification, since genes indicative of specified MHB, including *engrailed 3* and *pax2a* are normally expressed in laminin mutants. Separating the effects of region-specific signaling pathways in positioning the MHB from their possible role in later MHBC morphogenesis, as well as determining the cell biology underlying MHBC morphogenesis will be the focus of future analyses.

FIGURE LEGENDS

Fig. 1. Zebrafish MHB morphogenesis occurs between 17 and 24 hpf, and requires laminin but not ventricle inflation.

(A-C) Brightfield and fluorescent images and schematics of wild type (WT) MHBC formation. (D) WT embryo at 24 hpf was stained with anti-laminin 1 antibody (green); nuclei were stained with propidium iodide (red). Laminin lines the basal surface of the neuroepithelium. (E) Brightfield image of *snk*, a ventricle inflation mutant, at 24 hpf. (F) *snk* embryo at 24 hpf stained as in D. (G) Brightfield image and schematic of *nok*, a ventricle inflation mutant, at 24 hpf. (H) *nok* embryo at 24 hpf stained as in as D. (I-K) Brightfield and fluorescent images and schematics of MHBC formation in the laminin mutant, *sly*. (L) *gup* embryo at 24 hpf stained as in D. Arrowheads indicate MHB at 21 hpf and MHBC at 24 hpf. F, forebrain; M, midbrain; H, hindbrain. Scale bars: A-C, E, G, I-K = 100 μm, D, F, H, L = 6 μm.

Fig. 2. MHBC formation requires cell shortening and basal constriction.

(A-C′) Live laser-scanning confocal imaging of wild type embryos injected with memGFP mRNA at the one cell stage and imaged at 17, 21, and 24 hpf. Boxed regions from A-C are enlarged for panels A′-C′. Individual cells in the MHB are outlined, and a dividing cell is indicated by an arrow in B. Asterisks in A-C mark cells outlined in A′-C′. Cells with two asterisks are outside the MHB. (A′) At 17 hpf, cells at the MHB are similar in length to the cells in the surrounding tissue. (B′) At 21 hpf, cells at the MHB are shorter than the cells in the surrounding tissue. (C′) At 24 hpf, cells at the MHBC are constricted basally and expanded apically. In A- C′, some green fluorescence is visible within outlined cells since the plane of section contains the surface of the cell membrane. (D-I) Time-course of MHB morphogenesis beginning at 17 hpf. A single cell is outlined and followed through the time course. Cells at the MHB shorten relative to those surrounding

(n = 6 embryos). (J) Relative cell lengths at and outside the MHB in 21 hpf wild type embryos. Cells at the MHB were 0.76 times the length of those outside the MHB (+/- 0.06 s.d.) (n = 8 embryos, 3 cells at the MHB and 4 cells outside the MHB were measured per embryo). (K) Relative apical width of unwedged cells (those outside the MHBC) and basally constricted cells (at the MHBC) in wild type embryos at 24 hpf. Cells at the MHBC had 1.6 times the apical width of those outside the MHBC (+/- 0.29 s.d.) (n = 6 embryos, 2 cells at the MHBC and 3 cells outside the MHBC were measured per embryo). (L) Numbers of basally constricted cells at the MHBC in wild type embryos at 24 hpf (n = 9 embryos). Arrowheads indicate the MHBC. M, midbrain. Scale bars: A-C = 20 μm, A′-C′ = 9 μm, D-I = 30 μm.

Fig. 3. Basal constriction at the MHBC is laminin-dependent and not dependent on ventricle inflation.

(A-C′) Live laser-confocal imaging of wild type, *snk* and *nok* embryos at 24 hpf after injection with memGFP. Boxed regions in A-C are enlarged in panels A′-C′. Cells at the MHBC in (A-A′) wild type, (B-B′) *snk* and (C-C′) *nok* undergo basal constriction (see cell outlines). (D-F′) Imaging of *sly* mutants injected with memGFP mRNA at the one cell stage and imaged at 17, 21, and 24 hpf. Boxed regions in D-F are enlarged for panels D′-F′. (D′) At 17 hpf, MHB and surrounding cells are similar in length (see outlined cells). (E′) At 21 hpf, cells at the MHB are shorter than those surrounding. One cell at and one cell outside the MHB are outlined in yellow. Some cells are visible outside the neural tube. (F′) At 24 hpf, cells at the MHBC fail to basally constrict. For panels A-C and D-F asterisks indicate the cell that is outlined in the image below. Cells with two asterisks are outside MHB. Arrowheads indicate the MHBC. Dotted lines delineate the outside of the neural tube. Some green fluorescence is visible within outlined cells since the plane of section contains the surface of the cell membrane. Anterior is to the left in all images.

Scale bars: A-C = 22 mM, A′-C′ = 12 mM, D-F = 18 mM, D′-F′ = 9 mM. (**G**) Length of cells at the MHB relative to those outside the MHB in WT and *sly* mutants. At 21 hpf, cells at the MHB (at MHB) in *sly* mutants are 0.76 (+/- 0.094 s.d.) the length of those outside the MHB (outside MHB), as in WT embryos (WT data is the same as from Figure 2) (n = 6 embryos, 2 cells at MHB, 3 cells outside MHB were measured per embryo). (H) Graph compares the apical width of cells outside MHBC to cells at MHBC in WT, *sly*, *snk*, and *nok* embryos at 24 hpf. Basally constricted cells at the MHBC do not apparently show corresponding apical expansion *snk* and *nok* (n = 3 embryos each mutant, 2 cells at MHBC, 3 cells outside MHBC were measured per embryo). Cells at the MHBC in *sly* mutants that have shortened, but are not constricted basally, are also not expanded apically (n = 6 embryos, 3 cells at MHBC, 4 cells outside MHBC were measured per embryo).

Fig. 4. Patterning gene expression is normal in sly mutants during MHBC formation.

(A-H) Wild type and *sly* mutants were analyzed by in situ hybridization for *pax2a* and *krox20* at 17, 20, and 24 hpf. Gene expression at 17 hpf was normal in *sly* compared to wild type shown in panels A and B. At 20 hpf gene expression remained normal, shown dorsally C, D and laterally E, F. At 24 hpf *pax2a* and *krox20* are still expressed normally in *sly* mutants compared to wild type panels G, H. (I-J) Wild type and *sly* mutants were analyzed for expression of *engrailed 3* (*eng3*) and *krox20* at 24 hpf. In *sly* mutants, the *eng3* expression domain appeared to be extended along the neural tube around the MHB relative to wild type. This is because the MHB tissue in the mutant is also elongated due to the lack of a sharp MHBC and MHB fold, indicating that gene expression in the MHB at the time of MHBC formation is the same in wild type embryos and in *sly* mutants. The bracket marks the MHB region in each embryo. Anterior is to the left in all images.

Fig. 5. Levels of proliferation and cell death in laminin mutants are normal.

(A-C) Wild type and laminin mutant embryos were fixed and stained with PH3 antibody as a marker for cell proliferation at 22 hpf and the cells in the MHB were counted and compared between wild type and laminin mutants. Representative images of PH3 stained wild type and *sly* embryos are seen in panels A and B respectively. Quantification of PH3 positive cells indicated that there was no difference in the number of positive cells in the MHB of laminin mutants compared to wild type controls, panel C. (n = 3 control, n = 5 laminin mutants; 3 *sly*, 2 *gup*) (D-E) Wild type and laminin mutants were assayed by TUNEL to determine amount of apoptosis at 22 hpf. Cells in the MHB were counted and compared between wild type and laminin mutants. Representative images of TUNEL stained wild type and *sly* mutants are seen in panels D and E respectively. Differences in refractility between D and E are due to microscope settings. Quantification of TUNEL positive cells in the MHB of laminin mutants compared to wild type controls indicated that there was no difference in the number of positive cells, panel F. (n = 7 control, n = 5 laminin mutants, 3 *sly*, 2 *gup*). Anterior is to the left in all images. M, midbrain; H, hindbrain.

Fig. 6. Actin is localized basally at the MHBC in wild type embryos.

(A-D) Phalloidin stained wild type (A,C) and *sly* (B,D) embryos that were fixed at 24 hpf. Stained embryos were flat mounted in glycerol and imaged by confocal microscopy at 25X (A,B) and 100X (C,D). Arrows indicate points of basal actin accumulation in wild type embryos. Anterior is to the left in all images. Arrowhead indicates the MHBC in wild type and a bracket indicates the MHBC region in *sly* mutants. M, midbrain; H, hindbrain.

Fig. 7. Schematic of the two steps required in MHBC formation.

In step one, cells shorten at the MHB. In step two, 3 to 4 cells (in a plane of section) basally constrict, and expand apically, to form a sharp point at the MHBC. This second step is laminin dependent.

FIGURE 1

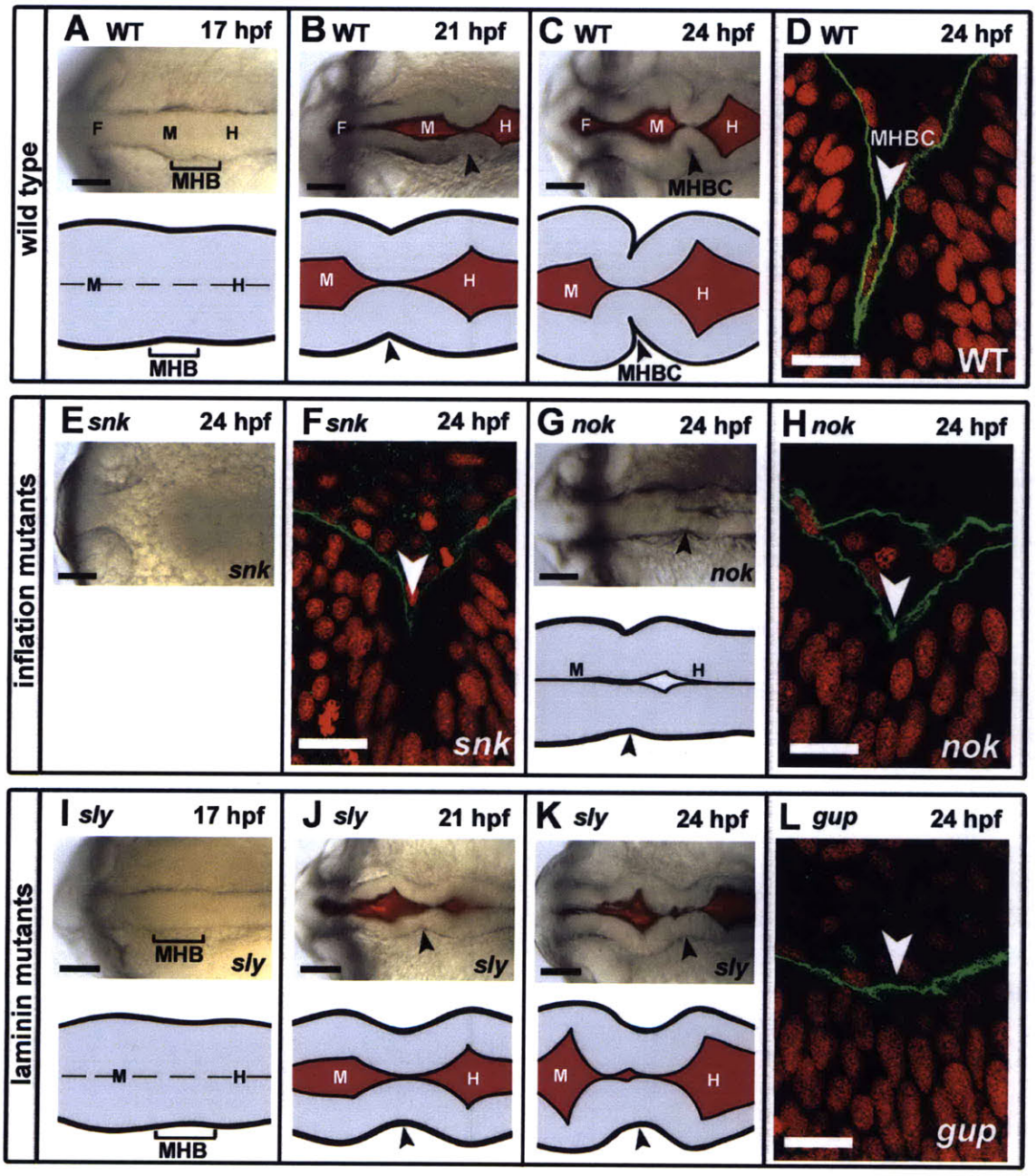
wild type
A WT 17 hpf
F
M
H
MHB
B WT 21 hpf
C WT 24 hpf
MHBC
D WT 24 hpf
WT
inflation mutants
E snk 24 hpf
snk
F snk 24 hpf
G nok 24 hpf
nok
H nok 24 hpf
laminin mutants
I sly 17 hpf
sly
J sly 21 hpf
K sly 24 hpf
L gup 24 hpf
gup

FIGURE 2

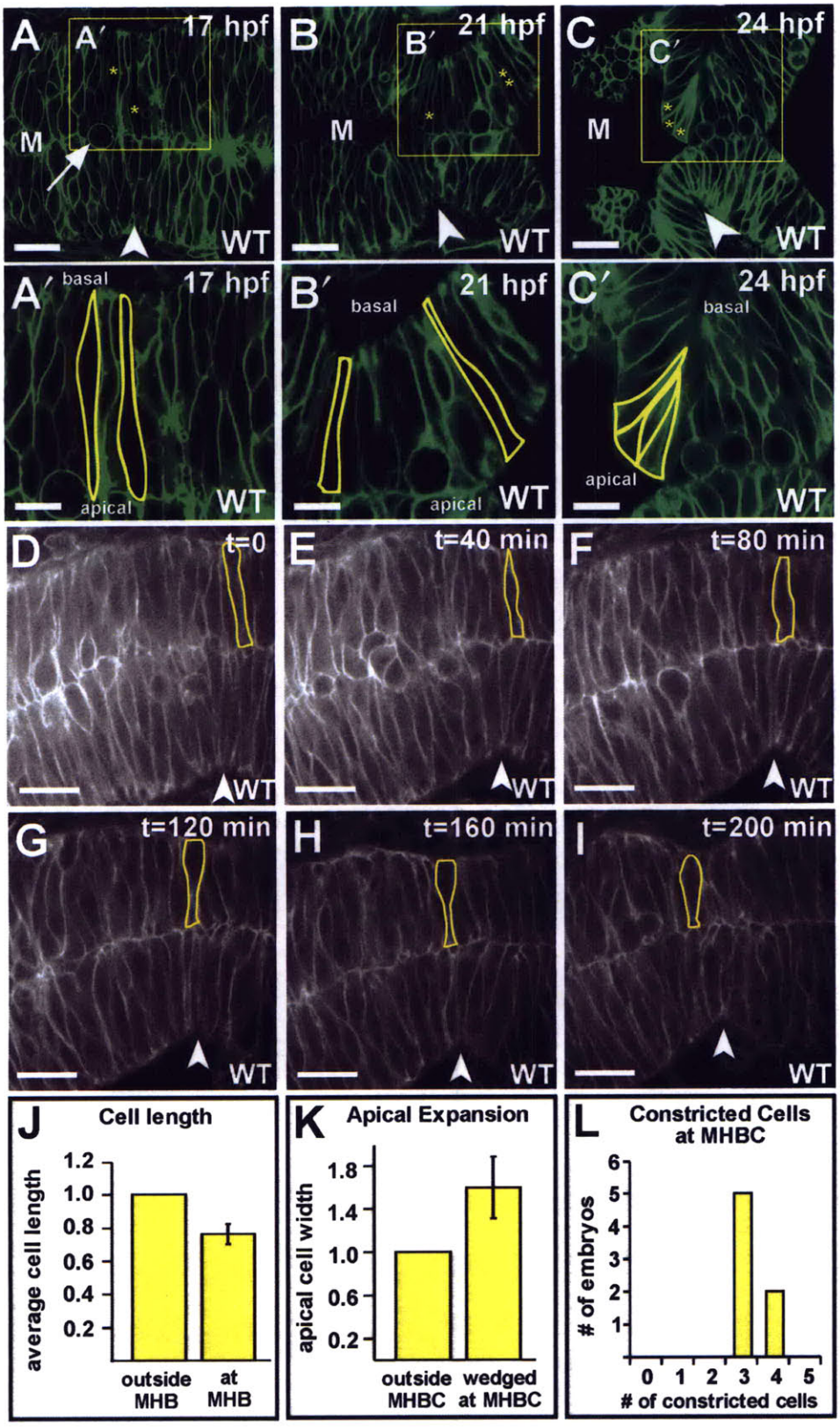
A
A′
17 hpf
M
WT
B
B′
21 hpf
M
WT
C
C′
24 hpf
M
WT
A′ basal
17 hpf
apical
WT
B′
basal
21 hpf
apical
WT
C′
24 hpf
basal
apical
WT
D
t=0
WT
E
t=40 min
WT
F
t=80 min
WT
G
t=120 min
WT
H
t=160 min
WT
I
t=200 min
WT
J
Cell length
average cell length
1.2
1.0
0.8
0.6
0.4
0.2
outside MHB
at MHB
K
Apical Expansion
apical cell width
1.8
1.4
1.0
0.6
0.2
outside MHBC
wedged at MHBC
L
Constricted Cells at MHBC
# of embryos
6
5
4
3
2
1
0 1 2 3 4 5
# of constricted cells

FIGURE 3

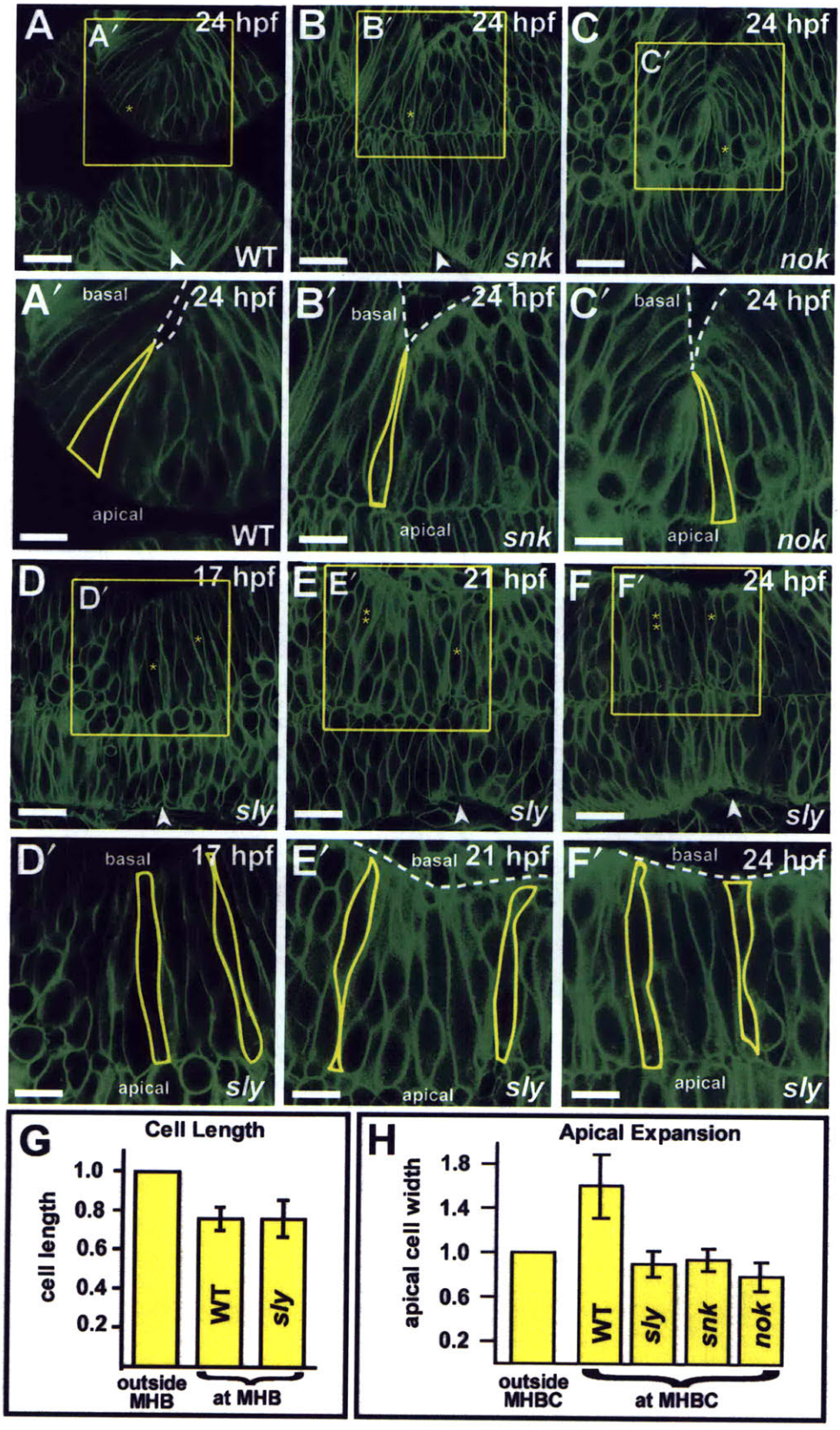
A
A′
24 hpf
WT
B
B′
24 hpf
snk
C
C′
24 hpf
nok
A′
basal
24 hpf
apical
WT
B′
basal
24 hpf
apical
snk
C′
basal
24 hpf
apical
nok
D
D′
17 hpf
sly
E
E′
21 hpf
sly
F
F′
24 hpf
sly
D′
basal
17 hpf
apical
sly
E′
basal
21 hpf
apical
sly
F′
basal
24 hpf
apical
sly
G
Cell Length
cell length
1.0
0.8
0.6
0.4
0.2
WT
sly
outside MHB
at MHB
H
Apical Expansion
apical cell width
1.8
1.4
1.0
0.6
0.2
WT
sly
snk
nok
outside MHBC
at MHBC

FIGURE 4

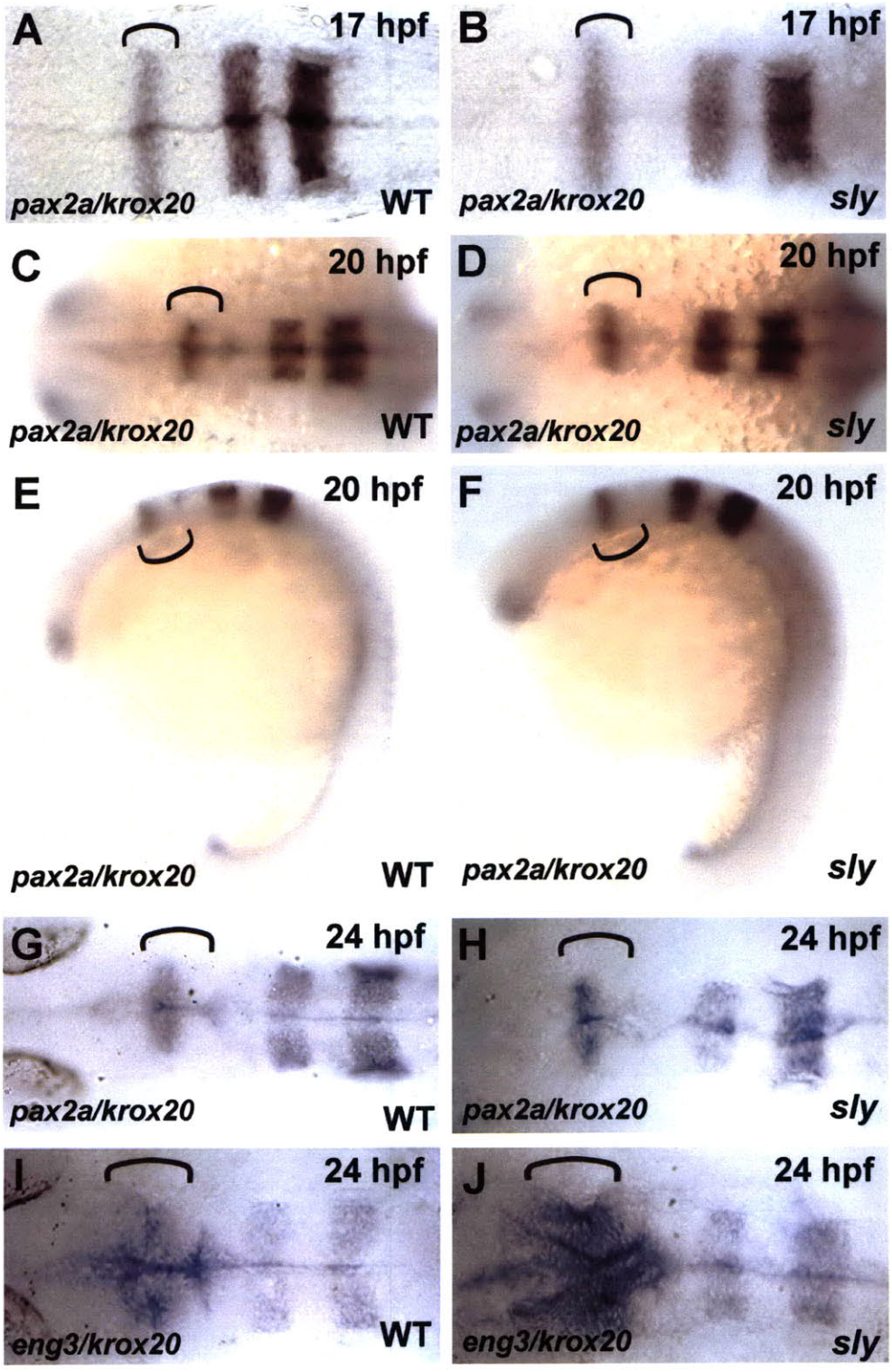
A
17 hpf
pax2a/krox20
WT
B
17 hpf
pax2a/krox20
sly
C
20 hpf
pax2a/krox20
WT
D
20 hpf
pax2a/krox20
sly
E
20 hpf
pax2a/krox20
WT
F
20 hpf
pax2a/krox20
sly
G
24 hpf
pax2a/krox20
WT
H
24 hpf
pax2a/krox20
sly
I
24 hpf
eng3/krox20
WT
J
24 hpf
eng3/krox20
sly

FIGURE 5

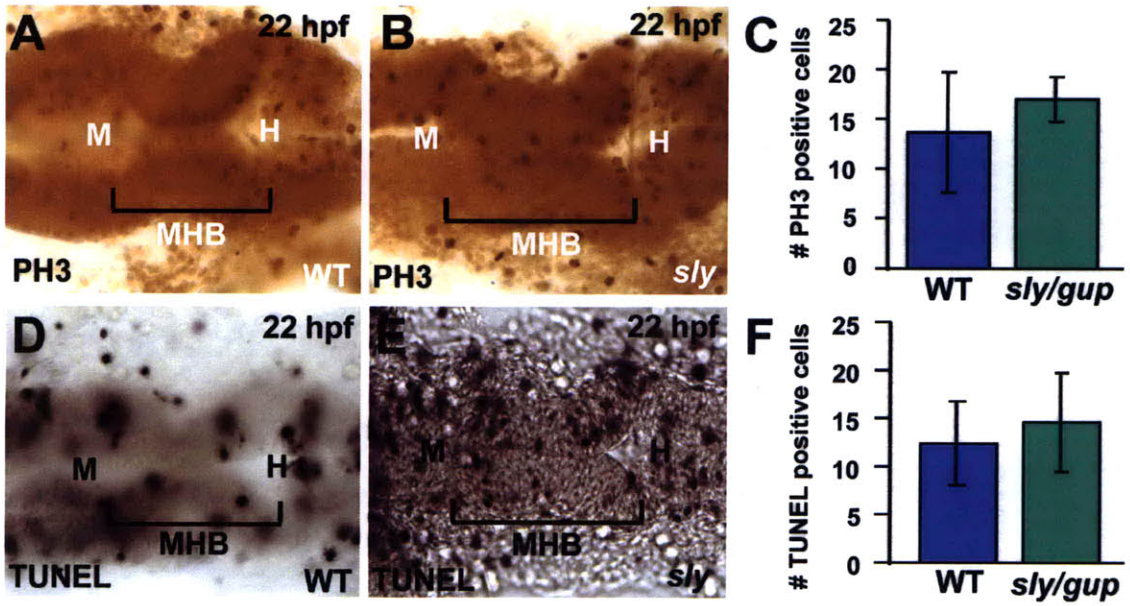
A
22 hpf
M
H
MHB
PH3
WT
B
22 hpf
M
H
MHB
PH3
sly
C
PH3 positive cells
25
20
15
10
5
0
WT
sly/gup
D
22 hpf
M
H
MHB
TUNEL
WT
E
22 hpf
M
H
MHB
TUNEL
sly
F
TUNEL positive cells
25
20
15
10
5
0
WT
sly/gup

FIGURE 6

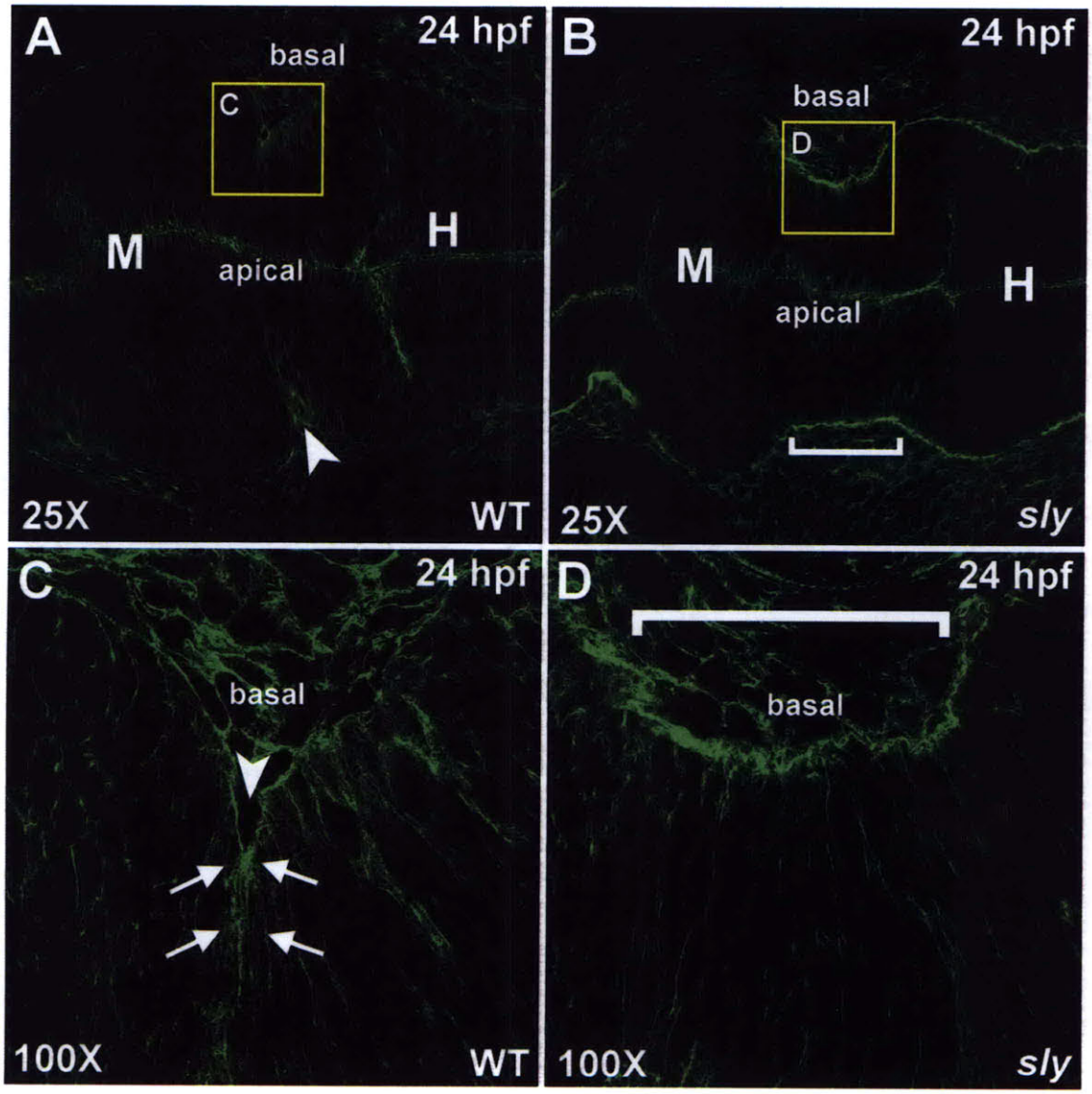
A
24 hpf
basal
C
M
H
apical
25X
WT
B
24 hpf
basal
D
M
H
apical
25X
sly
C
24 hpf
basal
100X
WT
D
24 hpf
basal
100X
sly

FIGURE 7

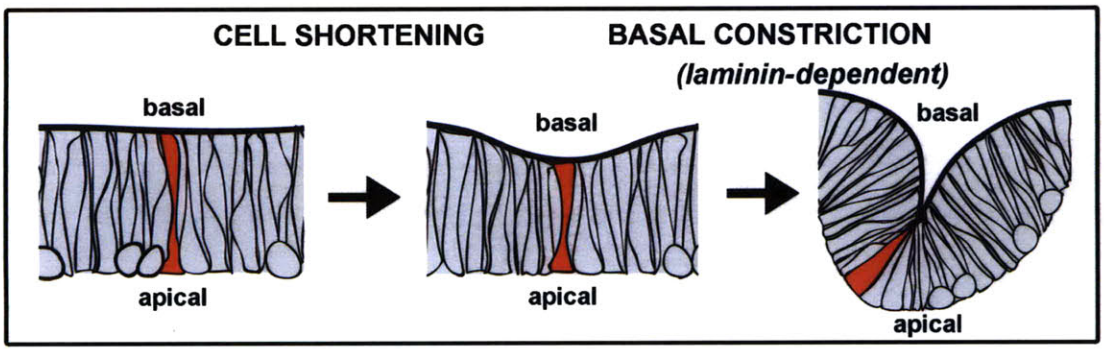
CELL SHORTENING
BASAL CONSTRICTION
(laminin-dependent)
basal
apical
basal
apical
basal
apical

REFERENCES

Amsterdam, A., Nissen, R. M., Sun, Z., Swindell, E. C., Farrington, S. and Hopkins, N. (2004). Identification of 315 genes essential for early zebrafish development. *Proc Natl Acad Sci U S A* **101**, 12792-7.

Bard, J. B. and Ross, A. S. (1982a). The morphogenesis of the ciliary body of the avian eye. I. Lateral cell detachment facilitates epithelial folding. *Dev Biol* **92**, 73-86.

Bard, J. B. and Ross, A. S. (1982b). The morphogenesis of the ciliary body of the avian eye. II. Differential enlargement causes an epithelium to form radial folds. *Dev Biol* **92**, 87-96.

Berdougo, E., Coleman, H., Lee, D. H., Stainier, D. Y. and Yelon, D. (2003). Mutation of weak atrium/atrial myosin heavy chain disrupts atrial function and influences ventricular morphogenesis in zebrafish. *Development* **130**, 6121-9.

Bernfield, M., Banerjee, S. D., Koda, J. E. and Rapraeger, A. C. (1984). Remodelling of the basement membrane: morphogenesis and maturation. *Ciba Found Symp* **108**, 179-96.

Brand, M., Heisenberg, C. P., Jiang, Y. J., Beuchle, D., Lun, K., Furutani-Seiki, M., Granato, M., Haffter, P., Hammerschmidt, M., Kane, D. A. et al. (1996). Mutations in zebrafish genes affecting the formation of the boundary between midbrain and hindbrain. *Development* **123**, 179-90.

Desmond, M. E. and Levitan, M. L. (2002). Brain expansion in the chick embryo initiated by experimentally produced occlusion of the spinal neurocoel. *Anat Rec* **268**, 147-59.

Fristrom, D. (1988). The cellular basis of epithelial morphogenesis. A review. *Tissue Cell* **20**, 645-90.

Garcia-Alonso, L., Fetter, R. D. and Goodman, C. S. (1996). Genetic analysis of Laminin A in Drosophila: extracellular matrix containing laminin A is required for ocellar axon pathfinding. *Development* **122**, 2611-21.

Haigo, S. L., Hildebrand, J. D., Harland, R. M. and Wallingford, J. B. (2003). Shroom induces apical constriction and is required for hingepoint formation during neural tube closure. *Curr Biol* **13**, 2125-37.

Hidalgo-Sanchez, M., Millet, S., Bloch-Gallego, E. and Alvarado-Mallart, R. M. (2005). Specification of the meso-isthmo-cerebellar region: the Otx2/Gbx2 boundary. *Brain Res Brain Res Rev* **49**, 134-49.

Hove, J. R., Koster, R. W., Forouhar, A. S., Acevedo-Bolton, G., Fraser, S. E. and Gharib, M. (2003). Intracardiac fluid forces are an essential epigenetic factor for embryonic cardiogenesis. *Nature* **421**, 172-7.

Jiang, Y. J., Brand, M., Heisenberg, C. P., Beuchle, D., Furutani-Seiki, M., Kelsh, R. N., Warga, R. M., Granato, M., Haffter, P., Hammerschmidt, M. et al. (1996). Mutations affecting neurogenesis and brain morphology in the zebrafish, Danio rerio. *Development* **123**, 205-16.

Joyner, A. L. (1996). Engrailed, Wnt and Pax genes regulate midbrain--hindbrain development. *Trends Genet* **12**, 15-20.

Karlstrom, R. O., Trowe, T., Klostermann, S., Baier, H., Brand, M., Crawford, A. D., Grunewald, B., Haffter, P., Hoffmann, H., Meyer, S. U. et al. (1996). Zebrafish mutations affecting retinotectal axon pathfinding. *Development* **123**, 427-38.

Kimmel, C. B., Ballard, W. W., Kimmel, S. R., Ullmann, B. and Schilling, T. F. (1995). Stages of embryonic development of the zebrafish. *Dev Dyn* **203**, 253-310.

Lee, C., Scherr, H. M. and Wallingford, J. B. (2007). Shroom family proteins regulate gamma-tubulin distribution and microtubule architecture during epithelial cell shape change. *Development* **134**, 1431-41.

Louvi, A., Alexandre, P., Metin, C., Wurst, W. and Wassef, M. (2003). The isthmic neuroepithelium is essential for cerebellar midline fusion. *Development* **130**, 5319-30.

Lowery, L. A. and Sive, H. (2005). Initial formation of zebrafish brain ventricles occurs independently of circulation and requires the nagie oko and snakehead/atp1a1a.1 gene products. *Development* **132**, 2057-67.

Malicki, J., Neuhauss, S. C., Schier, A. F., Solnica-Krezel, L., Stemple, D. L., Stainier, D. Y., Abdelilah, S., Zwartkruis, F., Rangini, Z. and Driever, W. (1996). Mutations affecting development of the zebrafish retina. *Development* **123**, 263-73.

Miner, J. H., Li, C., Mudd, J. L., Go, G. and Sutherland, A. E. (2004). Compositional and structural requirements for laminin and basement membranes during mouse embryo implantation and gastrulation. *Development* **131**, 2247-56.

Miner, J. H. and Yurchenco, P. D. (2004). Laminin functions in tissue morphogenesis. *Annu Rev Cell Dev Biol* **20**, 255-84.

Parsons, M. J., Pollard, S. M., Saude, L., Feldman, B., Coutinho, P., Hirst, E. M. and Stemple, D. L. (2002). Zebrafish mutants identify an essential role for laminins in notochord formation. *Development* **129**, 3137-46.

Patel, V. N., Rebustini, I. T. and Hoffman, M. P. (2006). Salivary gland branching morphogenesis. *Differentiation* **74**, 349-64.

Paulus, J. D. and Halloran, M. C. (2006). Zebrafish bashful/laminin-alpha 1 mutants exhibit multiple axon guidance defects. *Dev Dyn* **235**, 213-24.

Pilot, F. and Lecuit, T. (2005). Compartmentalized morphogenesis in epithelia: from cell to tissue shape. *Dev Dyn* **232**, 685-94.

Pollard, S. M., Parsons, M. J., Kamei, M., Kettleborough, R. N., Thomas, K. A., Pham, V. N., Bae, M. K., Scott, A., Weinstein, B. M. and Stemple, D. L. (2006). Essential and overlapping roles for laminin alpha chains in notochord and blood vessel formation. *Dev Biol* **289**, 64-76.

Puelles, L. and Martinez-de-la-Torre, M. (1987). Autoradiographic and Golgi study on the early development of n. isthmi principalis and adjacent grisea in the chick embryo: a tridimensional viewpoint. *Anat Embryol (Berl)* **176**, 19-34.

Rhinn, M. and Brand, M. (2001). The midbrain--hindbrain boundary organizer. *Curr Opin Neurobiol* **11**, 34-42.

Sato, T., Joyner, A. L. and Nakamura, H. (2004). How does Fgf signaling from the isthmic organizer induce midbrain and cerebellum development? *Dev Growth Differ* **46**, 487-94.

Schier, A. F., Neuhauss, S. C., Harvey, M., Malicki, J., Solnica-Krezel, L., Stainier, D. Y., Zwartkruis, F., Abdelilah, S., Stemple, D. L., Rangini, Z. et al. (1996). Mutations affecting the development of the embryonic zebrafish brain. *Development* **123**, 165-78.

Schock, F. and Perrimon, N. (2002). Molecular mechanisms of epithelial morphogenesis. *Annu Rev Cell Dev Biol* **18**, 463-93.

Scott, A. and Stemple, D. L. (2005). Zebrafish notochordal basement membrane: signaling and structure. *Curr Top Dev Biol* **65**, 229-53.

Seidman, J. G. and Seidman, C. (2001). The genetic basis for cardiomyopathy: from mutation identification to mechanistic paradigms. *Cell* **104**, 557-67.

Smith, J. L., Schoenwolf, G. C. and Quan, J. (1994). Quantitative analyses of neuroepithelial cell shapes during bending of the mouse neural plate. *J Comp Neurol* **342**, 144-51.

Stemple, D. L. (2002). Pioneering work in vertebrate neural development. *Dev Cell* **2**, 687-8.

Svoboda, K. K. and O'Shea, K. S. (1987). An analysis of cell shape and the neuroepithelial basal lamina during optic vesicle formation in the mouse embryo. *Development* **100**, 185-200.

Sweeton, D., Parks, S., Costa, M. and Wieschaus, E. (1991). Gastrulation in Drosophila: the formation of the ventral furrow and posterior midgut invaginations. *Development* **112**, 775-89.

Wei, X. and Malicki, J. (2002). nagie oko, encoding a MAGUK-family protein, is essential for cellular patterning of the retina. *Nat Genet* **31**, 150-7.

Westerfield, M. (1995). The Zebrafish Book: A guide for the laboratory use of zebrafish. University of Oregon Press.

Zagris, N., Christopoulos, M. and Giakoumaki, A. (2004). Developmentally regulated expression and functional role of alpha 7 integrin in the chick embryo. *Dev Growth Differ* **46**, 299-307.

3

Basal constriction at the midbrain-hindbrain boundary constriction is regulated by Wnt5, FAK and Gsk3β

CONTRIBUTIONS

This work was completed with the help of Jennifer Gutzman who drew the foundation for the models in figure 1, performed the *in situ* hybridization of *wnt5*, and provided the brightfield image of the *pax2a* mutant. I performed the remainder of the experiments, analysis, and drafted the document.

ABSTRACT

Basal constriction is a recently described cell shape change that occurs during epithelial morphogenesis during development of the midbrain-hindbrain boundary constriction (MHBC) (Gutzman et al., 2008). This process involves constriction of cells at their basal surface and is accompanied by expansion at the apical surface. Using 3D reconstruction, we show that MHBC cells are wedge-shaped, and that basal constriction occurs prior to apical expansion. MHBC formation involves basal constriction in a narrow band of epithelium, suggesting that it is regulated by locally active signals. *wnt5*, one candidate signal, is expressed at the MHBC immediately prior to and during basal constriction. We have confirmed this expression pattern at cellular resolution, and loss-of-function analysis shows that Wnt5 is required for basal constriction. Another candidate signaling regulator is focal adhesion kinase (FAK), which is known to be active on the basal surface of epithelia. Consistent with a role in basal constriction, FAK is specifically autophosphorylated in a region encompassing the MHBC as determined by immunostaining. Loss-of-function analysis shows that FAK is required for basal constriction, and transplant analysis confirms that this requirement is local to the MHBC. FAK activation is strongly reduced in Wnt5 loss-of-function embryos, indicating that Wnt5 function is required to activate FAK within the MHBC region. Gsk3β is a constitutively active kinase previously shown to be downregulated by both Wnt5 and FAK. We show that overexpression of dominant-negative Gsk3β rescues basal constriction in both Wnt5 and FAK loss-of-function embryos, suggesting that Wnt5 and FAK inhibit Gsk3β to regulate basal constriction. Together, these data suggest that basal constriction occurs at the MHBC due to local Wnt5 function, which activates FAK, in turn leading to downregulation of Gsk3β. This study is the first to uncover the signals regulating basal constriction.

INTRODUCTION

Epithelial morphogenesis shapes the vertebrate brain during development. The bending and folding of the neuroepithelium is driven by cell shape changes within the tissue. For example, apical constriction is required for bending of the neural plate during neurulation (Haigo et al., 2003) and changes in cell shape both within and between the rhombomeres, or subdivisions within the tissue, are required for shaping of the hindbrain (Gutzman and Sive, 2010). A poorly understood cell shape change, basal constriction, is required to bend the neural tube at the basal surface to form the midbrain-hindbrain boundary constriction, or MHBC (Gutzman et al., 2008).

The MHBC is the first major bend to form during vertebrate brain development and later becomes the tectum in the posterior midbrain and the cerebellum in the anterior hindbrain (Louvi et al., 2003). This region is an important organizing center in the developing embryo and is patterned by Fgf and β-catenin-dependent Wnt signaling early in neurulation (Brand et al., 1996; Joyner, 1996; Puelles and Martinez-de-la-Torre, 1987; Sato et al., 2004). Mutant embryos lacking signaling through these pathways fail to properly specify the tissue at the MHBC and, thus, fail to form an MHB (Buckles et al., 2004; Lun and Brand, 1998; Reifers et al., 1998). However, the role of these signaling pathways in the later steps of MHBC morphogenesis has not been addressed.

Basal constriction at the MHBC occurs in a small subset of cells during a narrow window of development. This suggests that the upstream signal initiating the cell shape change must be tightly spatially restricted. Intriguingly, Wnt5, a member of the non-canonical Wnt signaling pathway, is expressed at the MHB immediately prior to and during basal constriction (Montero-Balaguer et al., 2006). Non-canonical Wnt signaling drives cell shape changes and cell movement during development through its regulation of the actin and microtubule cytoskeletons (Choi and Sokol, 2009; Gao and Chen, 2010; Karner et al., 2009; Kilian et al., 2003; Komiya and Habas, 2008). Wnt5 specifically

appears to regulate cell shape changes during bud evagination in *Hydra* (Philipp et al., 2009). Zebrafish mutants lacking both Wnt5 and Wnt11, another non-canonical Wnt signaling ligand, fail to complete neurulation (Ciruna et al., 2006). These roles of Wnt5 in cell shape change led us to consider a possible role in regulating basal constriction during MHBC morphogenesis.

We define basal constriction as the reduction of the basal surface of an epithelial cell. This process requires laminin during MHBC formation (Gutzman et al., 2008), and β1-integrin has been implicated in basal constriction during optic cup morphogenesis in *Medaka* (Martinez-Morales et al., 2009). Both of these components are basally localized and together regulate adherence of epithelial cells to the underlying basement membrane (Gutzman et al., 2008; Martinez-Morales et al., 2009; Miner and Yurchenco, 2004). During basal constriction, remodeling of the basal cell surface requires both the reduction of adhesion to decrease the basal surface and maintenance of adherence to prevent apoptosis (Frisch et al., 1996). Focal adhesion kinase, a non-receptor tyrosine kinase, is a regulator of adhesion during migration, a process that requires a similar balance of adhesion and release (Schaller, 2010). During focal adhesion assembly, FAK is activated by recruitment to nascent focal adhesions concomitant with autophosphorylation at Tyr397. Once autophosphorylated, FAK's kinase activity is induced and, it binds signaling factors including Src and Rho-effectors, as well as structural components such as paxillin and talin (Parsons, 2003; Schaller, 2010). Paxillin and talin bind both actin and integrins, thereby linking the cytoskeleton to the extracellular matrix (Horwitz et al., 1986; Schaller, 2001).

Gsk3β is a constitutively active kinase first identified as a regulator of glycogen synthesis through AKT/PI3K signaling (Cross et al., 1995). It has since been studied in detail as a central negative regulator of the canonical Wnt signaling pathway. As part of a degradation complex, it prevents cytoplasmic accumulation of β-catenin and its

subsequent transcriptional activation (van Amerongen and Nusse, 2009). In addition, Gsk3β plays a role establishing and maintaining cell polarity in conjunction with Cdc42, the Par proteins, and APC (Etienne-Manneville and Hall, 2003; Shi et al., 2004; Siegrist and Doe, 2007). This is tied to roles in cell migration, neurite outgrowth, and axon pathfinding, particularly through its interactions with APC and the corresponding stabilization of microtubules (Gao and Chen, 2010; Hur and Zhou, 2010; Salinas, 2007; Siegrist and Doe, 2007; Wen et al., 2004; Zumbrunn et al., 2001). Recent studies have implicated Gsk3β in the non-canonical Wnt signaling pathway, including downstream of Wnt5 (Philipp et al., 2009; Terrand et al., 2009; Torii et al., 2008).

Here, we define signals that regulate basal constriction at the MHBC. We show that Wnt5 is expressed in a narrow band and signals at the MHBC upstream of FAK to drive basal constriction, and this phenotype can be rescued by downregulation of Gsk3β. These data comprise a new pathway by which basal constriction is regulated during brain development.

EXPERIMENTAL PROCEDURES

Zebrafish husbandry and lines

Zebrafish lines were maintained and stages determined as previously described (Kimmel et al., 1995; Westerfield, 1995). Strains used include wild type AB; Tg(*hs*::Dkk1-GFP) (Stoick-Cooper et al., 2007); Tg(GFP::*hsp70*::dnFgfR1) (Lee et al., 2005); *fgf8*^{ti282a} (Brand et al., 1996); and *pax2a*^{tu29a} (Brand et al., 1996).

mRNA and antisense MO injections

mRNA was transcribed with the mMessage mMachine kit (Ambion). These include membrane-bound GFP mRNA at 125pg/embryo (memGFP) (kindly provided by J. B.

Green, Dana-Farber Cancer Institute Boston, MA), membrane-bound Cherry mRNA at 50pg/embryo (memCherry) (kindly provided by Dr. Roger Tsien, University of California San Diego), GFP-tubulin mRNA at 150pg/embryo (kindly provided by Dr. Frank Gertler, MIT) and human FAK (hFAK) mRNA at 400pg/embryo (accession number BC035404) (purchased from Open Biosystems, EHS1001-5481173). Splice site-blocking MO antisense oligonucleotides (MO) were injected into embryos at the one-cell stage (0.75ng FAK exon 12/13 splice donor: 5-GTGTGTTTGGGTTCTCACCTTTCTG-3; 3ng Wnt5 exon5/6 splice donor: 5-TGTTTATTTCCTCACCATTCTTCCG-3 (Kim et al., 2005; Robu et al., 2007); standard control MO 5-CCTCTTACCTCAGTTACAATTTATA-3 (Gene Tools). Each was co-injected with 1.5x p53 MO 5-GCGCCATTGCTTTGCAAGAATTG-3 (Gene Tools).

Live imaging of embryos

Live imaging by brightfield microscopy was carried out as previously described (Lowery and Sive, 2005). mRNA injections and live confocal imaging were performed as described (Graeden and Sive, 2009) Briefly, embryos were mounted inverted in 0.7% agarose (Sigma) and imaged by fluorescent, laser-scanning confocal microscopy (Zeiss LSM510).

Mosaic analysis

Embryos were injected with memGFP mRNA plus MO (donors) or memCherry mRNA plus MO (hosts) at the single cell stage. Cells were transplanted from donors at sphere stage into hosts at shield stage targeted to the presumptive MHBC region (Woo and Fraser, 1995). Transplanted embryos were imaged at 24 hpf by laser-scanning confocal microscopy. A total of 6 embryos were analyzed for control-to-control transplant

experiments. A total of 4 embryos were analyzed for FAK morphant-to-control transplant experiments. This was based on the incorporation of donor cells into the region of the MHBC.

Rescue experiments

Embryos were injected with equal amounts control or inhibitory morpholino as well as equal amounts total mRNA. This included total memGFP when needed for imaging by scanning confocal microscopy. A minimum of 6 embryos were imaged by scanning confocal microscopy and analyzed for basal constriction for each condition.

Three-dimensional (3D) cell reconstruction

Confocal images were imported into 3D Doctor (Able Software). Individual cells at the MHBC were manually outlined in each *z*-section and rendered in 3D.

Quantification of cell width

The width of six cells at the MHBC from each of three embryos was measured at 300x zoom using Imaris (Bitplane) software. Measurements were averaged and error bars reflect standard deviation for each condition.

Immunohistochemistry

Embryos were fixed in 4% paraformaldehyde (for all but vinculin and ZO-1) or Dent's (70% methanol: 30% DMSO) (for vinculin and ZO-1); some dehydrated in methanol before rehydrating into PBT (anti-laminin); blocked in 2% normal goat serum, 1% BSA, and 0.1% Triton-X100 in PBT; incubated overnight at 4°C in primary antibody (anti-phosphoY397-FAK, 44-624, Biosource, 1:200; anti-laminin, L-9393, Sigma, 1:150; anti-

aPKC (C-20), SC-216, Santa Cruz Biotechnology, 1:1000; anti-ZO1, 33-9100, Invitrogen, 1:200; anti-vinculin (hVIN-1), V9264, Sigma, 1:200; anti-phospho861-FAK, 44-626G, Invitrogen, 1:200); then incubated in secondary antibody (goat anti-rabbit or anti-mouse IgG conjugated with Alexa Fluor 488, Invitrogen, 1:500). When appropriate, some were stained in combination with propidium iodide (PI) (P3566, Invitrogen, 1:1000) 15 minutes at room temperature. Actin staining was as previously described (Gutzman et al., 2008). Images were collected using scanning confocal microscopy (Zeiss LSM510) and analyzed using Imaris (Bitplane), LSM software (Zeiss) and Photoshop (Microsoft).

RT-PCR and sequencing

Primers used for RT-PCR: FAK exon 11 forward 5-CACCTTGCCAACTTCACTCA-3; FAK exon 22 reverse 5-GTGAATCGTGGGCGTTTACT-3; EF1α forward, 5-GATGCACCACGAGTCTCTGA-3; and EF1α reverse, 5-TGATGACCTGAGCGTTGAAG-3. FAK PCR products were cloned into pGEM using the pGEM T-Easy Vector System Kit (Promega) and sequenced.

In situ hybridization

RNA probes containing digoxigenin-11-UTP were synthesized from linearized plasmid DNA for *pax2.1* (Krauss et al., 1991) and *fgf8* (Reifers et al., 1998) as described (Harland, 1991). Standard methods for hybridization and for single color labeling were used as described elsewhere (Sagerstrom et al., 1996). After staining, embryos de-yolked, flat-mounted in glycerol and imaged with a Nikon compound microscope.

RESULTS

Basal constriction forms wedge-shaped cells at the MHBC

We have previously established that cells shorten prior to basal constriction and subsequent apical expansion during morphogenesis at the midbrain-hindbrain boundary constriction (MHBC) in zebrafish (Gutzman et al., 2008). Here, we have increased the resolution of our analysis to determine the order of the steps involved and have assayed for the three-dimensional shape of the cells undergoing basal constriction.

MHB morphogenesis begins at 17 hpf. At this stage, the MHB is composed of uniform columnar epithelial cells with an average basal width of 2.14 +/- 0.59μm (Fig. 1A, E, E', I, M). By 21 hpf, the cells at the MHB have shortened, as previously described (Gutzman et al., 2008) (Fig. 1B, F, F'). 3D reconstruction and quantification of these cells indicates that they have begun to constrict at their basal surface to approximately two-thirds their original basal width (1.44 +/- 0.40μm) (Fig. 1J, M). By between 23 and 24 hpf, cells at the MHBC have constricted completely, to a basal width of 0.50 +/- 0.18μm, forming a wedge shape (Fig. 1C, G, G', K, M). Subsequent to basal constriction, these cells expand apically (Fig. D, H, H', L, M). The order of these events suggests that cell shortening may be required for the later basal constriction, and apical expansion may be dependent upon both prior cell shortening and basal constriction. The wedge shape of these cells suggests the mechanism by which the constriction occurs. Force applied circumferentially around the basal cell surface would result in cone-shaped cells (Martin et al., 2009; Pilot and Lecuit, 2005). Therefore, formation of wedge-shaped cells indicates that force is applied unequally to constrict the cells in the antero-posterior and not the dorso-ventral direction.

Early patterning signals are not required at time of MHBC morphogenesis

The MHB is patterned starting at 10 hpf, early in neurulation. This is initiated by *otx2, gbx2* and *pax2* expression followed by *fgf8* and several members of the canonical Wnt signaling pathway, including *wnt1, wnt3a,* and *wnt10b* (Buckles et al., 2004; Hidalgo-Sanchez et al., 2005; Reifers et al., 1998). These signaling pathways are required for tissue specification and formation of the MHB, as determined by mutant analysis (Buckles et al., 2004; Burgess et al., 2002; Lun and Brand, 1998; Reifers et al., 1998; Reim and Brand, 2002). Mutant analysis cannot separate the early role of these genes in tissue specification from their possible later role in morphogenesis. Using inducible promoters driving antagonists of these pathways, we have performed loss-of-function analysis just prior to MHB morphogenesis.

FGF signaling is a key regulator of the MHB: Fgf8 implanted on a bead is sufficient to drive formation of an ectopic MHB in the chick midbrain (Crossley et al., 1996; Martinez et al., 1999). Three Fgf receptors, *fgf1-3*, are expressed in the developing neural tube (Walshe and Mason, 2000). Of these, FgfR1 is expressed at and required for regulation of the MHB (Rohner et al., 2009; Trokovic et al., 2003). The Poss lab constructed a transgenic line expressing dominant-negative FgfR1 under control of a heat shock promoter that ablates FGF signaling in a temporally specific manner (Lee et al., 2005). This promoter is bi-directional and induces transcription of GFP as a marker when it is activated. All transgenic embryos were screened for GFP as an indication of activation of the promoter. Heat shock treatment of wild type embryos did not affect their development as assayed by brightfield microscopy (Fig. 2A, B). Heat shock of the GFP::*hs*::FgfR1 transgenic embryos at 10 hpf prevented MHB morphogenesis (Fig. 2E) and phenocopied the Fgf8 mutant, *acerebellar* (Fig. 2C; (Reifers et al., 1998). However, embryos treated with heat shock at 17 hpf were unaffected when compared to control

embryos (Fig. 2G). This suggests that while FGF signaling is required for early MHB patterning, it is not required later for morphogenesis and basal constriction.

Canonical β-catenin-dependent Wnt signaling is also required for patterning at the MHB. Buckles et al performed a triple knockdown experiment of Wnt1, Wnt3a, and Wnt10b, three partially redundant components of this pathway all expressed at the MHB early in neurulation (Buckles et al., 2004). These embryos failed to form an MHB, phenocopying *no isthmus*, a mutant of a downstream component of the Wnt pathway, *pax2a* (Lun and Brand, 1998). Dkk1 is an antagonist of Wnt binding to its receptor, Fz, and appears to primarily inhibit canonical Wnt signaling (Glinka et al., 1998; Kazanskaya et al., 2000). We used a transgenic line expressing Dkk1 under control of a heat shock promoter (Stoick-Cooper et al., 2007) to ablate canonical Wnt signaling at 10 hpf during patterning and at 17 hpf just prior to MHB morphogenesis. Embryos treated at 10 hpf phenocopied the *pax2* mutant line (Fig. 2D, F). MHB morphogenesis was unaffected by treatment at 17 hpf (Fig. 2H). This suggests that, like FGF signaling, canonical Wnt signaling is required for patterning, but not for morphogenesis at the MHB.

Wnt5 is expressed at the MHBC and is required for basal constriction

Gene expression of patterning components such as *wnt1* and *fgf8* is restricted to the MHB as early as 10 hpf and is maintained through the completion of MHBC morphogenesis at 25 hpf (Buckles et al., 2004; Lekven et al., 2003; Reifers et al., 1998). We hypothesized that transcription of genes required specifically for morphogenesis would be initiated just prior to the start of MHB formation at 16 or 17 hpf and that this signal would be spatially restricted to the cells undergoing basal constriction. Previously published data suggested that *wnt5* expression might correlate with MHB morphogenesis both temporally and spatially (Hollyday et al., 1995; Montero-Balaguer et

al., 2006). We repeated expression analysis in higher resolution to address the question of whether *wnt5* is expressed in the basally constricting cells prior to and during constriction. At 18 hpf and 21 hpf, *wnt5* was expressed at the MHBC with some general expression present in the rest of the brain as shown by *in situ* hybridization (Fig. 3A, B). By 24 hpf, *wnt5* expression was restricted specifically to the MHBC, apparently in and just posterior to the basally constricting cells (Fig. 3C). A sense probe control did not stain in the brain, showing that binding was specific (Fig. 3D).

Based on the specificity of the expression pattern, we hypothesized that Wnt5 might play a role in regulating basal constriction. To test this, we co-injected a previously published splice-site antisense morpholino-modified oligonucleotide (hereafter, morpholino or MO) targeting Wnt5 and assayed for MHBC morphogenesis by brightfield microscopy. This morpholino was reported to cause mis-splicing and is specific, as shown by mRNA rescue (Kim et al., 2005; Robu et al., 2007). Injection of a control morpholino did not affect MHB morphogenesis (Fig. 3E). Embryos injected with Wnt5 morpholino failed to form a deep bend in the tissue at the MHBC (Fig. 3F). These embryos also exhibited a truncated tail suggestive of the somite defects expected based on the known mutant phenotype (Fig. 3F; Hammerschmidt et al., 1996; Westfall et al., 2003). These mutant lines have not been described as having an MHB defect. However, these mutants are the result of point mutations, and therefore, are likely to be hypomorphic (Hammerschmidt et al., 1996; Kilian et al., 2003; Lele et al., 2001; Mullins et al., 1994). Alternatively, the basal constriction defect may not be described due a lack of resolution in the assays used to describe the phenotype.

To determine if the MHB morphogenesis defect was caused by a loss of early tissue specification, we performed in situ hybridization against two genes required for patterning of the MHB, *fgf8* and *pax2* (Hidalgo-Sanchez et al., 2005). Both markers were strongly expressed at the MHB in control and Wnt5 morphant embryos (Fig. 3G-J).

We then performed confocal microscopy analysis on live embryos co-injected with membrane-bound GFP (memGFP) and morpholino at 24 hpf to assay for basal constriction at the MHBC. While basal constriction was unaffected in control embryos (Fig. 3K, K'), cells at the MHBC in Wnt5 loss-of-function embryos failed to undergo the cell shape change, supporting our hypothesis (Fig. 3L, L'). 3D reconstruction of the cells at the MHBC confirmed the lack of basal constriction in the Wnt5 morphant cells. While the cells in the control morphants formed a wedge-shape and were fully basally constricted, the cells in the Wnt5 morphants appeared columnar (Fig. 3M, N).

FAK is required specifically at the MBHC for basal constriction

During basal constriction, the basal surface of cells at the MHBC must be significantly remodeled. Focal adhesion kinase (FAK) is a regulator of basal remodeling, and its activation basally by autophosphorylation at Tyr397 is required for its localization to focal adhesions and its interactions with a host of protein binding partners (Parsons, 2003). We therefore hypothesized that autophosphorylated FAK would be localized to the MBHC and required for basal constriction. An antibody specific to FAK autophosphorylation stained both the apical and basal surfaces in the neural tube at 17, 21 and 24 hpf (Fig. 4A-C; Ridyard and Sanders, 1998). At 24 hpf, staining was enriched at the basal surface of the MHB (Fig. 4C) and at somite boundaries (Fig. 4D; Tsuda et al., 2010; Crawford et al., 2003).

Injection of a control morpholino did not affect morphogenesis of the MHB, but injection of a splice-site morpholino targeting Ptk2.1, one of the two genes encoding FAK in zebrafish, disrupted morphogenesis at the MHBC at 24 hpf (Fig. 4E, F; Crawford et al., 2003). To determine whether this defect in MHB formation was due to a loss of tissue specification, we performed *in situ* analysis of *fgf8* and *pax2*, two MHB patterning markers. Both were strongly expressed at the MHB in control embryos, and this was

recapitulated in the FAK loss-of-function embryos (Fig. 4G–J), indicating that the defect in these morphant embryos is not due to a defect in tissue patterning. We then assayed live embryos by confocal microscopy co-injected with morpholino and memGFP and found that basal constriction occurred normally in control embryos, but embryos lacking FAK function failed to undergo the cell shape change (Fig. 4K, K', L, L'). 3D reconstruction of the cells at the MHBC confirmed this phenotype (Fig. 4M, N). Quantification indicated that the degree of basal constriction in the FAK morphants is comparable to that of a 21 hpf wild-type embryo (compare quantification in Fig. 1Q to Fig. 9G). This may be explained by retention of some FAK function, since injection of higher levels of morpholino was toxic.

Loss of FAK function severely affects the gross morphology of the embryo (Fig. 4F). We wondered whether the loss of basal constriction was an indirect effect of FAK loss-of-function elsewhere in the embryo or, more specifically, in the neural tube. To address this, we transplanted cells from FAK morphant donors marked by memGFP into control embryo hosts marked by membrane-bound Cherry (memCherry). Transplants were completed just prior to shield stage (6 hpf) based on the fate map established by Woo and Fraser (Woo et al., 1995), and the resulting chimeras were assayed for basal constriction at 24 hpf. In all embryos assayed, the transplanted donor cells localized to the host neural tube. Embryos in which control morphant cells were transplanted into FAK morphant hosts were not viable.

Transplanting control donor cells into control hosts did not disrupt basal constriction of either the donor or host cells, as shown by confocal and 3D reconstruction (Fig. 4O, O', Q, host red cells outlined and 3D reconstructed in blue, donor green cells outlined and 3D reconstructed in yellow). When transplanted to the MHBC, FAK donor cells failed to undergo basal constriction as in the FAK morphant embryos (Fig. 4P, P', R, donor green cells outlined and 3D reconstructed in yellow). Therefore, basal constriction

in these cells cannot be rescued by control cells elsewhere in the neural tube or elsewhere in the embryo, indicating that FAK functions at the MHBC to drive basal constriction. Single FAK donor cells failed to integrate into the neuroepithelium so could not be assayed for basal constriction. Host cells at the MHBC in the mosaic embryos remained competent for basal constriction even when immediately adjacent to cells lacking FAK function (Fig. 4P, P', R, host red cells outlined and 3D reconstructed in blue). These data suggest that FAK function is specifically required in the cells at the MHB undergoing basal constriction.

FAK loss-of-function is specific and can be rescued by human FAK

To determine whether the morpholino targeting FAK is specific and FAK function conserved, we co-injected mRNA encoding human FAK with the FAK morpholino. Embryos co-injected with control morpholino and control mRNA appeared wild type (Fig. 5A – a) Embryos injected with FAK morpholino exhibited either a mild or severe phenotype. The mild phenotype exhibited a consistent tail morphology defect, but basal constriction sometimes occurred normally (Fig. 5A – b). The severe phenotype was used for confocal imaging of the MHBC to describe the effects of FAK on basal constriction, as it always exhibits a basal constriction defect, as well as a severe tail defects (Fig. 5A – c). Embryos with the severe morphology sometimes fail to complete neurulation. Embryos were screened for a neurulation defect, and basal constriction was not assayed in embryos exhibiting such defects. Injection of mRNA encoding human FAK (hFAK) did not generate a noticeable phenotype (Fig. 5A – d). Co-injection of hFAK with the FAK morpholino resulted in partially rescued embryos. In comparison to the severe FAK loss-of-function embryos, hFAK mRNA rescued both the brain and tail phenotypes to a significant degree (Fig. 5A – e). Co-injection with hFAK appears to rescue the tail phenotype in comparison with mild FAK morphants. A noticeable change in the brain

phenotype was not observed by brightfield microscopy. This partial rescue result is consistent with the data from rescues performed by other members of our lab on other morpholinos (Chang and Sive, unpublished). The penetrance of the phenotype and the mRNA rescue are quantified in Fig. 5B.

The FAK morpholino targets the splice site at the 3' end of exon 12. RT-PCR confirmed mis-splicing and the formation of two new mRNA species (Fig. 5C). When sequenced, these were identified as mRNA fragments containing wild type sequence through exon 12 and the addition of a small amount of intronic sequence. In both cases, nonsense mutations in the intronic inclusion resulted in truncated mRNA products lacking the autophosphorylation site at Tyr397 required for FAK activation (Calalb et al., 1995) (Fig. 5D).

Epithelial integrity is maintained in FAK loss-of-function embryos

FAK has been implicated in the formation and maintenance of epithelial integrity both through its role in cadherin-mediated cell-cell junctions (Avizienyte and Frame, 2005; Yano et al., 2004) and in its regulation of the basement membrane (Ilic et al., 2004). FAK also regulates the actin and microtubule cytoskeletons (Gupton and Gertler, 2010; Mitra et al., 2005; Schober et al., 2007; Serrels et al., 2007; Tsuda et al., 2010; Wu et al., 2004; Xie et al., 2003). It is possible that loss of basal constriction in FAK morphants is due to loss of epithelial integrity. This is of particular concern since laminin is required for basal constriction (Gutzman et al., 2008). As determined by immunohistochemistry, laminin lines the neural tube in control embryos with no breaks through the midbrain, hindbrain, and MHBC, forming a sharp point at the MHBC (Fig. 6A, A', A"). This staining is grossly normal in the FAK morphants (Fig. 6B). A few distinct breaks in the staining suggest regions of laminin degradation. It appears that cells in those regions may be extruding from the epithelium as indicated by the

movement of nuclei across the plane of the laminin staining (Fig. 6B', B"). However, these breaks do not necessarily occur at the MHBC, suggesting that loss of basal constriction in these embryos is not due to local disruption of the laminin. The actin cytoskeleton, as shown by phalloidin staining, is enriched at the MHBC in control morphants as previously published, and this enrichment is also observed in the FAK morphants as compared to control embryos (Fig. 6D, D', E, E'; (Gutzman et al., 2008). The microtubule cytoskeleton was assayed by live confocal imaging of GFP-β-tubulin-injected embryos at 24 hpf. As in control embryos, the microtubule cytoskeleton in FAK loss-of-function embryos exhibits apical-basal arrays (Fig. 6F, F', G, G'). ZO-1, a marker of apical junctions (Gumbiner, 1987), is localized to the apical side of the neuroepithelium similarly in control and FAK loss-of-function embryos (Fig. 6H, H', I, I'), as is aPKC, a marker of cell polarity (Izumi et al., 1998) (Fig. 6J, J', K, K'). While we cannot rule out subtle changes in epithelial cohesion or function resulting from loss of FAK function, taken together, these data suggest that the loss of basal constriction in the FAK loss-of-function embryos is unlikely to be due to a general loss of epithelial integrity.

FAK may not regulate mature focal adhesions during basal constriction

According to its published functions and localization in other systems, we hypothesized that FAK staining would correspond to focal adhesions in the neural tube (Schaller et al., 1992). Vinculin is a structural adapter protein localized to focal adhesions early in their development and important for actin binding at adhesions (Carisey and Ballestrem). Surprisingly, vinculin was not visible by antibody staining in the neural tube at 24 hpf, though it does stain at the somite boundaries in the same embryos (Fig. 7A). This was repeated at 48 hpf (Fig. 7B). By 72 hpf, staining showed vinculin enrichment both at the MHB and in the retina, as well as at the somite boundaries (Fig.

7C). We also stained with an antibody specific to FAK phosphorylated at Tyr861, a target of Src phosphorylation signaling at adhesions (Crawford et al., 2003; Mitra et al., 2005). Again, staining failed to detect the phospho-protein in the brain at 24 hpf, though the antibody stained at somite boundaries in the same embryos (Fig. 7D). At 48 hpf, faint staining was visible in the retina with strong staining in the somites (Fig. 7E). Not until 72 hpf was staining visible in the brain, where it was again enriched at the MHB and in the retina as for vinculin (Fig. 7F). These data suggest that mature focal adhesions may not be established in the brain during MHBC morphogenesis and basal constriction. In conjunction with the data showing that loss of FAK does not disrupt epithelial integrity in the neural tube, these data lead us to consider other ways in which FAK might be regulating basal constriction.

Wnt5 may be required for localization of activated FAK at the MHB

Wnt5 has previously been shown to regulate focal adhesion dynamics upstream of Dishevelled and to promote activation of FAK in migrating cells (Kurayoshi et al., 2006; Matsumoto et al., 2010). We have shown in this study that FAK and Wnt5 are both required for basal constriction at the MHBC. This led us to hypothesize that Wnt5 regulates basal constriction through the downstream activation of FAK, in which case FAK activation at the MHBC would be lost in Wnt5 loss-of-function embryos. Consistent with this hypothesis, autophosphorylated FAK is enriched at the MHB and the somite boundaries in control embryos at 24 hpf, as described above (Fig. 8A, A'). Preliminary experiments suggest that enrichment at the MHB and possibly at the somite boundaries may be lost in embryos injected with Wnt5 morpholino (Fig. 8B, B'). These data would suggest that FAK activation at the MHBC is dependent upon Wnt5. We are currently planning a control experiment to test whether rescue of the Wnt5 loss-of-function phenotype by co-injection with mRNA also will rescue the phospho-FAK enrichment at

the MHBC. An additional experiment will test whether downregulation of FAK phosphorylation in Wnt5 loss-of-function embryos can be detected and quantified by Western blot. Present data indicate an intriguing result consistent with a model in which FAK acts downstream of Wnt5 to regulate basal constriction.

Wnt5 and FAK signal through Gsk3β to regulate basal constriction

Gsk3β is a constitutively active kinase that acts as an inhibitor of canonical Wnt signaling. In complex with APC and Axin, Gsk3β phosphorylates β-catenin, the downstream canonical Wnt effector. This prevents its cytoplasmic accumulation, nuclear translocation, and transcriptional activity (Doble and Woodgett, 2003). In other contexts, Gsk3β regulates the microtubule cytoskeleton in β-catenin-independent pathways, often referred to as non-canonical Wnt signaling (Ciani et al., 2004; van Amerongen and Nusse, 2009). Gsk3β has also recently been shown to signal downstream of Wnt5, a ligand generally thought to activate non-canonical Wnt signaling (Terrand et al., 2009; Torii et al., 2008). Wnt5 primarily signals through Rho and Jnk, independent of the canonical, or β-catenin-dependent, Wnt pathway (Hardy et al., 2008; Kilian et al., 2003; Wallingford et al., 2001; Westfall et al., 2003; Zhang et al., 2006). However, recent data from *Hydra* suggests that, during evagination, Wnt5 may also be involved with cross-talk between the canonical and non-canonical Wnt signaling pathways (Philipp et al., 2009). Given the interplay between Wnt5 and Gsk3β, we hypothesized that inhibition of Gsk3β by Wnt5 might be required for basal constriction. To test this hypothesis, we used a kinase-dead Gsk3β (dnGsk3β), which acts as a well-characterized dominant-negative during embryogenesis (Pierce and Kimelman, 1995; Torres et al., 1999; Yost et al., 1996).

Injection of control morpholino and memGFP control mRNA resulted in wild type MHBC morphogenesis and basal constriction (Fig. 9A, B, B'). Injection of low levels

of mRNA encoding dnGsk3β resulted in a posteriorized head most noticeably characterized by an eyeless phenotype (Fig. 9C). Basal constriction occurred normally in these embryos (Fig. 9D, D'). Injection of Wnt5 morpholino prevented basal constriction at the MHBC as described above (Fig. 9E, F, F'). Supporting our hypothesis, overexpression of dnGsk3β rescued the loss of basal constriction in Wnt5 morphants (Fig. 9G, H, H'). Quantification of basal constriction in these embryos confirmed the phenotype (Fig. 9M). A histogram describing quantification of the rescue is shown in Fig. 9R.

FAK is an important signaling kinase in addition to its role as a scaffolding protein in focal adhesions (Giancotti and Ruoslahti, 1999). It is a known regulator of Gsk3β as part of insulin signaling through the PI3K/Akt pathway (Huang et al., 2009; Huang et al., 2002) and signals downstream of Dishevelled, indicative of a role in Wnt signaling (Cohen et al., 2002). Given that both Wnt5 and FAK are required for basal constriction, and that Gsk3β is one of the few proteins of which they share regulation, we hypothesized that FAK might also regulate basal constriction through signaling with Gsk3β.

As also shown above, FAK loss-of-function resulted in embryos with truncated, up-turned tails and loss of basal constriction at the MHBC (Fig. 9I, J, J'). Co-injection of FAK morpholino and dnGsk3β mRNA resulted in a completely rescued embryo. Remarkably, both the basal constriction and tail defects from the FAK morphant embryos were rescued in addition to the loss of eyes in the embryos injected with dnGsk3β mRNA (Fig. 9C, D, D', K, L, L'). Quantification of the basal width of these embryos confirmed the phenotype (Fig. 9M). A histogram describing quantification of the rescue is shown in Fig. 9S.

To address whether this rescue was a response to non-specific modulation of Gsk3β signaling, we tested whether overexpression of wild type Gsk3β mRNA was also

capable of rescue. Control morpholino did not disrupt MHB morphogenesis (Fig. 9N.) Overexpression of Gsk3β by mRNA injection caused significant disruption of the embryo, including a neurulation defect (Fig. 9O). FAK morpholino injection caused malformation of the MHB and a tail extension defect, as described above (Fig. 9P). When co-injected with FAK morpholino, Gsk3β mRNA failed to rescue the neural tube or tail defects (Fig. 9Q). Quantification of these data are described by a histogram in Fig. 9T). This suggests that the rescue of basal constriction in FAK loss-of-function embryos is specific to the downregulation of Gsk3β.

In total, these data are consistent with a model in which Gsk3β regulates basal constriction downstream of Wnt5 activation of FAK.

FAK signaling to Gsk3β is independent of Akt

The best characterized signaling pathway connecting FAK to Gsk3β is through Akt (Huang et al., 2009; Huang et al., 2002). In this pathway, FAK phosphorylates and activates Akt, which then phosphorylates Gsk3β, inhibiting it. Akt is activated by phosphorylation at Thr308 in the activation loop of its kinase domain and Ser473, in the C-terminal hydrophobic motif (Vanhaesebroeck and Alessi, 2000). Mutation of these phosphorylation sites to alanine results in a dominant-negative Akt (Kotani et al., 1999). Myristolation causes constitutive membrane-localization of Akt, which results in a constitutively active protein (Ramaswamy et al., 1999). Because FAK positively regulates basal constriction, and its loss can be rescued by Gsk3β, we hypothesized that Akt would also positively regulate basal constriction. In this case, loss of Akt function would be expected to disrupt MHB morphogenesis, and constitutively active Akt would be expected to rescue the MHB defect in FAK morphant embryos. Counter to our hypothesis, overexpression of dominant negative Akt (dnAkt) exhibited a curled tail in comparison to control embryos, but a normal MHB, suggesting that Akt may not be

required for MHB morphogenesis (Fig. 10A – a, b). Overexpression of constitutively active Akt (caAkt) caused a slight defect in ventricle inflation in comparison to control or FAK morphant embryos, but a relatively normal MHB (Fig. 10B – a, b, c). Co-injection of caAkt with the FAK morpholino resulted in embryos with an abnormal MHB and tail, like the FAK morphants, but lacking complete ventricle inflation similar to the caAkt-injected embryos (Fig. 10B – d). Thus, we concluded that caAkt was unable to rescue the MHB defect. These data suggest that FAK is unlikely to inhibit Gsk3β and regulate MHB morphogenesis through Akt.

DISCUSSION

Basal constriction at the MHBC

The zebrafish MHBC is shaped by folding of the basal surface of the neuroepithelium during which a small subset of cells at the point of deepest constriction sequentially shorten, constrict basally, and expand apically (Gutzman et al., 2008). 3D reconstruction now shows that basal constriction results in wedge-shaped cells with the constriction occurring in the anterior-posterior plane and not in the dorso-ventral plane.

While we had previously established that cell shortening occurs prior to basal constriction and that basal constriction can occur even in the absence of apical expansion, we have now shown that apical expansion occurs only after the completion of basal constriction. This supports our previous conclusion that basal constriction, and not apical expansion, is an active process necessary to form the MHBC. It is possible, however, that basal constriction is dependent on the earlier cell shortening. Cell shortening occurs normally in laminin mutants, which suggests that cell-matrix adhesion may not be required for the process (Gutzman et al., 2008). Preliminary data from our lab suggests that non-muscle myosin II may be required for cell shortening (Gutzman,

unpublished), but we have not yet tested whether the additional factors shown to be required for basal constriction are also required for cell shortening.

Wnt5 in MHBC Morphogenesis

The signal required to position the MHBC and initiate basal constriction was previously unknown. Signaling through both the Fgf and canonical Wnt pathways is spatially restricted to the MHB, but not to the basally constricting cells (Buckles et al., 2004; Lekven et al., 2003; Reifers et al., 1998). Moreover, these genes are first expressed early in neurulation (Lun and Brand, 1998). Temporally specific inhibition of these pathways suggests that this signaling is not additionally required for MHBC morphogenesis. Localization of laminin, the only previously identified regulator of basal constriction, is not spatially or temporally restricted in the neural tube (Gutzman et al., 2008), leaving open the question of the upstream signal driving basal constriction. In this study, we show that Wnt5 is expressed specifically at the MHBC during morphogenesis and is required for basal constriction. Previously published data indicates that this expression is not present in the neural tube until the onset of morphogenesis at 18 hpf (Thisse et al., 2004). This suggests that Wnt5 may be the instructive signal positioning and initiating MHBC morphogenesis. While these experiments establish that Wnt5 is required for basal constriction, we have not yet determined if this signal is sufficient.

The role of cell-matrix interactions

We show here that FAK is required for basal constriction at the MHBC. Considering the additional requirement for laminin, this suggests an important role of cell-matrix adhesion in the process. Interactions between FAK and laminin have generally been at focal adhesions where they are connected by integrins, also previously

shown to play a role in basal constriction (Li et al., 2002; Parsons, 2003; Schock and Perrimon, 2002; Wederell and de Iongh, 2006). While immunostaining suggests that mature focal adhesions may not be present in the neural tube during this stage of development, there may be nascent cell-matrix adhesions that do not yet contain the two markers for which we stained. Staining for other focal adhesion components was not successful. Alternatively, FAK may be primarily required as a signal transducer during basal constriction. This is supported by the fact that it can be rescued by inhibition of another signaling component, Gsk3β. However, if this is the case, it is unclear how or if this signaling is connected to laminin, leaving the loss of basal constriction in laminin mutants unexplained.

The physical process of basal constriction

What directs basal constriction downstream of Wnt5, FAK, and Gsk3β? During basal constriction, the basal cell surface decreases, requiring that the attachment of the cell to the underlying extracellular matrix be remodeled, reducing adhesion to shrink the basal surface while retaining enough adhesion to maintain epithelial integrity and prevent apoptosis (Frisch et al., 1996). A model for maintaining this balance can be found in migrating cells. Migration requires binding to the substrate at the leading edge and release at the rear of the cell to allow the cell to pull itself forward over the substrate (Parsons et al., 2010). Disassembly of focal adhesions at the rear of the cell is driven by dynamin-mediated endocytosis in response to microtubule contacts; this is dependent on FAK (Ezratty et al., 2005). Intriguingly, Gsk3β phosphorylates dynamin, a primary mediator of endocytosis (Clayton et al., 2010). Together, these data suggest that endocytosis might be regulated by Wnt/FAK/Gsk3β to remodel the basal cell surface during basal constriction.

Model: A signaling pathway to regulate basal constriction

A model for regulation of basal constriction consistent with the data presented here is diagrammed in Fig. 11. In this model, Wnt5 signals to activate FAK. FAK then inhibits Gsk3β, possibly through an unidentified intermediate. This inhibition of Gsk3β promotes basal constriction. These components are unlikely to compose a complete pathway. Wnt5 activation of FAK presumably would require a receptor to connect the extracellular ligand with the intracellular kinase, though this receptor is unknown (Parsons, 2003; Wodarz and Nusse, 1998). Wnt5 signals through both Frizzled2 and Ryk in different developmental contexts, and one or both may be acting to regulate basal constriction (Lin et al., 2010; Kilian et al., 2003). Identifying the receptor for Wnt5 during basal constriction will provide useful clues about the downstream pathway.

Regulators of basal constriction downstream of Gsk3β are also unknown. It is possible that Gsk3β could activate β-catenin, as in canonical Wnt signaling (Cadigan and Liu, 2006). However, Dkk1 is an inhibitor of β-catenin-mediated Wnt signaling, and it does not inhibit MHBC morphogenesis (Kazanskaya et al., 2000; Stoick-Cooper et al., 2007). Rho, Rac and Jnk all participate in Wnt signal transduction to regulate the cytoskeleton and cell shape changes (Angers and Moon, 2009; Schlessinger et al., 2009; van Amerongen and Nusse, 2009). Future analyses will determine the role of these regulators in basal constriction.

FIGURE LEGENDS

Fig. 1 Basal constriction at the zebrafish MHBC occurs after prior to apical expansion and results in wedge-shaped cells

(A – D) Schematics of wild type (WT) MHBC formation. (E – H') Live scanning confocal imaging of wild type embryos injected with memGFP mRNA at the one cell stage and imaged at 17, 21, 23/24 and 24/25 hpf ($n > 8$ embryos each stage). Cells at the MHBC are outlined. (E, E') At 17 hpf, cells at the MHBC are similar in shape to those surrounding. (F, F') At 21 hpf, cells at the MHBC have shortened (Gutzman et al., 2008). (G, G') At 23/24 hpf, cells at the MHBC are constricted basally. (H, H') at 24/25 hpf, basally constricted cells have also expanded apically. (I-L) 3D reconstruction of cells using 3D Doctor (Able Software) (n = 2-3 cells from each of 3 embryos). Each reconstruction is shown next to a 45° rotation of the same image. (I) Columnar epithelial cells at the MHBC at 17 hpf are relatively uniform in shape when rotated. (J) At 21 hpf, cells at the MHBC have shortened and begun to constrict basally along their dorso-ventral axis. (K) At 23/24 hpf, basal constriction is complete in cells at the MHBC and these cells have become wedge-shaped. (L) At 24/25 hpf, cells at the MHBC have expanded apically. (M) Histogram comparing the basal width of cells at each time point. Six cells in each of three embryos were measured for each time point. The basal width decreases progressively over time. Basal constriction is completed by 23/24 hpf. Anterior is left. Arrowheads indicate the MHBC. MB, midbrain. HB, hindbrain. Error bars reflect standard deviation. Scale bars: E–H' = 9μm

Fig. 2 Early patterning genes are not required for later MHBC morphogenesis

(A – H) Brightfield images of the MHBC at 24 hpf. Arrowheads mark MHBC. (A) Wild type control embryo; untreated. (B) Wild type embryo; treated with heat shock 10-12 hpf.

(C) *fgf8* mutant embryo;, untreated. (D) *pax2a* mutant embryo, untreated. (E) Transgenic line expressing dnFgfR1 and GFP under control of a bi-directional heat shock promoter (Tg(GFP::*hs*::dnFgfR1)); treated with heat shock 10-12 hpf. Treatment recapitulates *fgf8* mutant phenotype. (F) Transgenic line expressing Dkk1-GFP under control of a heat shock promoter (Tg(*hs*::Dkk1-GFP)); treated 10 12 hpf. Treatment recapitulates *pax2a* mutant phenotype. (G) Tg(GFP::*hs*::dnFgfR1); treated with heat shock 17-19 hpf. Does not affect MHBC morphogenesis. (H) Tg(*hs*::Dkk1-GFP); treated with heat shock 17-19 hpf. Does not affect MHBC morphogenesis. Anterior is left. Arrowheads mark the MHBC. Scale bars: A–H = 100μm

Fig. 3 Wnt5 is expressed at the MHBC during morphogenesis and is required for basal constriction

(A – D) *In situ* hybridization of *wnt5* in wild type embryos. Embryos were stained, flat-mounted in glycerol and imaged with a compound light microscope. (A, B) *wnt5* is expressed at the MHBC at 18 and 21 hpf. (C) *wnt5* is expressed in and just posterior to the basally constricted cells at the MHBC at 24 hpf. (D) Sense control at 24 hpf shows no staining. (E – F) Brightfield images of morpholino injected embryos at 24 hpf. Boxed region is enlarged below. (E) Embryos injected with control MO exhibit normal MHBC morphogenesis. (F) Embryos injected with Wnt5 MO exhibit morphological defects at the MHBC and in the tail. (G – J) *in situ* hybridization of patterning controls, *fgf8* and *pax2a* are expressed at the MHBC at 18 hpf in control embryos (G, I) and Wnt5 morphants (H, J). (K – L') Embryos were co-injected with memGFP mRNA and MO (n = 10). Three cells at the MHBC are outlined. (K, K') Cells at the MHBC undergo basal constriction in control embryos. (L, L') Cells at the MHBC fail to undergo basal constriction in Wnt5 morphants. (M, N) Two cells in each of three embryos were reconstructed in 3D using 3D Doctor (Able Software). Reconstructed cell shown is

outlined in red above and rotated 45° to show side view. (M) MHBC cell in control embryo is constricted basally and wedge-shaped. (N) MHBC cell in Wnt5 morphants embryo is columnar. Anterior is left. Arrowheads mark the MHBC. MB, midbrain. HB, hindbrain. Error bars reflect standard deviation. Scale bars: E–F = 100μm; K–L' = 26μm

Fig. 4 Activated focal adhesion kinase (FAK) is enriched at the MHBC and is required locally for basal constriction

(A – D) Wild type embryos were stained with anti-phospho-FAK^{Y397} antibody, flat mounted in glycerol, and imaged by scanning confocal microscopy. (A, B) phospho-FAK^{Y397} is localized at the basal and apical sides of the neural tube at 18 and 21 hpf. (C) This staining is enriched at the MHBC at 24 hpf. (D) phospho-FAK^{Y397} is localized to somite boundaries at 24 hpf. (E , F) Brightfield images of morphants at 24 hpf. Boxed region is enlarged below. (E) Control morphants exhibit normal MHBC morphogenesis. (F) FAK morphants exhibit morphological defects at the MHBC and in the tail. (G-J) *in situ* hybridization of patterning controls, *fgf8* and *pax2a* are expressed at the MHBC at 18 hpf in control embryos (G, I) and FAK morphants (H, J). (K-L') Embryos were co-injected with memGFP mRNA and MO (n = 10). Three cells at the MHBC are outlined. (K, K') Cells at the MHBC undergo basal constriction in control embryos. (L, L') Cells at the MHBC fail to undergo basal constriction in FAK morphants. (M, N) Two cells in each of three embryos were reconstructed in 3D using 3D Doctor (Able Software). Reconstructed cell shown is outlined in red above and rotated 45° to show side view. (M) MHBC cell in control embryo is constricted basally and wedge-shaped. (N) MHBC cell in FAK morphant embryo is somewhat constricted at the basal surface, similar to WT embryos at 21 hpf (see Fig. 1J). (O – P') Mosaic analysis of FAK loss-of-function. Embryos were co-injected with memGFP (donor) or memCherry (host) and control or FAK MO. Cells from donor embryos were transplanted at sphere stage into host embryos

at shield stage (n = 4). Donor cells are outlined in yellow and host cells in blue. All cells were targeted to the neural tube. (O, O') Control donor and host cells basally constricted normally when transplanted to the MHBC. (P, P') Cells from FAK morphants donors transplanted into control hosts failed to undergo basal constriction at the MHBC. Basal constriction occurred normally in control host cells, even when immediately adjacent to FAK morphant donor cells. Arrow marks host cell outlined in (P'). (P) In the corner box, a more ventral slice shows the same cell more clearly. (Q) Two cells in each of three embryos were reconstructed in 3D as in (N, M). Reconstructed cells are those outlined in the same color above. Control cells undergo basal constriction and become wedge-shaped in all cases. FAK morphant donor cells fail to undergo basal constriction, as in FAK morphants. Anterior is left. Arrowheads mark the MHBC. MB, midbrain. HB, hindbrain. Scale bars: A–C = 20μm; E–F = 70μm; K–L', O', P' = 13μm; O, P = 24μm

Fig. 5 FAK morpholino phenotype can be rescued and generates aberrant mRNA products

(A) Brightfield images at 24 hpf show rescue of FAK morphants with co-injection of human FAK mRNA. Anterior is left. Arrowheads mark the MHBC. (a) Control MO embryo. (b, c) FAK MO injection generates mild and severe phenotypes. (d) Co-injection of human FAK mRNA with control MO did not affect morphogenesis. (e) FAK morphants were rescued by co-injection of human FAK mRNA at the one-cell stage. (B) Histogram shows quantification of the rescue by percent of embryos exhibiting wild type (WT), mild FAK morphant or severe FAK morphant phenotypes (n > 48 embryos for each condition). (C) RT-PCR from control and FAK morphants embryo. FAK MO injection results in total loss of the wild type mRNA product and two truncated mRNA products. (D) Aberrant mRNA products were caused by intronic inclusions resulting in early nonsense codons. Schematics describe the basic structure of the FAK protein with

corresponding schematics for each truncation. In both cases, the truncation eliminates the necessary autophosphorylation site at Y397. Scale bars: A – a–e: 100μm

Fig. 6 Epithelial integrity and cytoskeleton are intact in FAK loss-of-function embryos

(A-C") Embryos fixed at 24 hpf were stained with anti-laminin antibody (green) and propidium iodide (red) to mark the nuclei, flat-mounted in glycerol, and imaged by scanning confocal microscopy. Regions boxed above are enlarged below. (A, A', A") Laminin staining is continuous at the basal surface in control embryos. (B – C") Two FAK morphants shown. Laminin staining is generally intact with small breaks. Cell nuclei cross the laminin staining suggesting extrusion from the epithelium. Arrows indicate nuclei crossing the line of the laminin staining. (D – E') Phalloidin stains actin in embryos fixed at 24 hpf. Regions boxed above are enlarged below. Actin is enriched at the basally constricting cells in control and FAK morphants. (F – G') Embryos injected with GFP-tubulin mRNA were imaged at 24 hpf. Images are full stacks reconstructed using Imaris (Bitplane). Microtubules are oriented in apical-basal arrays. (H, I) Antibody staining for ZO-1 (green) marks the apical junctions, localized at the apical epithelial surface. Propidium iodide (red) stains the nuclei. (H', I') ZO-1 staining without propidium iodide. Arrows mark small regions of aberrant ZO-1 staining, but junctions appear grossly intact. (J – K') aPKC antibody staining indicates that cell polarity is not disrupted in FAK morphants. Anterior is left. Arrowheads mark the MHBC. Scale bars: A–C" = 30μm; D–E' = 35μm; F–G' = 20μm; H–I' = 35μm; J–K' = 25μm

Fig. 7 Focal adhesion markers are not present in neural tube during basal constriction

(A – C) Wild type embryos stained with anti-vinculin antibody (green). Propidium iodide stains nuclei (red). (A, B) Vinculin staining is not present in the brain at 24 or 48 hpf, but marks somite boundaries in the same embryos. (C) Vinculin stains the brain and somite boundaries at 72 hpf. (D – F) Wild type embryos stained with anti-phospho-FAK^{Y861} antibody (green). Propidium iodide stains nuclei (red). (A, B) phospho-FAK^{Y861} staining is not present in the brain at 24 or 48 hpf, but marks somite boundaries in the same embryos. (C) phospho-FAK^{Y861} stains the brain and somite boundaries at 72 hpf. Scale bars: brain A, D = 80μm; B, E = 70μm; C, F = 70μm; somites A, D = 85μm; B, E = 80μm; C,F = 125μm

Fig. 8 FAK phosphorylation at the MHBC is dependent on Wnt5

(A, B) Wild type embryos fixed at 24 hpf and stained for phospho-FAK^{Y397}, flat-mounted in glycerol, and imaged by scanning confocal microscopy (n >8 each condition). (A) phospho-FAK^{Y397} staining is enriched at the MHBC and the somite boundaries in control morphants. (B) phospho-FAK^{Y397} enrichment at the MHBC is lost and all other staining reduced in Wnt5 morphants. Anterior is left. Arrowheads mark the MHBC. Scale bars: brain A, B = 25μm; somites A, B = 45μm

Fig. 9 Overexpression of dnGsk3β rescues basal constriction in Wnt5 and FAK loss-of-function embryos

(A, C, E, G, I, K) Brightfield images of embryos at 24 hpf co-injected with morpholino and mRNA as described. (B, B', D, D', F, F', H, H', J, J', L, L') Embryos co-injected with morpholino and mRNA as described with additional memGFP for imaging. Three cells at the MHBC are outlined below. (A, B, B') Control morphants co-injected with control mRNA exhibit normal MHBC morphogenesis and basal constriction (n = 6). (C, D, D') Control morphants co-injected with dnGsk3β mRNA exhibit an eyeless phenotype, but

undergo basal constriction normally (n = 9). (E, F, F') Wnt5 morphants co-injected with control mRNA exhibit abnormal MHBC morphogenesis, tail defects, and fail to undergo basal constriction (n = 6). (G, H, H') Wnt5 morphants co-injected with dnGsk3β mRNA exhibit a loss of eyes and tail defects, but basal constriction occurs normally (n = 6). (I, J, J') FAK morphants co-injected with control mRNA exhibit abnormal MHBC morphogenesis, tail defects, and fail to undergo basal constriction (n = 7). (K, L, L') FAK morphants co-injected with dnGsk3β mRNA have eyes, normal tail morphology, and undergo basal constriction (n = 9). (M) Histogram describes quantification of basal width of these embryos (6 cells in each of 3 embryos each condition). (N – Q) Overexpression of Gsk3β fails to rescue MHBC morphogenesis defect in FAK morphants. (N) Control morphants co-injected with control mRNA exhibit normal MHBC morphogenesis. (O) Control morphants co-injected with Gsk3β mRNA exhibit neurulation defects and a malformed tail. (P) FAK morphants co-injected with control mRNA exhibit abnormal MHBC morphogenesis and a malformed tail. (Q) FAK morphants co-injected with Gsk3β mRNA exhibit gross morphology defects throughout the embryo, including the MHBC. (R – T) Histograms describe quantification in terms of normal and abnormal embryos. Co-injection with dnGsk3β mRNA rescues the Wnt5 and FAK morphant phenotypes. Co-injection of Gsk3β mRNA fails to rescue the FAK morphant phenotypes (n > 25 embryos each condition). Anterior is left. Arrowheads mark the MHBC. MB, midbrain. HB, hindbrain. Scale bars: A, C, E, G, I, K, N–Q = 100μm; B, D, F, H, J, L = 26μm; B', D', F', H', J', L' = 13μm

Fig. 10 FAK does not appear to regulate basal constriction through signaling to Akt

(A) Loss of Akt does not prevent MHBC morphogenesis. Brightfield images of embryos at 24 hpf. (a) Control mRNA-injected embryos exhibit normal MHBC morphology. (b)

Embryos injected with 400 pg dominant-negative Akt (dnAkt) mRNA have a curved tail, but normal MHBC morphology. (B) Constitutively-active Akt (caAkt) does not rescue MHBC morphogenesis in FAK morphants. (a) Control morphants co-injected with control mRNA exhibit normal MHBC morphogenesis. (b) Control morphants co-injected with caAkt mRNA exhibit a neurulation defect characterized by tissue folds within the brain ventricles. (c) FAK morphants exhibit abnormal MHBC and tail morphogenesis. (d) FAK morphants co-injected with caAkt lose all brain ventricle morphology, fail to form an MHBC, and exhibit tail defects. Anterior is left. Arrowheads mark the MHBC. Scale bars: A–B = 100μm

Fig. 11 Model: Regulation of Basal Constriction

Shown here is a diagram of one possible model describing the regulation of basal constriction at the MHBC consistent with results presented here. Wnt5 activates FAK via signaling through an unknown receptor. This promotes basal constriction by downregulating Gsk3β.

FIGURE 1

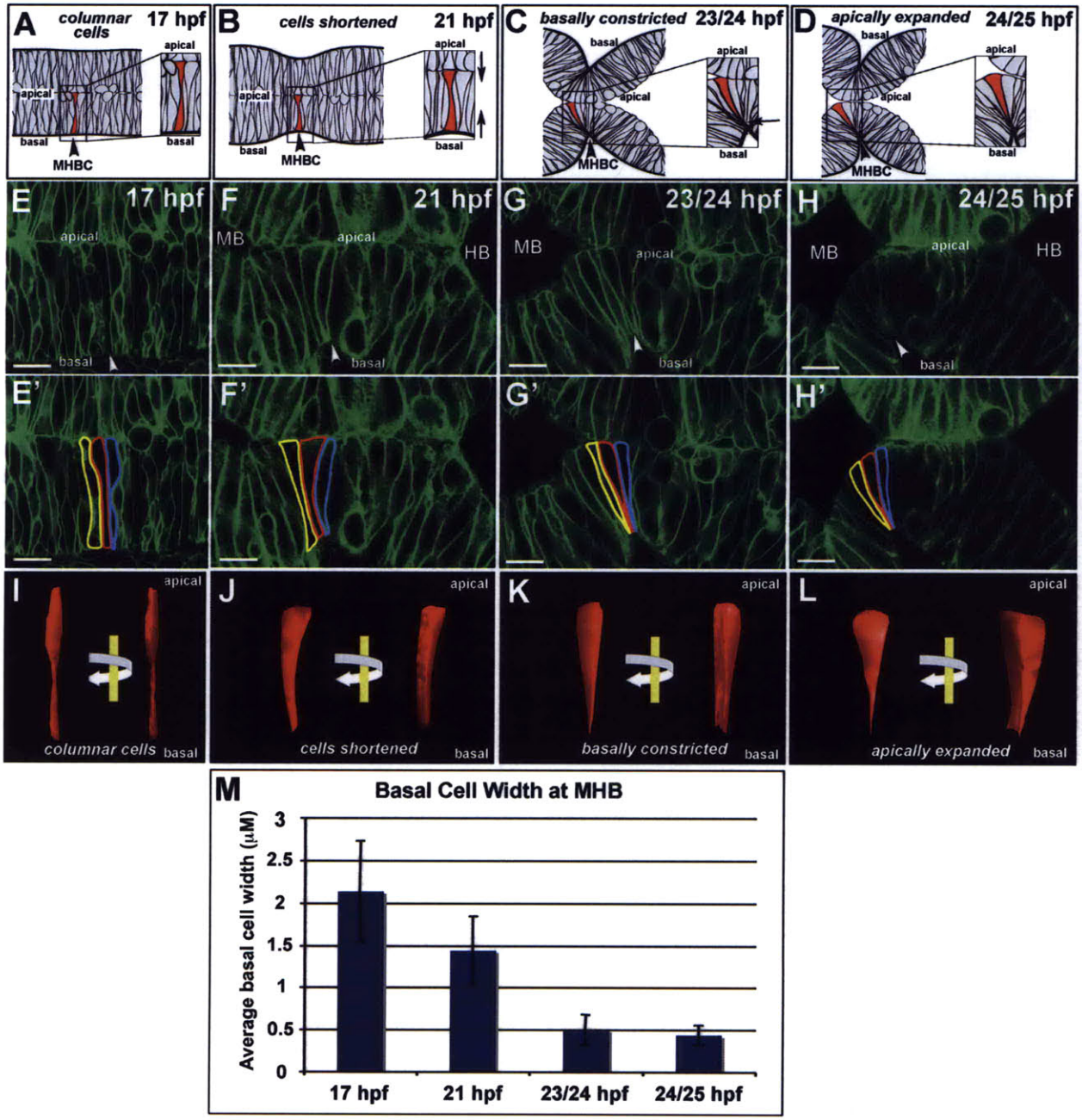
A columnar cells 17 hpf
apical
basal
MHBC
B cells shortened 21 hpf
C basally constricted 23/24 hpf
D apically expanded 24/25 hpf
E 17 hpf
F 21 hpf
G 23/24 hpf
H 24/25 hpf
MB
HB
E'
F'
G'
H'
I
J
K
L
columnar cells
cells shortened
basally constricted
apically expanded
M
Basal Cell Width at MHB
Average basal cell width (μM)
0
0.5
1
1.5
2
2.5
3
17 hpf
21 hpf
23/24 hpf
24/25 hpf

FIGURE 2

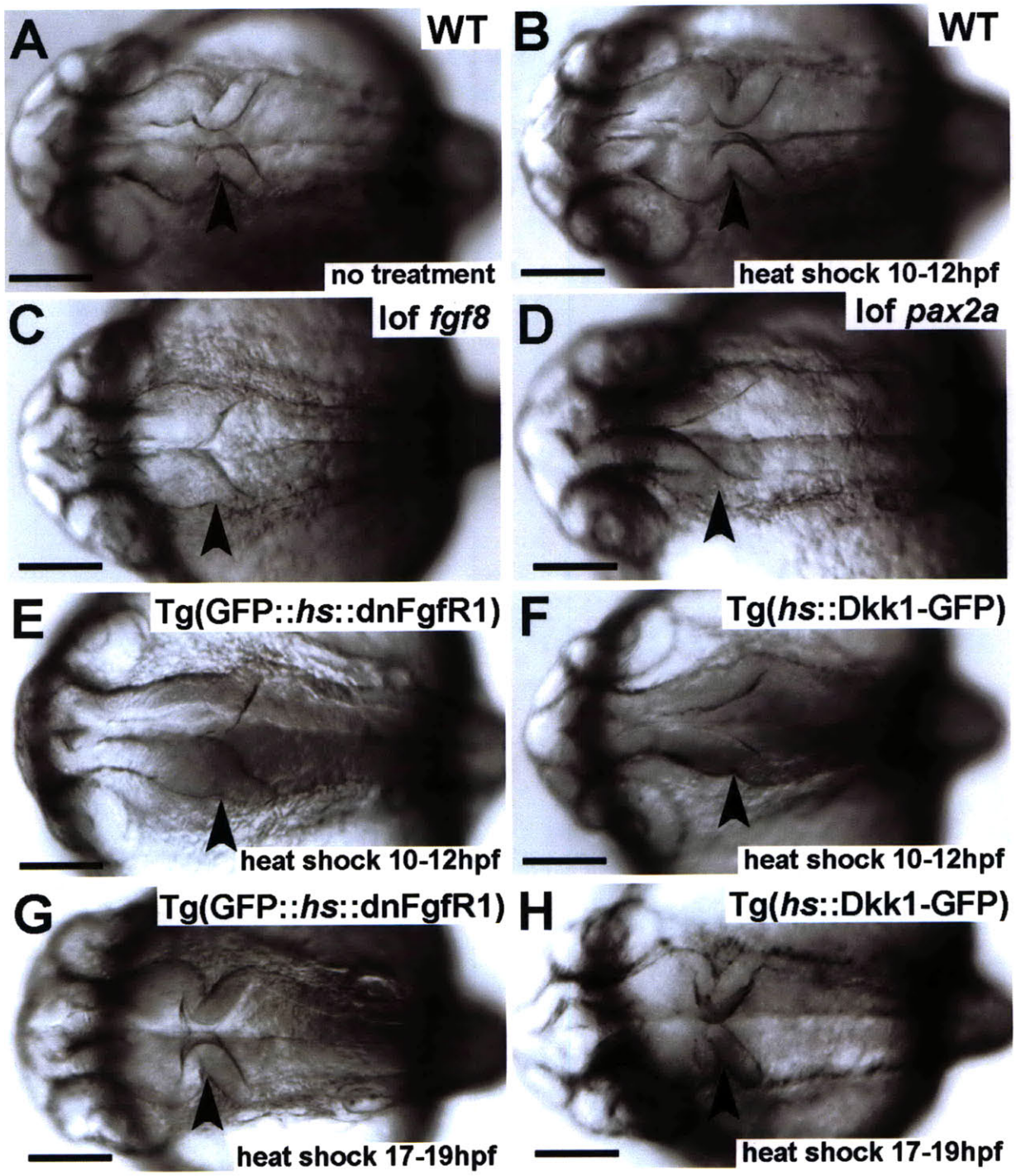
A
WT
no treatment
B
WT
heat shock 10-12hpf
C
lof *fgf8*
D
lof *pax2a*
E
Tg(GFP::*hs*::dnFgfR1)
heat shock 10-12hpf
F
Tg(*hs*::Dkk1-GFP)
heat shock 10-12hpf
G
Tg(GFP::*hs*::dnFgfR1)
heat shock 17-19hpf
H
Tg(*hs*::Dkk1-GFP)
heat shock 17-19hpf

FIGURE 3

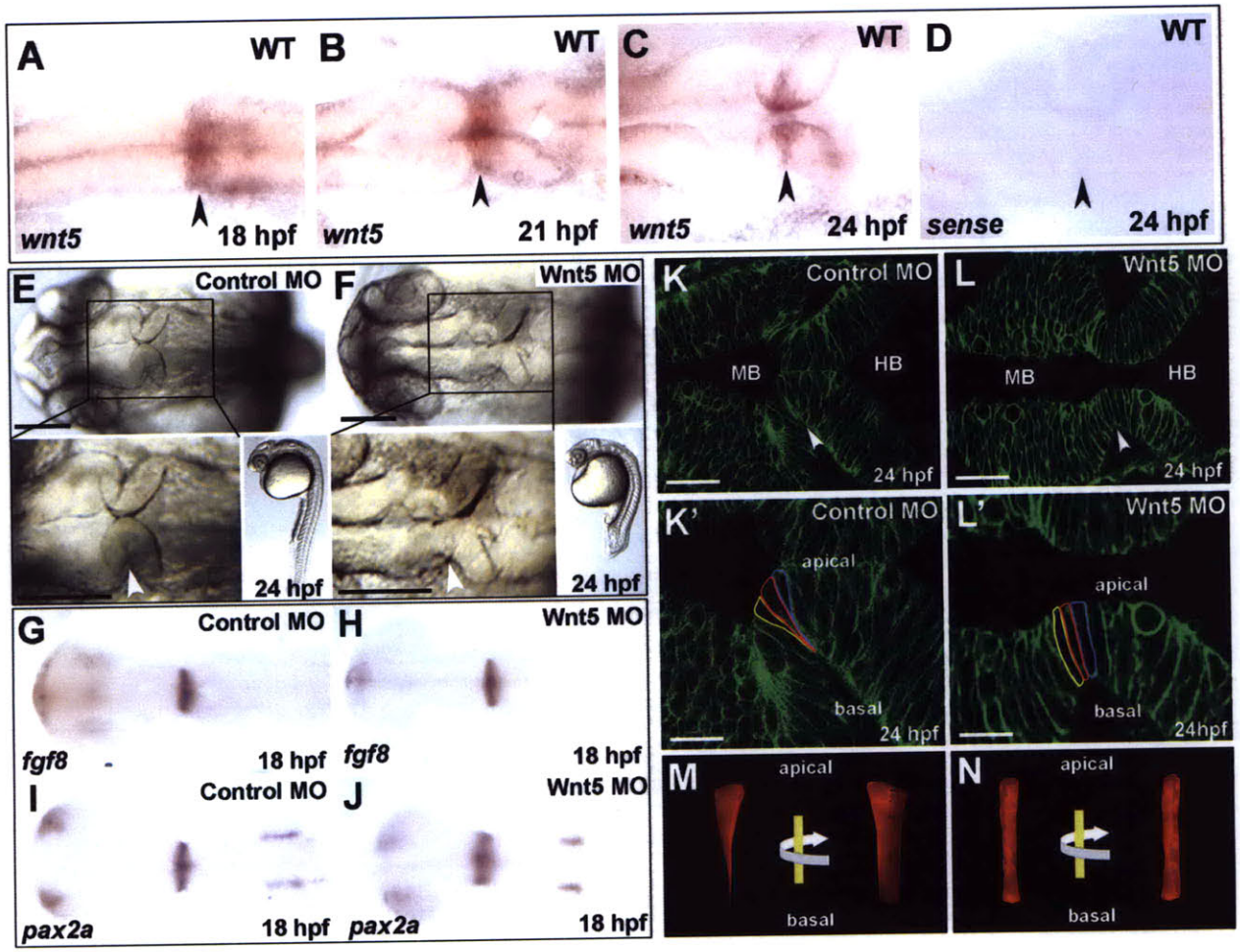
A
WT
wnt5
18 hpf
B
WT
wnt5
21 hpf
C
WT
wnt5
24 hpf
D
WT
sense
24 hpf
E
Control MO
24 hpf
F
Wnt5 MO
24 hpf
K
Control MO
MB
HB
24 hpf
L
Wnt5 MO
MB
HB
24 hpf
K'
Control MO
apical
basal
24 hpf
L'
Wnt5 MO
apical
basal
24hpf
G
Control MO
fgf8
18 hpf
H
Wnt5 MO
fgf8
18 hpf
I
Control MO
pax2a
18 hpf
J
Wnt5 MO
pax2a
18 hpf
M
apical
basal
N
apical
basal

FIGURE 4

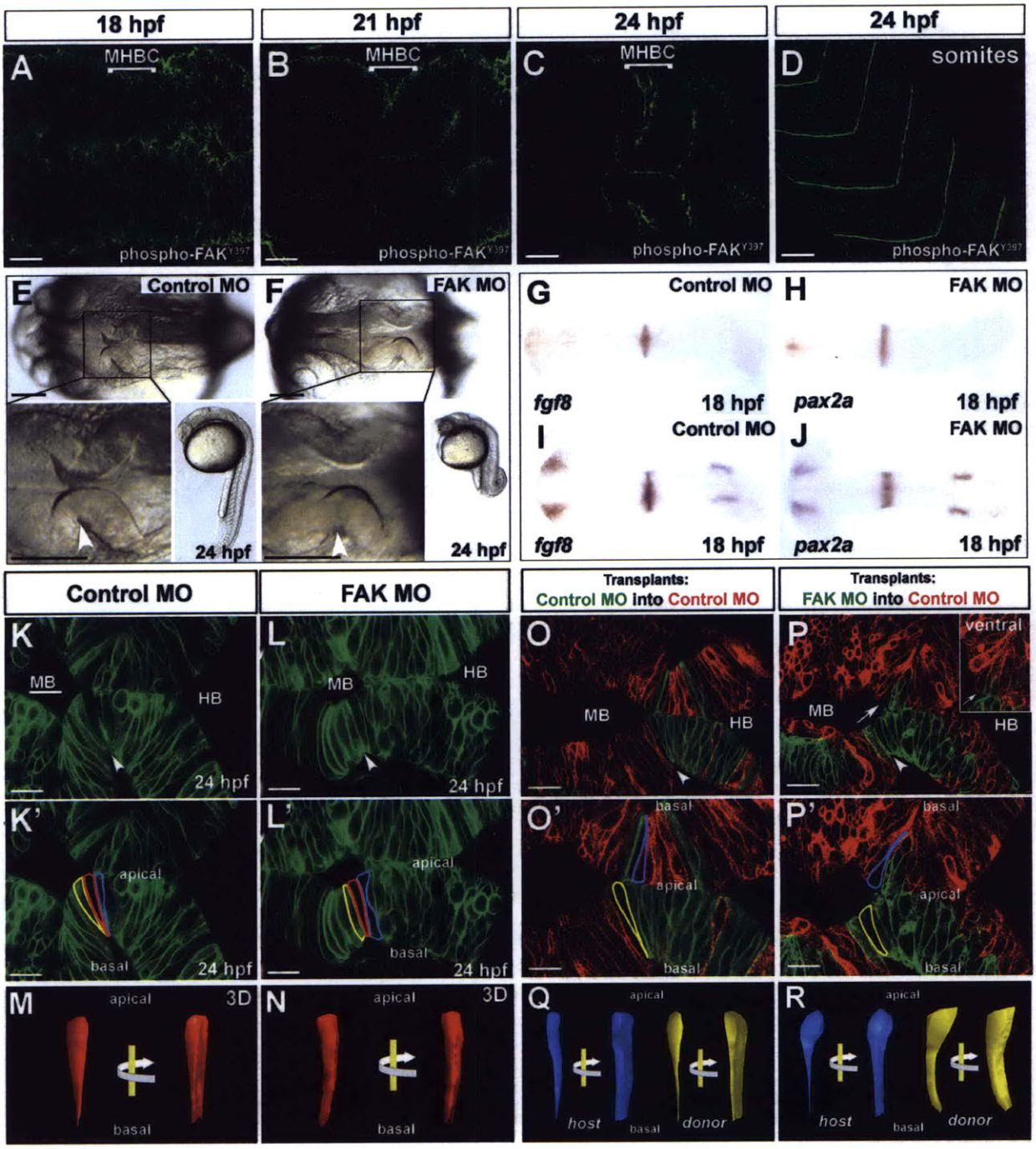
18 hpf
21 hpf
24 hpf
24 hpf
A
MHBC
phospho-FAK Y397
B
MHBC
phospho-FAK Y397
C
MHBC
phospho-FAK Y397
D
somites
phospho-FAK Y397
E
Control MO
24 hpf
F
FAK MO
24 hpf
G
Control MO
fgf8
18 hpf
H
FAK MO
pax2a
18 hpf
I
Control MO
fgf8
18 hpf
J
FAK MO
pax2a
18 hpf
Control MO
FAK MO
Transplants:
Control MO into Control MO
Transplants:
FAK MO into Control MO
K
MB
HB
24 hpf
L
MB
HB
24 hpf
O
MB
HB
P
ventral
MB
HB
K'
apical
basal
24 hpf
L'
apical
basal
24 hpf
O'
basal
apical
basal
P'
basal
apical
basal
M
apical
3D
basal
N
apical
3D
basal
Q
apical
host
basal
donor
R
apical
host
basal
donor

FIGURE 5

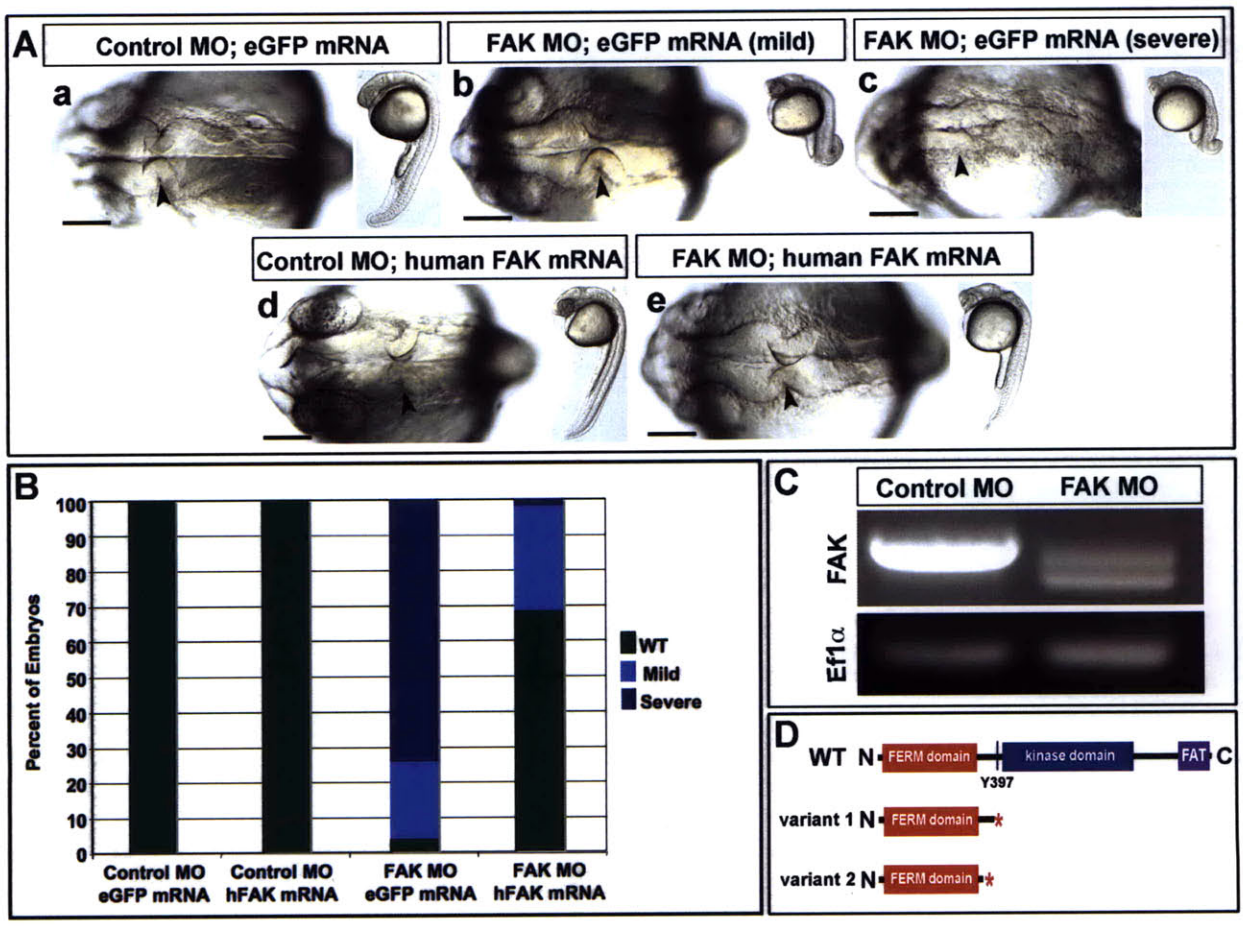
A
Control MO; eGFP mRNA
FAK MO; eGFP mRNA (mild)
FAK MO; eGFP mRNA (severe)
a
b
c
Control MO; human FAK mRNA
FAK MO; human FAK mRNA
d
e
B
Percent of Embryos
100
90
80
70
60
50
40
30
20
10
0
Control MO eGFP mRNA
Control MO hFAK mRNA
FAK MO eGFP mRNA
FAK MO hFAK mRNA
WT
Mild
Severe
C
Control MO
FAK MO
FAK
Ef1α
D
WT N
FERM domain
kinase domain
FAT
C
Y397
variant 1 N
FERM domain
variant 2 N
FERM domain

FIGURE 6

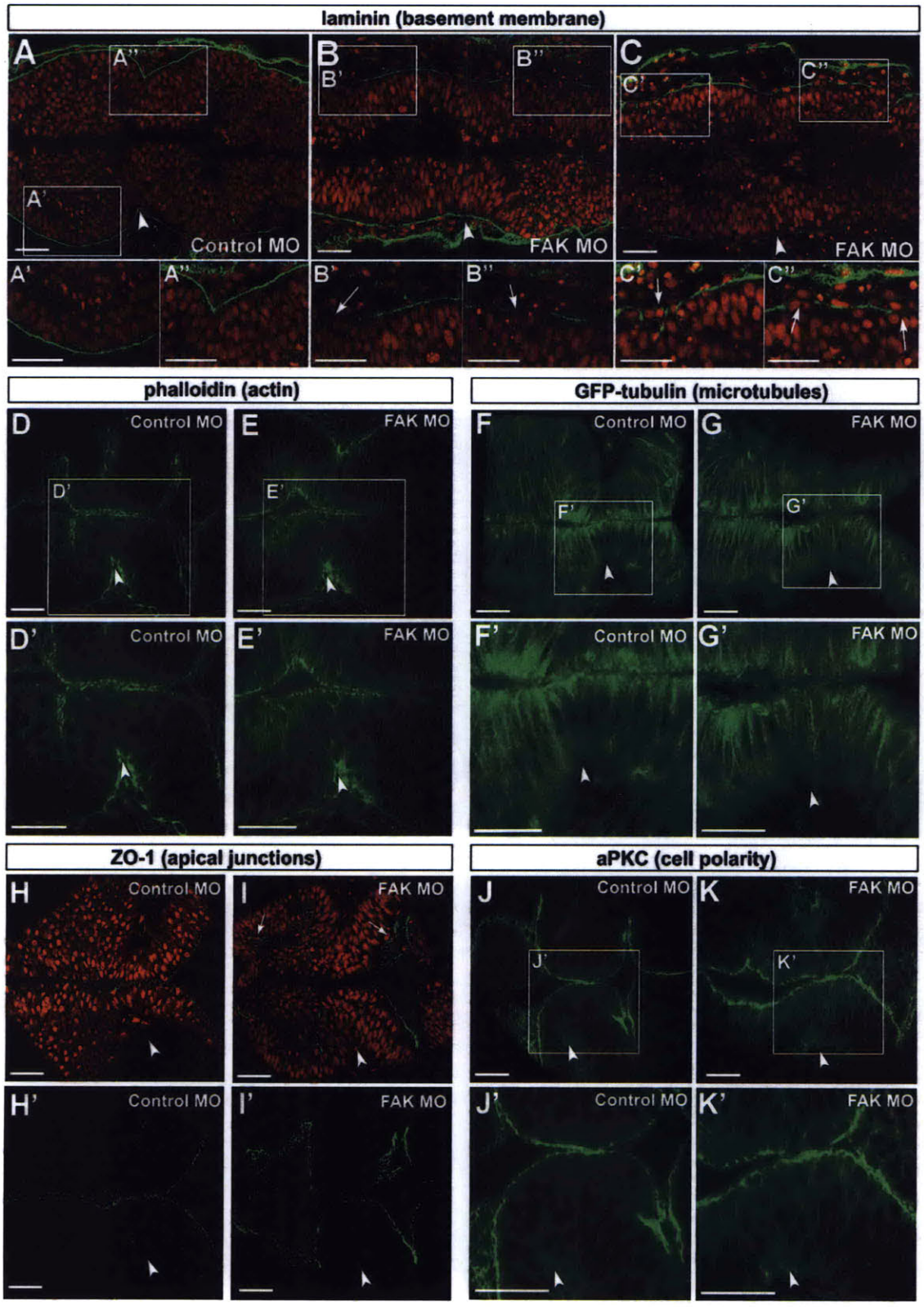
laminin (basement membrane)
A
A''
A'
Control MO
B
B'
B''
FAK MO
C
C'
C''
FAK MO
A'
A''
B'
B''
C'
C''
phalloidin (actin)
D
Control MO
D'
E
FAK MO
E'
D'
Control MO
E'
FAK MO
GFP-tubulin (microtubules)
F
Control MO
F'
G
FAK MO
G'
F'
Control MO
G'
FAK MO
ZO-1 (apical junctions)
H
Control MO
I
FAK MO
H'
Control MO
I'
FAK MO
aPKC (cell polarity)
J
Control MO
J'
K
FAK MO
K'
J'
Control MO
K'
FAK MO

FIGURE 7

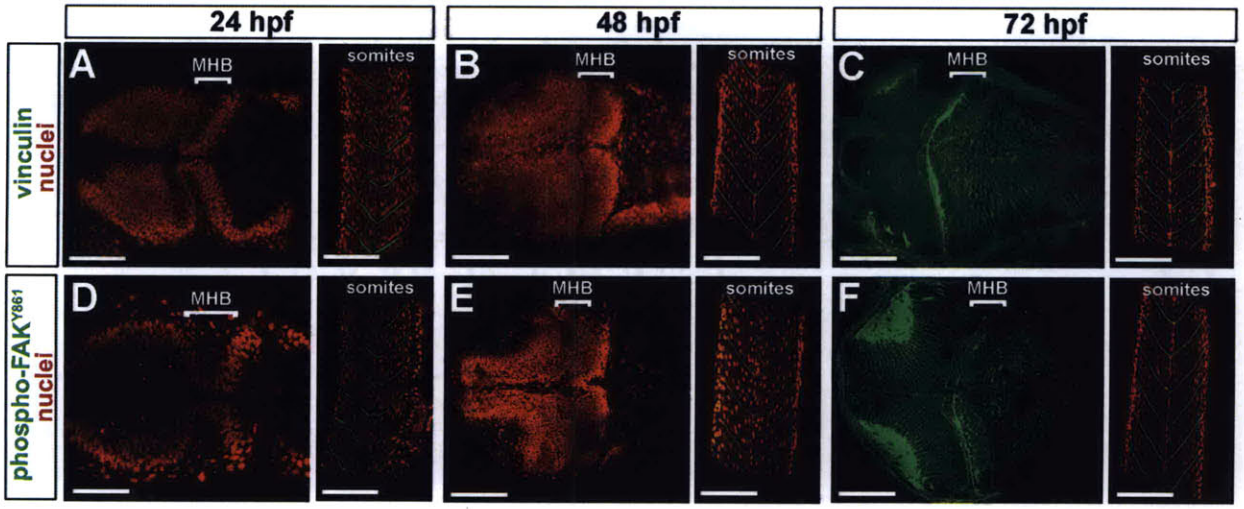
24 hpf
48 hpf
72 hpf
vinculin
nuclei
phospho-FAK Y861
nuclei
A
B
C
D
E
F
MHB
somites

FIGURE 8

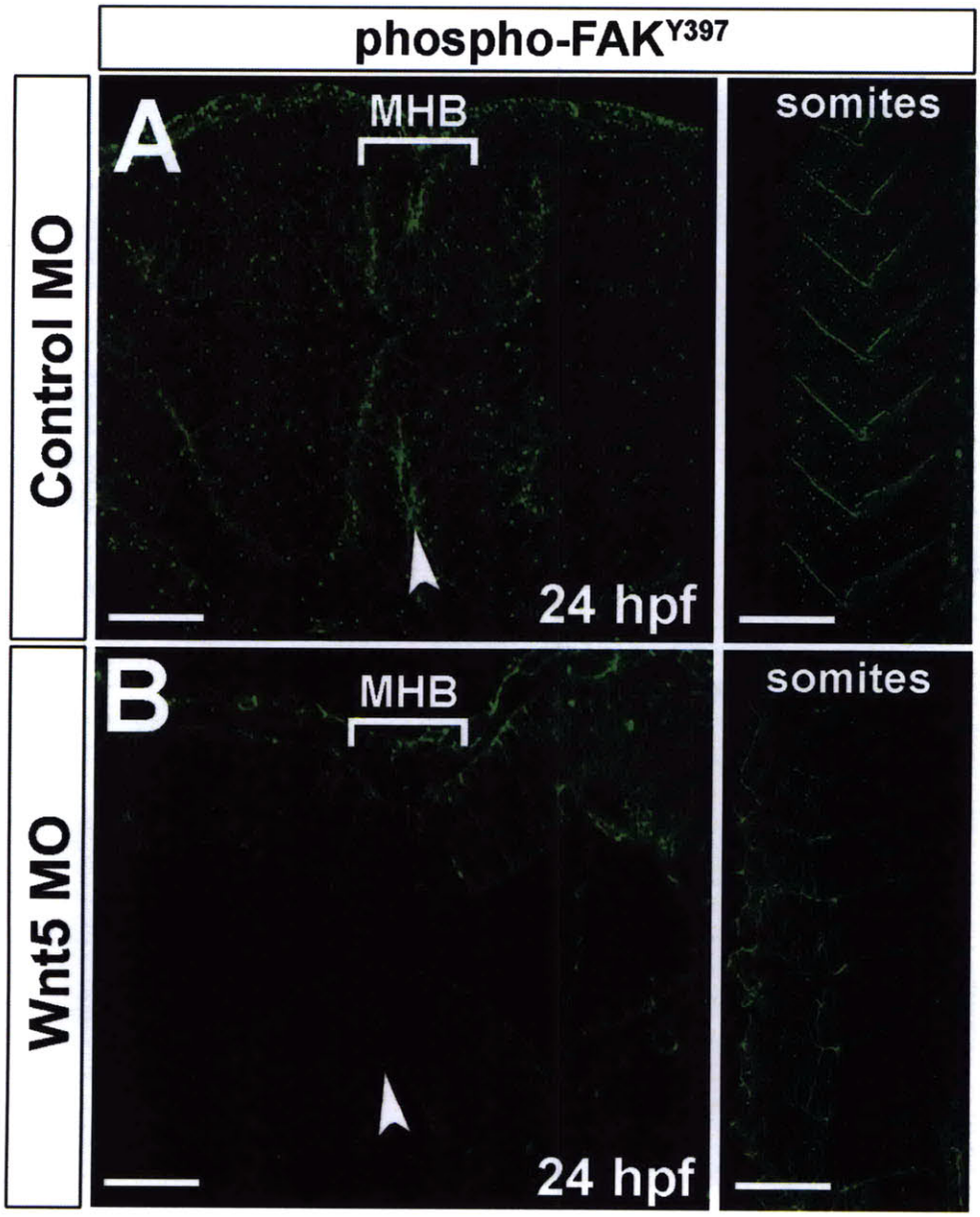
phospho-FAK^{Y397}
Control MO
A
MHB
somites
24 hpf
Wnt5 MO
B
MHB
somites
24 hpf

FIGURE 9

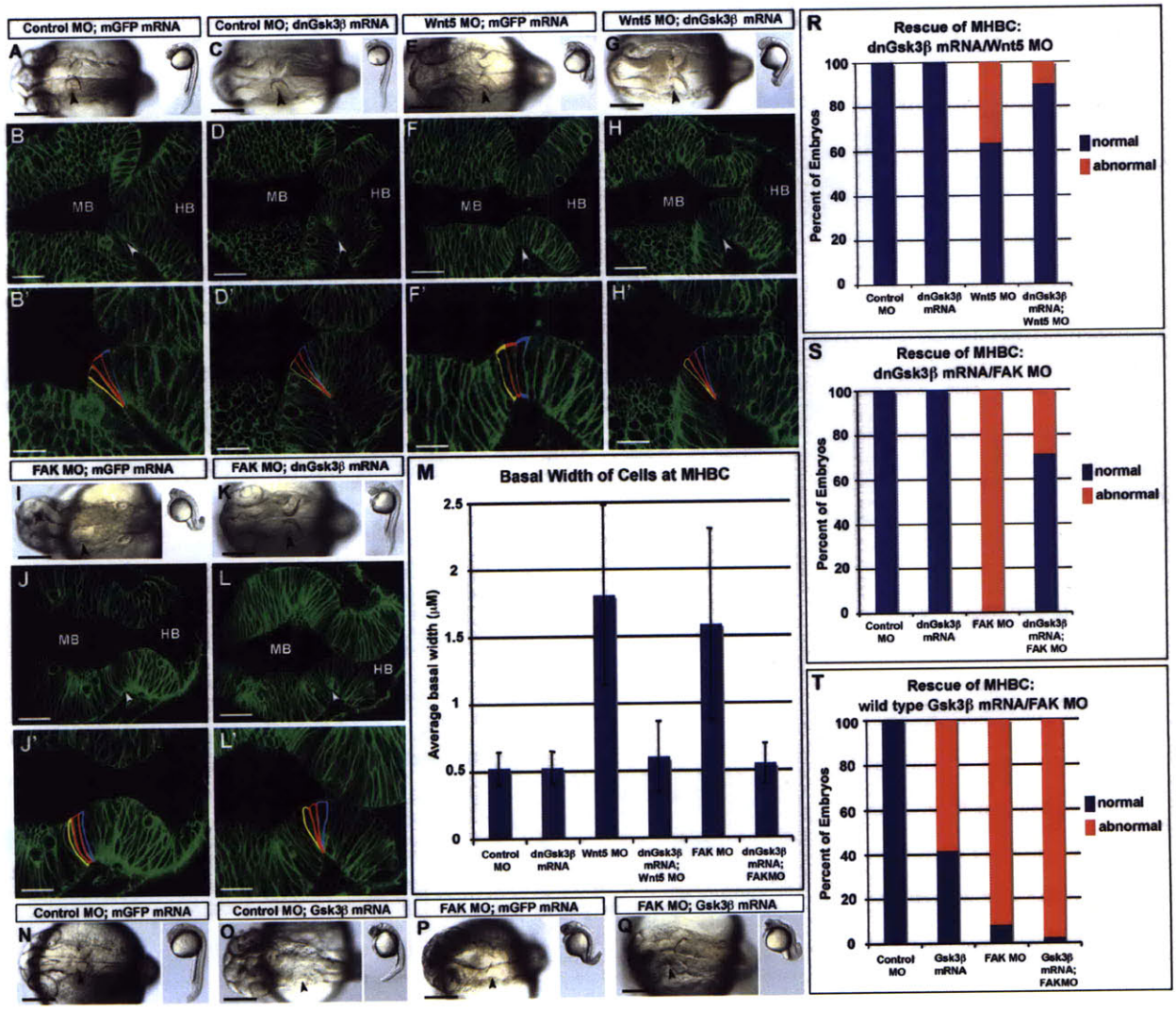
Control MO; mGFP mRNA
Control MO; dnGsk3β mRNA
Wnt5 MO; mGFP mRNA
Wnt5 MO; dnGsk3β mRNA
A
C
E
G
B
D
F
H
MB
HB
B'
D'
F'
H'
FAK MO; mGFP mRNA
FAK MO; dnGsk3β mRNA
I
K
J
L
J'
L'
M
Basal Width of Cells at MHBC
Average basal width (μM)
2.5
2
1.5
1
0.5
0
Control MO
dnGsk3β mRNA
Wnt5 MO
dnGsk3β mRNA; Wnt5 MO
FAK MO
dnGsk3β mRNA; FAKMO
Control MO; mGFP mRNA
Control MO; Gsk3β mRNA
FAK MO; mGFP mRNA
FAK MO; Gsk3β mRNA
N
O
P
Q
R
Rescue of MHBC:
dnGsk3β mRNA/Wnt5 MO
Percent of Embryos
100
80
60
40
20
0
normal
abnormal
Control MO
dnGsk3β mRNA
Wnt5 MO
dnGsk3β mRNA; Wnt5 MO
S
Rescue of MHBC:
dnGsk3β mRNA/FAK MO
dnGsk3β mRNA; FAK MO
T
Rescue of MHBC:
wild type Gsk3β mRNA/FAK MO
Gsk3β mRNA
Gsk3β mRNA; FAKMO

FIGURE 10

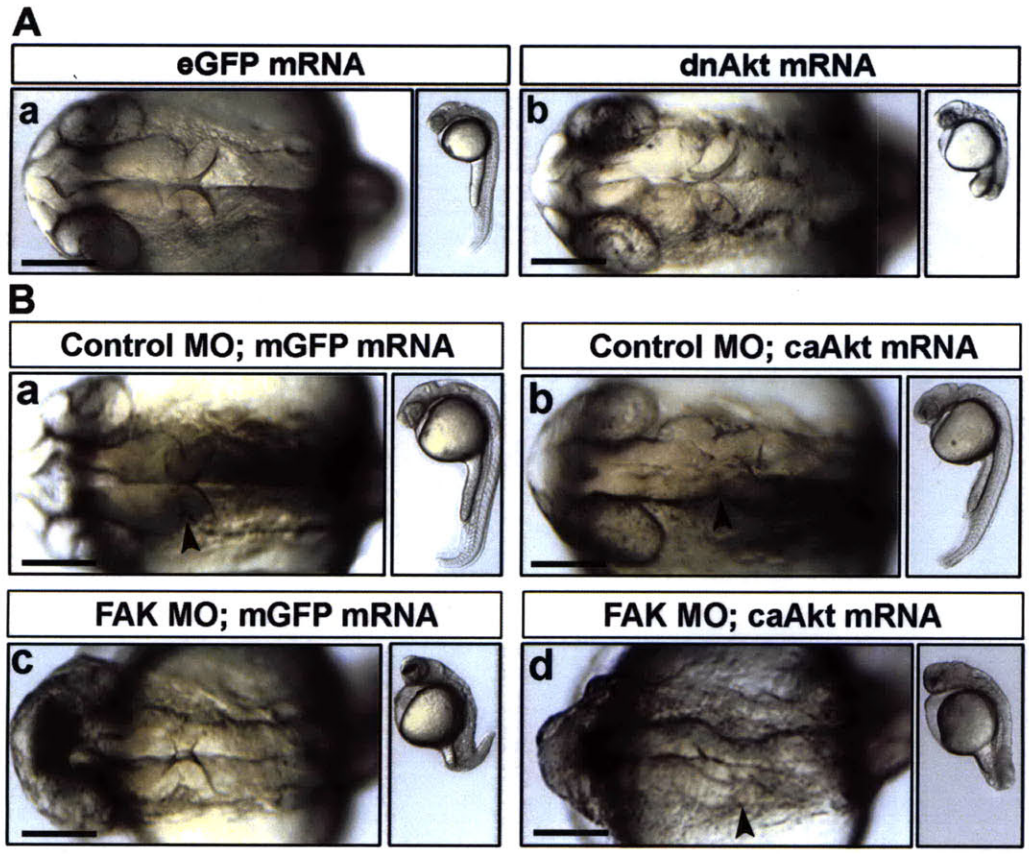
A
eGFP mRNA
dnAkt mRNA
a
b
B
Control MO; mGFP mRNA
Control MO; caAkt mRNA
a
b
FAK MO; mGFP mRNA
FAK MO; caAkt mRNA
c
d

FIGURE 11

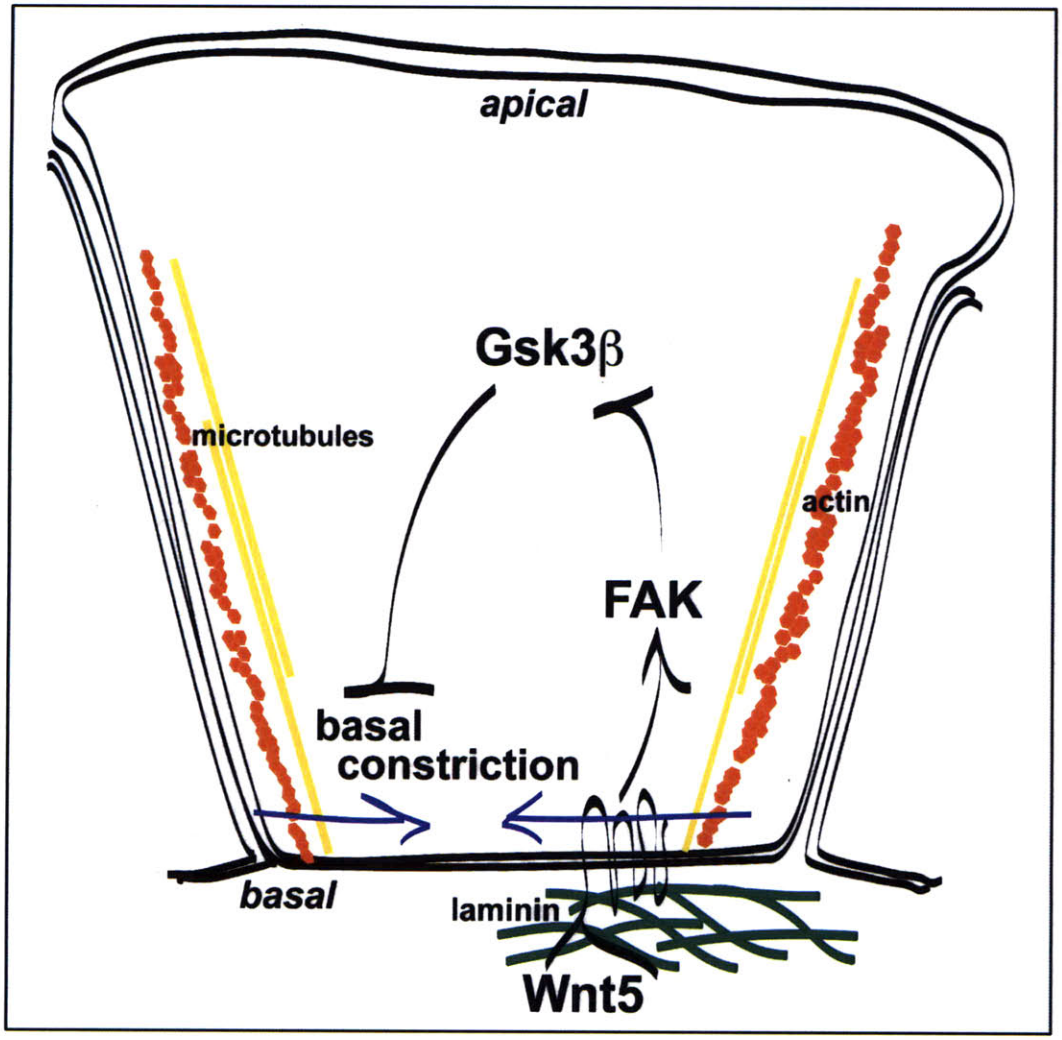
apical
Gsk3β
microtubules
actin
FAK
basal
constriction
basal
laminin
Wnt5

REFERENCES

Angers, S. and Moon, R. T. (2009). Proximal events in Wnt signal transduction. *Nat Rev Mol Cell Biol* **10**, 468-77.

Avizienyte, E. and Frame, M. C. (2005). Src and FAK signalling controls adhesion fate and the epithelial-to-mesenchymal transition. *Curr Opin Cell Biol* **17**, 542-7.

Brand, M., Heisenberg, C. P., Jiang, Y. J., Beuchle, D., Lun, K., Furutani-Seiki, M., Granato, M., Haffter, P., Hammerschmidt, M., Kane, D. A. et al. (1996). Mutations in zebrafish genes affecting the formation of the boundary between midbrain and hindbrain. *Development* **123**, 179-90.

Buckles, G. R., Thorpe, C. J., Ramel, M. C. and Lekven, A. C. (2004). Combinatorial Wnt control of zebrafish midbrain-hindbrain boundary formation. *Mech Dev* **121**, 437-47.

Burgess, S., Reim, G., Chen, W., Hopkins, N. and Brand, M. (2002). The zebrafish spiel-ohne-grenzen (spg) gene encodes the POU domain protein Pou2 related to mammalian Oct4 and is essential for formation of the midbrain and hindbrain, and for pre-gastrula morphogenesis. *Development* **129**, 905-16.

Cadigan, K. M. and Liu, Y. I. (2006). Wnt signaling: complexity at the surface. *J Cell Sci* **119**, 395-402.

Calalb, M. B., Polte, T. R. and Hanks, S. K. (1995). Tyrosine phosphorylation of focal adhesion kinase at sites in the catalytic domain regulates kinase activity: a role for Src family kinases. *Mol Cell Biol* **15**, 954-63.

Carisey, A. and Ballestrem, C. (2010). Vinculin, an adapter protein in control of cell adhesion signalling. *Eur J Cell Biol.*

Choi, S. C. and Sokol, S. Y. (2009). The involvement of lethal giant larvae and Wnt signaling in bottle cell formation in Xenopus embryos. *Dev Biol* **336**, 68-75.

Ciani, L., Krylova, O., Smalley, M. J., Dale, T. C. and Salinas, P. C. (2004). A divergent canonical WNT-signaling pathway regulates microtubule dynamics: dishevelled signals locally to stabilize microtubules. *J Cell Biol* **164**, 243-53.

Ciruna, B., Jenny, A., Lee, D., Mlodzik, M. and Schier, A. F. (2006). Planar cell polarity signalling couples cell division and morphogenesis during neurulation. *Nature* **439**, 220-4.

Clayton, E. L., Sue, N., Smillie, K. J., O'Leary, T., Bache, N., Cheung, G., Cole, A. R., Wyllie, D. J., Sutherland, C., Robinson, P. J. et al. (2010). Dynamin I phosphorylation by GSK3 controls activity-dependent bulk endocytosis of synaptic vesicles. *Nat Neurosci* **13**, 845-51.

Cohen, E. D., Mariol, M. C., Wallace, R. M., Weyers, J., Kamberov, Y. G., Pradel, J. and Wilder, E. L. (2002). DWnt4 regulates cell movement and focal adhesion kinase during Drosophila ovarian morphogenesis. *Dev Cell* **2**, 437-48.

Crawford, B. D., Henry, C. A., Clason, T. A., Becker, A. L. and Hille, M. B. (2003). Activity and distribution of paxillin, focal adhesion kinase, and cadherin indicate cooperative roles during zebrafish morphogenesis. *Mol Biol Cell* **14**, 3065-81.

Cross, D. A., Alessi, D. R., Cohen, P., Andjelkovich, M. and Hemmings, B. A. (1995). Inhibition of glycogen synthase kinase-3 by insulin mediated by protein kinase B. *Nature* **378**, 785-9.

Crossley, P. H., Martinez, S. and Martin, G. R. (1996). Midbrain development induced by FGF8 in the chick embryo. *Nature* **380**, 66-8.

Doble, B. W. and Woodgett, J. R. (2003). GSK-3: tricks of the trade for a multi-tasking kinase. *J Cell Sci* **116**, 1175-86.

Etienne-Manneville, S. and Hall, A. (2003). Cdc42 regulates GSK-3beta and adenomatous polyposis coli to control cell polarity. *Nature* **421**, 753-6.

Ezratty, E. J., Partridge, M. A. and Gundersen, G. G. (2005). Microtubule-induced focal adhesion disassembly is mediated by dynamin and focal adhesion kinase. *Nat Cell Biol* **7**, 581-90.

Frisch, S. M., Vuori, K., Kelaita, D. and Sicks, S. (1996). A role for Jun-N-terminal kinase in anoikis; suppression by bcl-2 and crmA. *J Cell Biol* **135**, 1377-82.

Gao, C. and Chen, Y. G. (2010). Dishevelled: The hub of Wnt signaling. *Cell Signal* **22**, 717-27.

Giancotti, F. G. and Ruoslahti, E. (1999). Integrin signaling. *Science* **285**, 1028-32.

Glinka, A., Wu, W., Delius, H., Monaghan, A. P., Blumenstock, C. and Niehrs, C. (1998). Dickkopf-1 is a member of a new family of secreted proteins and functions in head induction. *Nature* **391**, 357-62.

Graeden, E. and Sive, H. (2009). Live imaging of the zebrafish embryonic brain by confocal microscopy. *J Vis Exp.*

Gumbiner, B. (1987). Structure, biochemistry, and assembly of epithelial tight junctions. *Am J Physiol* **253**, C749-58.

Gupton, S. L. and Gertler, F. B. (2010). Integrin signaling switches the cytoskeletal and exocytic machinery that drives neuritogenesis. *Dev Cell* **18**, 725-36.

Gutzman, J. H., Graeden, E. G., Lowery, L. A., Holley, H. S. and Sive, H. (2008). Formation of the zebrafish midbrain-hindbrain boundary constriction requires laminin-dependent basal constriction. *Mech Dev* **125**, 974-83.

Gutzman, J. H. and Sive, H. (2010). Epithelial relaxation mediated by the myosin phosphatase regulator Mypt1 is required for brain ventricle lumen expansion and hindbrain morphogenesis. *Development* **137**, 795-804.

Haigo, S. L., Hildebrand, J. D., Harland, R. M. and Wallingford, J. B. (2003). Shroom induces apical constriction and is required for hingepoint formation during neural tube closure. *Curr Biol* **13**, 2125-37.

Hammerschmidt, M., Pelegri, F., Mullins, M. C., Kane, D. A., Brand, M., van Eeden, F. J., Furutani-Seiki, M., Granato, M., Haffter, P., Heisenberg, C. P. et al. (1996). Mutations affecting morphogenesis during gastrulation and tail formation in the zebrafish, Danio rerio. *Development* **123**, 143-51.

Hardy, K. M., Garriock, R. J., Yatskievych, T. A., D'Agostino, S. L., Antin, P. B. and Krieg, P. A. (2008). Non-canonical Wnt signaling through Wnt5a/b and a novel Wnt11 gene, Wnt11b, regulates cell migration during avian gastrulation. *Dev Biol* **320**, 391-401.

Harland, R. M. (1991). In situ hybridization: an improved whole-mount method for Xenopus embryos. *Methods Cell Biol* **36**, 685-95.

Hidalgo-Sanchez, M., Millet, S., Bloch-Gallego, E. and Alvarado-Mallart, R. M. (2005). Specification of the meso-isthmo-cerebellar region: the Otx2/Gbx2 boundary. *Brain Res Brain Res Rev* **49**, 134-49.

Hollyday, M., McMahon, J. A. and McMahon, A. P. (1995). Wnt expression patterns in chick embryo nervous system. *Mech Dev* **52**, 9-25.

Horwitz, A., Duggan, K., Buck, C., Beckerle, M. C. and Burridge, K. (1986). Interaction of plasma membrane fibronectin receptor with talin--a transmembrane linkage. *Nature* **320**, 531-3.

Huang, C. Y., Liang, C. M., Chu, C. L. and Liang, S. M. (2009). Albumin fibrillization induces apoptosis via integrin/FAK/Akt pathway. *BMC Biotechnol* **9**, 2.

Huang, D., Cheung, A. T., Parsons, J. T. and Bryer-Ash, M. (2002). Focal adhesion kinase (FAK) regulates insulin-stimulated glycogen synthesis in hepatocytes. *J Biol Chem* **277**, 18151-60.

Hur, E. M. and Zhou, F. Q. (2010). GSK3 signalling in neural development. *Nat Rev Neurosci* **11**, 539-51.

Ilic, D., Kovacic, B., Johkura, K., Schlaepfer, D. D., Tomasevic, N., Han, Q., Kim, J. B., Howerton, K., Baumbusch, C., Ogiwara, N. et al. (2004). FAK promotes organization of fibronectin matrix and fibrillar adhesions. *J Cell Sci* **117**, 177-87.

Izumi, Y., Hirose, T., Tamai, Y., Hirai, S., Nagashima, Y., Fujimoto, T., Tabuse, Y., Kemphues, K. J. and Ohno, S. (1998). An atypical PKC directly associates and colocalizes at the epithelial tight junction with ASIP, a mammalian homologue of Caenorhabditis elegans polarity protein PAR-3. *J Cell Biol* **143**, 95-106.

Joyner, A. L. (1996). Engrailed, Wnt and Pax genes regulate midbrain--hindbrain development. *Trends Genet* **12**, 15-20.

Karner, C. M., Chirumamilla, R., Aoki, S., Igarashi, P., Wallingford, J. B. and Carroll, T. J. (2009). Wnt9b signaling regulates planar cell polarity and kidney tubule morphogenesis. *Nat Genet* **41**, 793-9.

Kazanskaya, O., Glinka, A. and Niehrs, C. (2000). The role of Xenopus dickkopf1 in prechordal plate specification and neural patterning. *Development* **127**, 4981-92.

Kilian, B., Mansukoski, H., Barbosa, F. C., Ulrich, F., Tada, M. and Heisenberg, C. P. (2003). The role of Ppt/Wnt5 in regulating cell shape and movement during zebrafish gastrulation. *Mech Dev* **120**, 467-76.

Kim, H. J., Schleiffarth, J. R., Jessurun, J., Sumanas, S., Petryk, A., Lin, S. and Ekker, S. C. (2005). Wnt5 signaling in vertebrate pancreas development. *BMC Biol* **3**, 23.

Kimmel, C. B., Ballard, W. W., Kimmel, S. R., Ullmann, B. and Schilling, T. F. (1995). Stages of embryonic development of the zebrafish. *Dev Dyn* **203**, 253-310.

Komiya, Y. and Habas, R. (2008). Wnt signal transduction pathways. *Organogenesis* **4**, 68-75.

Kotani, K., Ogawa, W., Hino, Y., Kitamura, T., Ueno, H., Sano, W., Sutherland, C., Granner, D. K. and Kasuga, M. (1999). Dominant negative forms of Akt (protein kinase B) and atypical protein kinase Clambda do not prevent insulin inhibition of phosphoenolpyruvate carboxykinase gene transcription. *J Biol Chem* **274**, 21305-12.

Krauss, S., Johansen, T., Korzh, V. and Fjose, A. (1991). Expression of the zebrafish paired box gene pax[zf-b] during early neurogenesis. *Development* **113**, 1193-206.

Kurayoshi, M., Oue, N., Yamamoto, H., Kishida, M., Inoue, A., Asahara, T., Yasui, W. and Kikuchi, A. (2006). Expression of Wnt-5a is correlated with aggressiveness of gastric cancer by stimulating cell migration and invasion. *Cancer Res* **66**, 10439-48.

Lee, Y., Grill, S., Sanchez, A., Murphy-Ryan, M. and Poss, K. D. (2005). Fgf signaling instructs position-dependent growth rate during zebrafish fin regeneration. *Development* **132**, 5173-83.

Lekven, A. C., Buckles, G. R., Kostakis, N. and Moon, R. T. (2003). Wnt1 and wnt10b function redundantly at the zebrafish midbrain-hindbrain boundary. *Dev Biol* **254**, 172-87.

Lele, Z., Bakkers, J. and Hammerschmidt, M. (2001). Morpholino phenocopies of the swirl, snailhouse, somitabun, minifin, silberblick, and pipetail mutations. *Genesis* **30**, 190-4.

Li, L., Okura, M. and Imamoto, A. (2002). Focal adhesions require catalytic activity of Src family kinases to mediate integrin-matrix adhesion. *Mol Cell Biol* **22**, 1203-17.

Louvi, A., Alexandre, P., Metin, C., Wurst, W. and Wassef, M. (2003). The isthmic neuroepithelium is essential for cerebellar midline fusion. *Development* **130**, 5319-30.

Lowery, L. A. and Sive, H. (2005). Initial formation of zebrafish brain ventricles occurs independently of circulation and requires the nagie oko and snakehead/atp1a1a.1 gene products. *Development* **132**, 2057-67.

Lun, K. and Brand, M. (1998). A series of no isthmus (noi) alleles of the zebrafish pax2.1 gene reveals multiple signaling events in development of the midbrain-hindbrain boundary. *Development* **125**, 3049-62.

Martin, A. C., Kaschube, M. and Wieschaus, E. F. (2009). Pulsed contractions of an actin-myosin network drive apical constriction. *Nature* **457**, 495-9.

Martinez, S., Crossley, P. H., Cobos, I., Rubenstein, J. L. and Martin, G. R. (1999). FGF8 induces formation of an ectopic isthmic organizer and isthmocerebellar development via a repressive effect on Otx2 expression. *Development* **126**, 1189-200.

Martinez-Morales, J. R., Rembold, M., Greger, K., Simpson, J. C., Brown, K. E., Quiring, R., Pepperkok, R., Martin-Bermudo, M. D., Himmelbauer, H. and Wittbrodt, J. (2009). ojoplano-mediated basal constriction is essential for optic cup morphogenesis. *Development* **136**, 2165-75.

Matsumoto, S., Fumoto, K., Okamoto, T., Kaibuchi, K. and Kikuchi, A. (2010). Binding of APC and dishevelled mediates Wnt5a-regulated focal adhesion dynamics in migrating cells. *EMBO J* **29**, 1192-204.

Miner, J. H. and Yurchenco, P. D. (2004). Laminin functions in tissue morphogenesis. *Annu Rev Cell Dev Biol* **20**, 255-84.

Mitra, S. K., Hanson, D. A. and Schlaepfer, D. D. (2005). Focal adhesion kinase: in command and control of cell motility. *Nat Rev Mol Cell Biol* **6**, 56-68.

Montero-Balaguer, M., Lang, M. R., Sachdev, S. W., Knappmeyer, C., Stewart, R. A., De La Guardia, A., Hatzopoulos, A. K. and Knapik, E. W. (2006). The mother superior mutation ablates foxd3 activity in neural crest progenitor cells and depletes neural crest derivatives in zebrafish. *Dev Dyn* **235**, 3199-212.

Mullins, M. C., Hammerschmidt, M., Haffter, P. and Nusslein-Volhard, C. (1994). Large-scale mutagenesis in the zebrafish: in search of genes controlling development in a vertebrate. *Curr Biol* **4**, 189-202.

Parsons, J. T. (2003). Focal adhesion kinase: the first ten years. *J Cell Sci* **116**, 1409-16.

Parsons, J. T., Horwitz, A. R. and Schwartz, M. A. (2010). Cell adhesion: integrating cytoskeletal dynamics and cellular tension. *Nat Rev Mol Cell Biol* **11**, 633-43.

Philipp, I., Aufschnaiter, R., Ozbek, S., Pontasch, S., Jenewein, M., Watanabe, H., Rentzsch, F., Holstein, T. W. and Hobmayer, B. (2009).

Wnt/beta-catenin and noncanonical Wnt signaling interact in tissue evagination in the simple eumetazoan Hydra. *Proc Natl Acad Sci U S A* **106**, 4290-5.

Pierce, S. B. and Kimelman, D. (1995). Regulation of Spemann organizer formation by the intracellular kinase Xgsk-3. *Development* **121**, 755-65.

Pilot, F. and Lecuit, T. (2005). Compartmentalized morphogenesis in epithelia: from cell to tissue shape. *Dev Dyn* **232**, 685-94.

Puelles, L. and Martinez-de-la-Torre, M. (1987). Autoradiographic and Golgi study on the early development of n. isthmi principalis and adjacent grisea in the chick embryo: a tridimensional viewpoint. *Anat Embryol (Berl)* **176**, 19-34.

Ramaswamy, S., Nakamura, N., Vazquez, F., Batt, D. B., Perera, S., Roberts, T. M. and Sellers, W. R. (1999). Regulation of G1 progression by the PTEN tumor suppressor protein is linked to inhibition of the phosphatidylinositol 3-kinase/Akt pathway. *Proc Natl Acad Sci U S A* **96**, 2110-5.

Reifers, F., Bohli, H., Walsh, E. C., Crossley, P. H., Stainier, D. Y. and Brand, M. (1998). Fgf8 is mutated in zebrafish acerebellar (ace) mutants and is required for maintenance of midbrain-hindbrain boundary development and somitogenesis. *Development* **125**, 2381-95.

Reim, G. and Brand, M. (2002). Spiel-ohne-grenzen/pou2 mediates regional competence to respond to Fgf8 during zebrafish early neural development. *Development* **129**, 917-33.

Ridyard, M. S. and Sanders, E. J. (1998). Cellular phenotype transformation during early embryogenesis: a role for focal adhesion kinase? *Biochem Cell Biol* **76**, 45-58.

Robu, M. E., Larson, J. D., Nasevicius, A., Beiraghi, S., Brenner, C., Farber, S. A. and Ekker, S. C. (2007). p53 activation by knockdown technologies. *PLoS Genet* **3**, e78.

Rohner, N., Bercsenyi, M., Orban, L., Kolanczyk, M. E., Linke, D., Brand, M., Nusslein-Volhard, C. and Harris, M. P. (2009). Duplication of fgfr1 permits Fgf signaling to serve as a target for selection during domestication. *Curr Biol* **19**, 1642-7.

Sagerstrom, C. G., Grinbalt, Y. and Sive, H. (1996). Anteroposterior patterning in the zebrafish, Danio rerio: an explant assay reveals inductive and suppressive cell interactions. *Development* **122**, 1873-83.

Salinas, P. C. (2007). Modulation of the microtubule cytoskeleton: a role for a divergent canonical Wnt pathway. *Trends Cell Biol* **17**, 333-42.

Sato, T., Joyner, A. L. and Nakamura, H. (2004). How does Fgf signaling from the isthmic organizer induce midbrain and cerebellum development? *Dev Growth Differ* **46**, 487-94.

Schaller, M. D. (2001). Paxillin: a focal adhesion-associated adaptor protein. *Oncogene* **20**, 6459-72.

Schaller, M. D. (2010). Cellular functions of FAK kinases: insight into molecular mechanisms and novel functions. *J Cell Sci* **123**, 1007-13.

Schaller, M. D., Borgman, C. A., Cobb, B. S., Vines, R. R., Reynolds, A. B. and Parsons, J. T. (1992). pp125FAK a structurally distinctive protein-tyrosine kinase associated with focal adhesions. *Proc Natl Acad Sci U S A* **89**, 5192-6.

Schlessinger, K., Hall, A. and Tolwinski, N. (2009). Wnt signaling pathways meet Rho GTPases. *Genes Dev* **23**, 265-77.

Schober, M., Raghavan, S., Nikolova, M., Polak, L., Pasolli, H. A., Beggs, H. E., Reichardt, L. F. and Fuchs, E. (2007). Focal adhesion kinase modulates tension signaling to control actin and focal adhesion dynamics. *J Cell Biol* **176**, 667-80.

Schock, F. and Perrimon, N. (2002). Molecular mechanisms of epithelial morphogenesis. *Annu Rev Cell Dev Biol* **18**, 463-93.

Serrels, B., Serrels, A., Brunton, V. G., Holt, M., McLean, G. W., Gray, C. H., Jones, G. E. and Frame, M. C. (2007). Focal adhesion kinase controls actin assembly via a FERM-mediated interaction with the Arp2/3 complex. *Nat Cell Biol* **9**, 1046-56.

Shi, S. H., Cheng, T., Jan, L. Y. and Jan, Y. N. (2004). APC and GSK-3beta are involved in mPar3 targeting to the nascent axon and establishment of neuronal polarity. *Curr Biol* **14**, 2025-32.

Siegrist, S. E. and Doe, C. Q. (2007). Microtubule-induced cortical cell polarity. *Genes Dev* **21**, 483-96.

Stoick-Cooper, C. L., Weidinger, G., Riehle, K. J., Hubbert, C., Major, M. B., Fausto, N. and Moon, R. T. (2007). Distinct Wnt signaling pathways have opposing roles in appendage regeneration. *Development* **134**, 479-89.

Terrand, J., Bruban, V., Zhou, L., Gong, W., El Asmar, Z., May, P., Zurhove, K., Haffner, P., Philippe, C., Woldt, E. et al. (2009). LRP1 controls intracellular cholesterol storage and fatty acid synthesis through modulation of Wnt signaling. *J Biol Chem* **284**, 381-8.

Thisse, B., Heyer, V., Lux, A., Alunni, V., Degrave, A., Seiliez, I., Kirchner, J., Parkhill, J. P. and Thisse, C. (2004). Spatial and temporal expression of the zebrafish genome by large-scale in situ hybridization screening. *Methods Cell Biol* **77**, 505-19.

Torii, K., Nishizawa, K., Kawasaki, A., Yamashita, Y., Katada, M., Ito, M., Nishimoto, I., Terashita, K., Aiso, S. and Matsuoka, M. (2008). Anti-apoptotic action of Wnt5a in dermal fibroblasts is mediated by the PKA signaling pathways. *Cell Signal* **20**, 1256-66.

Torres, M. A., Eldar-Finkelman, H., Krebs, E. G. and Moon, R. T. (1999). Regulation of ribosomal S6 protein kinase-p90(rsk), glycogen synthase kinase 3, and beta-catenin in early Xenopus development. *Mol Cell Biol* **19**, 1427-37.

Trokovic, R., Trokovic, N., Hernesniemi, S., Pirvola, U., Vogt Weisenhorn, D. M., Rossant, J., McMahon, A. P., Wurst, W. and Partanen, J. (2003). FGFR1 is independently required in both developing mid- and hindbrain for sustained response to isthmic signals. *EMBO J* **22**, 1811-23.

Tsuda, S., Kitagawa, T., Takashima, S., Asakawa, S., Shimizu, N., Mitani, H., Shima, A., Tsutsumi, M., Hori, H., Naruse, K. et al. (2010). FAK-mediated extracellular signals are essential for interkinetic nuclear migration and planar divisions in the neuroepithelium. *J Cell Sci* **123**, 484-96.

van Amerongen, R. and Nusse, R. (2009). Towards an integrated view of Wnt signaling in development. *Development* **136**, 3205-14.

Vanhaesebroeck, B. and Alessi, D. R. (2000). The PI3K-PDK1 connection: more than just a road to PKB. *Biochem J* **346 Pt 3**, 561-76.

Wallingford, J. B., Vogeli, K. M. and Harland, R. M. (2001). Regulation of convergent extension in Xenopus by Wnt5a and Frizzled-8 is independent of the canonical Wnt pathway. *Int J Dev Biol* **45**, 225-7.

Walshe, J. and Mason, I. (2000). Expression of FGFR1, FGFR2 and FGFR3 during early neural development in the chick embryo. *Mech Dev* **90**, 103-10.

Wederell, E. D. and de Iongh, R. U. (2006). Extracellular matrix and integrin signaling in lens development and cataract. *Semin Cell Dev Biol* **17**, 759-76.

Wen, Y., Eng, C. H., Schmoranzer, J., Cabrera-Poch, N., Morris, E. J., Chen, M., Wallar, B. J., Alberts, A. S. and Gundersen, G. G. (2004). EB1 and APC bind to mDia to stabilize microtubules downstream of Rho and promote cell migration. *Nat Cell Biol* **6**, 820-30.

Westerfield, M. (1995). The Zebrafish Book: A guide for the laboratory use of zebrafish.: University of Oregon Press.

Westfall, T. A., Brimeyer, R., Twedt, J., Gladon, J., Olberding, A., Furutani-Seiki, M. and Slusarski, D. C. (2003). Wnt-5/pipetail functions in vertebrate axis formation as a negative regulator of Wnt/beta-catenin activity. *J Cell Biol* **162**, 889-98.

Wodarz, A. and Nusse, R. (1998). Mechanisms of Wnt signaling in development. *Annu Rev Cell Dev Biol* **14**, 59-88.

Woo, K. and Fraser, S. E. (1995). Order and coherence in the fate map of the zebrafish nervous system. *Development* **121**, 2595-609.

Woo, K., Shih, J. and Fraser, S. E. (1995). Fate maps of the zebrafish embryo. *Curr Opin Genet Dev* **5**, 439-43.

Wu, X., Suetsugu, S., Cooper, L. A., Takenawa, T. and Guan, J. L. (2004). Focal adhesion kinase regulation of N-WASP subcellular localization and function. *J Biol Chem* **279**, 9565-76.

Xie, Z., Sanada, K., Samuels, B. A., Shih, H. and Tsai, L. H. (2003). Serine 732 phosphorylation of FAK by Cdk5 is important for microtubule organization, nuclear movement, and neuronal migration. *Cell* **114**, 469-82.

Yano, H., Mazaki, Y., Kurokawa, K., Hanks, S. K., Matsuda, M. and Sabe, H. (2004). Roles played by a subset of integrin signaling molecules in cadherin-based cell-cell adhesion. *J Cell Biol* **166**, 283-95.

Yost, C., Torres, M., Miller, J. R., Huang, E., Kimelman, D. and Moon, R. T. (1996). The axis-inducing activity, stability, and subcellular distribution of beta-catenin is regulated in Xenopus embryos by glycogen synthase kinase 3. *Genes Dev* **10**, 1443-54.

Zhang, L., Gao, X., Wen, J., Ning, Y. and Chen, Y. G. (2006). Dapper 1 antagonizes Wnt signaling by promoting dishevelled degradation. *J Biol Chem* **281**, 8607-12.

Zumbrunn, J., Kinoshita, K., Hyman, A. A. and Nathke, I. S. (2001). Binding of the adenomatous polyposis coli protein to microtubules increases microtubule stability and is regulated by GSK3 beta phosphorylation. *Curr Biol* **11**, 44-9.

4

Future Directions

CONTRIBUTIONS

This work was completed solely by me, aided by helpful discussions with Jennifer Gutzman.

INTRODUCTION

In this thesis, I have established basal constriction as a mechanism of epithelial morphogenesis during MHBC formation in zebrafish. This process is dependent on laminin and requires Wnt5, FAK, and the subsequent inhibition of Gsk3β with preliminary results suggesting that Wnt5 may be upstream of FAK. However, many questions remain about this newly described mechanism of epithelial morphogenesis. In this chapter, I address some of the most salient questions and propose experiments by which to answer them.

FUTURE DIRECTIONS

Further analysis of the pathway regulating basal constriction

I have identified the first known regulators of basal constriction, but further analysis is needed to describe the interactions between the known players and identify the full complement of pathway components. I would hypothesize that Wnt5 signals through a receptor to activate intracellular FAK, an non-receptor kinase, to regulate basal constriction. Wnt5 is known to signal through both Frizzled-2, a well established Wnt signaling receptor, and an alternate receptor, Ryk, to activate distinct downstream signaling pathways (Harris and Beckendorf, 2007; Lin et al., 2010). Wnt5 signaling through Ryk activates Src family tyrosine-kinases during axon pathfinding in *Drosophila* (Wouda et al., 2008), while Wnt5 signaling through both Ryk and Fz2 drives directional cell migration during convergent extension in zebrafish gastrulation (Kilian et al., 2003; Lin et al., 2010). If Wnt5 signaling through Frz2 is required for basal constriction, then injection of a morpholino targeting Frz2 (Kilian et al., 2003) would be expected to phenocopy the Wnt5 loss-of-function basal constriction phenotype. Signaling of Wnt5 through the Ryk receptor could be similarly tested with a Ryk morpholino (Lin et al., 2010). In either case, the role of the identified receptor in this pathway could be

confirmed by rescue of basal constriction in the loss-of-function embryos by overexpression of dominant-negative Gsk3β (Pierce and Kimelman, 1995).

I have also not identified how Wnt5 and FAK inhibit Gsk3β. Gsk3β is generally inhibited by phosphorylation at Ser9; this suggests a hypothesis that Ser9 phosphorylation would be lost in Wnt5 and FAK loss-of-function embryos. This could be tested by Western analysis comparing the levels of Gsk3β Ser9 phosphorylation in the brain tissue of control and morphant embryos. Preliminary experiments have been inconclusive. Gsk3β also appears to be regulated in a phosphorylation-independent manner since a knock-in mouse lacking the inhibitory phosphorylation site develops normally (Hur and Zhou, 2010).

Which brain regions are competent for basal constriction? Is Wnt5 sufficient to initiate basal constriction?

As shown in chapter 3, the specificity of the *wnt5* expression pattern and its loss-of-function phenotype are consistent with it signaling to position and initiate basal constriction at the MHBC. These data do not address whether *wnt5* expression is a sufficient signal or whether additional factors determine competence for basal constriction. It has previously been shown that regions in the midbrain are competent for formation of an ectopic MHBC, but basal constriction has not been examined in this case (Crossley et al., 1996; Martinez et al., 1999). Wild type *wnt5* expression is restricted to a narrow band of tissue (though it is not clear exactly where the signal lies relative to basally constricting cells) and is required for basal constriction in a set of 3–4 cells approximately 10 cells deep on each side of the neural tube (~70 cells total). If *wnt5* is sufficient for basal constriction at the MHBC and a larger region of cells is competent for basal constriction, then expanding the expression domain of *wnt5* in the anterior-posterior dimension would result in a wider band of basally constricted cells at the

MHBC – perhaps 5–7 cells instead of 3–4. This hypothesis could be tested by ectopically expressing *wnt5* in an expanded region over the MHBC. *engrailed2b* (*eng2b*) is expressed in a larger domain of the MHBC and posterior midbrain (Thisse et al., 2004). Expression of *wnt5* under control of the *eng2b* promoter would expand its expression domain. A larger number of basally constricted cells at the MHBC would suggest that a larger domain of cells are competent for basal constriction and that *wnt5* expression is sufficient to drive the process. A negative result would suggest that either *wnt5* is insufficient to initiate basal constriction or that the cells near the MHBC are incompetent for basal constriction. However, a positive result would suggest that *wnt5* expression is sufficient to induce basal constriction at the MHBC. In this case, ectopic expression under control of additional promoters with region-specific brain expression could be used to address whether other regions of the developing brain are also competent for basal constriction.

Regulation of basal constriction by laminin

I have not yet determined whether the Wnt5, FAK, and Gsk3β regulatory pathway is affected by laminin, also shown to be required for basal constriction. The extracellular matrix is an important regulator of growth factor signaling (reviewed in (Walker et al., 2005). Therefore, I would hypothesize that laminin is required for Wnt5 activation of FAK upstream of Gsk3β. The activation of FAK by laminin could be tested by assaying for FAK autophosphorylation in laminin mutants. A decrease in FAK phosphorylation at the MHBC in the laminin mutants would support the hypothesis. If Gsk3β were inhibited by phosphorylation downstream of Wnt5 and FAK and acts downstream of laminin, then Gsk3β phosphorylation at Ser9 would be decreased in laminin mutants. This could be assayed by comparative Western, as described above. This hypothesis could also be tested by attempting rescue of basal constriction in the laminin mutants by

overexpression of constitutively-active FAK (Shi et al., 2009) or dominant-negative Gsk3β (Pierce and Kimelman, 1995). If laminin acts upstream of Wnt5/FAK/Gsk3β signaling, then overexpression of either of these constructs would be expected to rescue the loss of basal constriction in the laminin mutants.

Identifying new regulators of basal constriction at the MHBC

What other components regulate basal constriction at the MHBC? The regulators identified in this study were found using candidate analysis. While this has proven successful, a less targeted approach would likely identify both additional regulators and proteins of previously unidentified function required for this process. Basal constriction is spatially restricted to a very small number of cells. This suggests that they are regulated by signals that are also spatially restricted. I would hypothesize that the protein composition of the basally constricting cells as well as the phosphorylation state of the relevant regulators would be different in the basally constricting cells both in comparison to other neural cells in wild type embryos and in comparison to cells that fail to undergo basal constriction such as in the Wnt5 or FAK loss-of-function embryos. Comparative mass spectrometry is an unbiased approach that could be used to identify proteins specifically phosphorylated during basal constriction. Assuming this phosphorylation altered their activity, these would be candidate regulators of the process (Lemeer et al., 2007; Lin et al., 2009). A proteomic sample from the MHBC could be prepared by locally activating a UV-sensitive dye, such as Kaede, followed by FACS sorting to separate the fluorescent MHBC cells from the rest of the embryo (Pyati et al., 2006; Shkumatava et al., 2009). As a comparison sample, neural cells could be FACS-sorted from a line expressing GFP from a neural-specific promoter such as *miR124* (Shkumatava et al., 2009). Proteins revealed by mass spectrometry to be differentially present or differentially phosphorylated in the MHBC cells would be excellent candidates

for further study as regulators of basal constriction. It is possible, however, that there would not be sufficient resolution in the photo-activation of the Kaede dye to differentiate between the proteins present in the basally constricting cells as compared to other neural cells. In this case, temporally-specific knockdown of known basal constriction regulators (Wnt5 or FAK) could be used to compare the protein composition in these loss-of-function cells to the surrounding tissue. In collaboration with Dr. James Chen, we are designing photo-activatable morpholinos that can be activated in a temporally- and spatially-restricted manner. Once these photo-activatable morpholinos have been optimized, activation of Kaede dye in MHBC cells during basal constriction could be coordinated with activation of morpholinos that target Wnt5 or FAK. FACS sorting of these cells followed by mass spectrometry could be used to identify components that are differentially expressed or phosphorylated in the absence of the targeted proteins. The proteins identified in this assay could either be used as confirmation of those identified in the previous assay or could substitute in the case of ambiguous results in the first experiment described.

A connection with microtubules

In appendix 1, I show that depolymerization of microtubules just prior to morphogenesis inhibits basal constriction at the MHBC. Wnt5, FAK, and Gsk3β, shown in this study to be required in the regulation of basal constriction, all also regulate microtubules. Recently published data indicates that Wnt5 induces the interaction of Dishevelled and APC and localization of these proteins to the plus-ends of microtubules where they interact with FAK and stabilize the microtubules (Matsumoto et al., 2010). Gsk3β stabilizes microtubules through its inhibition of APC, a plus-end microtubule binding protein (Zumbrunn et al., 2001). FAK also stabilizes microtubules as a signaling intermediary between integrins and Rho (Palazzo et al., 2004). Together, these data

suggest a possible model in which Wnt5, FAK and Gsk3β might regulate basal constriction in part through stabilizing the microtubule cytoskeleton. EB1 is a plus-end microtubule binding protein that could be exploited to assay microtubule stability. Fluorescently tagged constructs of EB1 have previously been used in vertebrate embryos; this fluorescence corresponds with stabilized MT plus-ends (Rogers et al., 2004; Tirnauer et al., 2002). So as not to stabilize microtubules by overexpression of EB1, it should be expressed using the endogenous promoter. Co-injection of EB1-cherry and GFP-tubulin would allow microtubule dynamics to be compared in wild type embryos and embryos lacking Wnt5, FAK and Gsk3β function. If signaling through Wnt5, FAK and Gsk3β stabilizes microtubules, then the plus-ends of the microtubules would be subject to more frequent catastrophe in the loss-of-function mutants and EB1 fluorescence would be decreased.

Is there a role for endocytosis in basal constriction?

Endocytosis is one possible mechanism by which the basal cell surface could be reduced during basal constriction. In endocytosis, the cell internalizes portions of its membrane in vesicles (reviewed in (Doherty and McMahon, 2009). The process is initiated by the formation of a vesicle at the cell surface; the coiled-coil protein dynamin then pinches off the vesicle (Urrutia et al., 1997). As the vesicle is released, Rab5 mediates its fusion with the early endosome, at which point the vesicle becomes marked by Eea1 (Somsel Rodman and Wandinger-Ness, 2000). These vesicles are then trafficked into the cell along microtubules (Lee and Harland, 2010).

Dynamin-mediated endocytosis is required for the disassembly of focal adhesions in a microtubule- and FAK-dependent manner during cell migration in tissue culture (Ezratty et al., 2005). Microtubule-dependent endocytosis is required for apical constriction during *Xenopus* bottle cell formation (Lee and Harland, 2010). A

preliminary experiment suggests that dynamin may be required for basal constriction at the MHBC, and I have shown that intact microtubules are required for basal constriction (see Appendix 1). Taken together, these observations suggest that microtubule-dependent endocytosis may drive basal constriction. This model could be tested by loss-of-function analysis of both dynamin and Rab5. Staining for an early endosomal marker such as Eea1 could be used to assay for endocytosis during basal constriction. If endocytosis is required for the process, then Eea1 would be enriched in vesicles at the basal surface of cells undergoing basal constriction as compared to neighboring cells. Endocytosis could also be assayed by locally injecting a lipophilic dye that would mark the basal cell membrane and any vesicles taken up from that surface. Alternatively, electron microscopy could be used to visualize vesicle internalization (Lee and Harland, 2010). These results could be confirmed by comparison of basally constricting cells in control embryos as compared to cells that fail to undergo basal constriction in Wnt5 or FAK loss-of-function embryos.

CONCLUSION

The study described in this thesis is only a small introduction to the field of basal constriction in epithelial morphogenesis. The experiments described above suggest possible steps forward in building an understanding of this process in development. Basal constriction is a critical event in shaping the vertebrate brain; a better understanding of the mechanisms that drive it are likely to shine light on brain development, as well as more generally identify previously undescribed mechanisms of epithelial morphogenesis.

REFERENCES

Crossley, P. H., Martinez, S. and Martin, G. R. (1996). Midbrain development induced by FGF8 in the chick embryo. *Nature* **380**, 66-8.

Doherty, G. J. and McMahon, H. T. (2009). Mechanisms of endocytosis. *Annu Rev Biochem* **78**, 857-902.

Ezratty, E. J., Partridge, M. A. and Gundersen, G. G. (2005). Microtubule-induced focal adhesion disassembly is mediated by dynamin and focal adhesion kinase. *Nat Cell Biol* **7**, 581-90.

Harris, K. E. and Beckendorf, S. K. (2007). Different Wnt signals act through the Frizzled and RYK receptors during Drosophila salivary gland migration. *Development* **134**, 2017-25.

Hur, E. M. and Zhou, F. Q. (2010). GSK3 signalling in neural development. *Nat Rev Neurosci* **11**, 539-51.

Kilian, B., Mansukoski, H., Barbosa, F. C., Ulrich, F., Tada, M. and Heisenberg, C. P. (2003). The role of Ppt/Wnt5 in regulating cell shape and movement during zebrafish gastrulation. *Mech Dev* **120**, 467-76.

Lee, J. Y. and Harland, R. M. (2010). Endocytosis is required for efficient apical constriction during Xenopus gastrulation. *Curr Biol* **20**, 253-8.

Lemeer, S., Ruijtenbeek, R., Pinkse, M. W., Jopling, C., Heck, A. J., den Hertog, J. and Slijper, M. (2007). Endogenous phosphotyrosine signaling in zebrafish embryos. *Mol Cell Proteomics* **6**, 2088-99.

Lin, S., Baye, L. M., Westfall, T. A. and Slusarski, D. C. (2010). Wnt5b-Ryk pathway provides directional signals to regulate gastrulation movement. *J Cell Biol* **190**, 263-78.

Lin, Y., Chen, Y., Yang, X., Xu, D. and Liang, S. (2009). Proteome analysis of a single zebrafish embryo using three different digestion strategies coupled with liquid chromatography-tandem mass spectrometry. *Anal Biochem* **394**, 177-85.

Martinez, S., Crossley, P. H., Cobos, I., Rubenstein, J. L. and Martin, G. R. (1999). FGF8 induces formation of an ectopic isthmic organizer and isthmocerebellar development via a repressive effect on Otx2 expression. *Development* **126**, 1189-200.

Matsumoto, S., Fumoto, K., Okamoto, T., Kaibuchi, K. and Kikuchi, A. (2010). Binding of APC and dishevelled mediates Wnt5a-regulated focal adhesion dynamics in migrating cells. *EMBO J* **29**, 1192-204.

Palazzo, A. F., Eng, C. H., Schlaepfer, D. D., Marcantonio, E. E. and Gundersen, G. G. (2004). Localized stabilization of microtubules by integrin- and FAK-facilitated Rho signaling. *Science* **303**, 836-9.

Pierce, S. B. and Kimelman, D. (1995). Regulation of Spemann organizer formation by the intracellular kinase Xgsk-3. *Development* **121**, 755-65.

Pyati, U. J., Cooper, M. S., Davidson, A. J., Nechiporuk, A. and Kimelman, D. (2006). Sustained Bmp signaling is essential for cloaca development in zebrafish. *Development* **133**, 2275-84.

Rogers, S. L., Wiedemann, U., Hacker, U., Turck, C. and Vale, R. D. (2004). Drosophila RhoGEF2 associates with microtubule plus ends in an EB1-dependent manner. *Curr Biol* **14**, 1827-33.

Shi, J., Zeng, X., Zhou, M. and Chen, Q. (2009). Activation of ERK-FAK signaling pathway and enhancement of cell migration involved in the early interaction between oral keratinocytes and Candida albicans. *Mycopathologia* **167**, 1-7.

Shkumatava, A., Stark, A., Sive, H. and Bartel, D. P. (2009). Coherent but overlapping expression of microRNAs and their targets during vertebrate development. *Genes Dev* **23**, 466-81.

Somsel Rodman, J. and Wandinger-Ness, A. (2000). Rab GTPases coordinate endocytosis. *J Cell Sci* **113** Pt 2, 183-92.

Thisse, B., Heyer, V., Lux, A., Alunni, V., Degrave, A., Seiliez, I., Kirchner, J., Parkhill, J. P. and Thisse, C. (2004). Spatial and temporal expression of the zebrafish genome by large-scale in situ hybridization screening. *Methods Cell Biol* **77**, 505-19.

Tirnauer, J. S., Grego, S., Salmon, E. D. and Mitchison, T. J. (2002). EB1-microtubule interactions in Xenopus egg extracts: role of EB1 in microtubule stabilization and mechanisms of targeting to microtubules. *Mol Biol Cell* **13**, 3614-26.

Urrutia, R., Henley, J. R., Cook, T. and McNiven, M. A. (1997). The dynamins: redundant or distinct functions for an expanding family of related GTPases? *Proc Natl Acad Sci U S A* **94**, 377-84.

Walker, J. L., Fournier, A. K. and Assoian, R. K. (2005). Regulation of growth factor signaling and cell cycle progression by cell adhesion and adhesion-dependent changes in cellular tension. *Cytokine Growth Factor Rev* **16**, 395-405.

Wouda, R. R., Bansraj, M. R., de Jong, A. W., Noordermeer, J. N. and Fradkin, L. G. (2008). Src family kinases are required for WNT5 signaling through the Derailed/RYK receptor in the Drosophila embryonic central nervous system. *Development* **135**, 2277-87.

Zumbrunn, J., Kinoshita, K., Hyman, A. A. and Nathke, I. S. (2001). Binding of the adenomatous polyposis coli protein to microtubules increases microtubule stability and is regulated by GSK3 beta phosphorylation. *Curr Biol* **11**, 44-9.

Appendix 1

The role of microtubules in basal constriction

Contributions

I completed the experiments and writing for this section section.

INTRODUCTION

The actin and microtubule cytoskeletons -have been widely implicated in neural tube morphogenesis (Burnside, 1971; Lee et al., 2007; Suzuki et al., 2010). For example, actin is specifically recruited to the apical surface of apically constricting neuroepithelial cells during neural tube closure in Xenopus (Lee et al., 2007) and to the basal surface of basally constricting cells at the MHBC during its morphogenesis in zebrafish (Gutzman et al., 2008). Apico-basal microtubule arrays have been associated with cell elongation during neural tube closure in Xenopus (Burnside, 1971), and microtubules are a well-established regulator of neurogenesis (Conde and Caceres, 2009; Poulain and Sobel, 2010). We show here that the depolymerization of microtubules just prior to basal constriction at the MHBC prevents the cell shape change.

EXPERIMENTAL PROCEDURES

Nocodazole treatments

Embryos were treated with 1% DMSO or 1μM nocodazole (M1404, Sigma) dissolved in DMSO in embryo media. For analysis of cell shape, embryos treated for 1 hour at 30°C from 19-20 hpf and transferred to fresh embryo media until 24 hpf. To assay for microtubule depolymerization, embryos were imaged at 20 hpf, immediately after treatment.

Live imaging of embryos

mRNA injections and live confocal imaging were performed as described (Graeden and Sive, 2009). Briefly, single cell embryos were micro-injected with membrane-bound GFP mRNA (memGFP) (kindly provided by Dr. J. B. Green, Dana-Farber Cancer Institute Boston, MA) or GFP-tubulin mRNA (kindly provided by Dr. Frank Gertler, MIT) transcribed with the mMessage mMachine kit (Ambion). The embryos were mounted

inverted in 0.7% agarose (Sigma) and imaged by fluorescent, laser-scanning confocal microscopy (Zeiss LSM510) at 24 hpf.

RESULTS

Given its role in other cell shape changes during development, I hypothesized that microtubules might be required for basal constriction at the MHBC. Nocodazole is a well-characterized microtubule-depolymerizing agent (DeBrabander et al., 1975; Jacobs and Stevens, 1986; Samson et al., 1979; Solomon, 1980). Treatment with the nocodazole solvent, DMSO, had no effect on basal constriction (Fig. 1A, A'). However, treatment of embryos with nocodazole specifically from 19-20 hpf prevented basal constriction (Fig. 1B, B'). Injection of GFP-β-tubulin allows microtubules to be imaged in the live embryo. Microtubules are oriented in apical-basal arrays in cells at the MHB during basal constriction (Fig. 1C). Embryos injected with GFP-tubulin were treated with nocodazole from 19-20 hpf. This treatment appears to entirely depolymerize the microtubules (Fig. 1D). These results suggest that intact microtubules are required in the embryo at the onset of basal constriction.

DISCUSSION

There are several possible modes of action by which microtubules could be required for basal constriction. One interesting hypothesis is that microtubules may be required for endocytosis-mediated disassembly of focal adhesions, which we have hypothesized is required for basal constriction at the MHBC. Dynamin is a coiled-coil protein that pinches off endocytic vesicles (Urrutia et al., 1997). As the vesicle is released, Rab5 mediates the fusion of the endocytic vesicle with the early endosome at which point the vesicle becomes bound by Eea1 (Somsel Rodman and Wandinger-Ness, 2000). These vesicles are then trafficked into the cell along microtubules (Apodaca, 2001). Dynamin-

mediated endocytosis has been shown to be required for the disassembly of focal adhesions in a microtubule- and FAK-dependent manner during cell migration in tissue culture (Ezratty et al., 2009; Ezratty et al., 2005). The role of this process in cell shape change is supported by data showing that microtubule-dependent endocytosis is required for apical constriction during Xenopus bottle cell formation (Lee and Harland, 2010). One preliminary experiment suggests that dynamin may be required for basal constriction at the MHBC as well. This hypothesis could be tested by determining if dynamin and Rab5 are required for basal constriction and by assaying for endocytosis in the basally constricting cells at the MHBC.

An alternative hypothesis is that microtubules are required for apical expansion during basal constriction. Golgi-derived membrane traffic is also microtubule-dependent, suggesting that if biogenesis of membrane were required during apical or basal expansion, microtubules might well be required. This could be addressed by assaying for apical expansion at the MHBC after nocodazole treatment. However, because apical expansion does not occur until nearly four hours after the initiation of basal constriction and the time window when microtubules are required, this is unlikely to explain the data described here.

Finally, it is possible that microtubules are required to shorten the cells at the MHBC prior to basal constriction. Microtubules have not been shown to have an explicit role in cell shortening, but have been shown to be required for cell elongation during development of the mouse optic cup (Svoboda and O'Shea, 1987) and lens cell formation in sunfish (Dearry and Burnside, 1986; Troutt and Burnside, 1988). Thus, if microtubules were required for cell shortening, and cell shortening were required for subsequent basal constriction at the MHBC, this would explain their requirement in basal constriction. This could be tested by measuring cell length at the MHB at 21 hpf in embryos treated with nocodazole.

FIGURE LEGEND

Fig. 1 Nocodazole treatment just prior to basal constriction depolymerizes microtubules and prevents basal constriction

(A – B') Wild type embryos were injected with memGFP mRNA. Three cells at the MHBC are outlined below. Embryos were treated 19 – 20 hpf and imaged live at 24 hpf by scanning confocal microscopy. (A, A') Cells at the MHBC undergo basal constriction in DMSO-treated embryos. (B, B') Cells at the MHBC fail to undergo basal constriction after treatment with nocodazole. (C – D) Wild type embryos were injected with GFP-β-tubulin mRNA at the single cell stage, treated 19 – 20 hpf, and imaged immediately after treatment at 20 hpf. (C) Intact microtubules are oriented apical-basally as indicated by arrows. Circle highlights a dividing cell with a visible microtubule aster. (D) Microtubules are completely depolymerized by a one-hour treatment of nocodazole. Anterior is left. Arrowheads mark the MHBC.

FIGURE 1

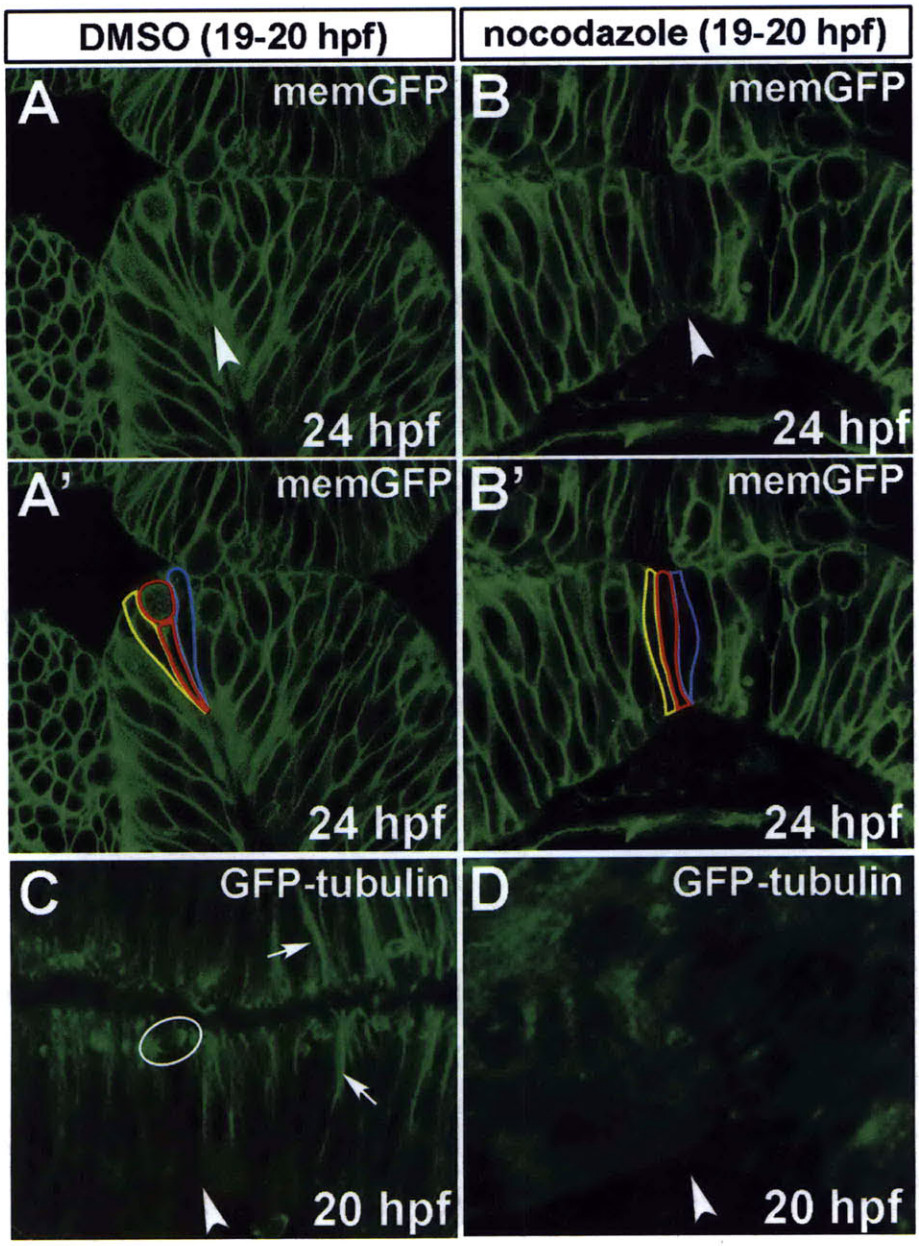
DMSO (19-20 hpf)
nocodazole (19-20 hpf)
A
memGFP
24 hpf
B
memGFP
24 hpf
A'
memGFP
24 hpf
B'
memGFP
24 hpf
C
GFP-tubulin
20 hpf
D
GFP-tubulin
20 hpf

REFERENCES

Apodaca, G. (2001). Endocytic traffic in polarized epithelial cells: role of the actin and microtubule cytoskeleton. *Traffic* **2**, 149-59.

Burnside, B. (1971). Microtubules and microfilaments in newt neuralation. *Dev Biol* **26**, 416-41.

Conde, C. and Caceres, A. (2009). Microtubule assembly, organization and dynamics in axons and dendrites. *Nat Rev Neurosci* **10**, 319-32.

Dearry, A. and Burnside, B. (1986). Dopaminergic regulation of cone retinomotor movement in isolated teleost retinas: I. Induction of cone contraction is mediated by D2 receptors. *J Neurochem* **46**, 1006-21.

DeBrabander, M., Aerts, F., Van de Veire, R. and Borgers, M. (1975). Evidence against interconversion of microtubules and filaments. *Nature* **253**, 119-20.

Ezratty, E. J., Bertaux, C., Marcantonio, E. E. and Gundersen, G. G. (2009). Clathrin mediates integrin endocytosis for focal adhesion disassembly in migrating cells. *J Cell Biol* **187**, 733-47.

Ezratty, E. J., Partridge, M. A. and Gundersen, G. G. (2005). Microtubule-induced focal adhesion disassembly is mediated by dynamin and focal adhesion kinase. *Nat Cell Biol* 7, 581-90.

Graeden, E. and Sive, H. (2009). Live imaging of the zebrafish embryonic brain by confocal microscopy. *J Vis Exp*.

Gutzman, J. H., Graeden, E. G., Lowery, L. A., Holley, H. S. and Sive, H. (2008). Formation of the zebrafish midbrain-hindbrain boundary constriction requires laminin-dependent basal constriction. *Mech Dev* **125**, 974-83.

Jacobs, J. R. and Stevens, J. K. (1986). Experimental modification of PC12 neurite shape with the microtubule-depolymerizing drug Nocodazole: a serial electron microscopic study of neurite shape control. *J Cell Biol* **103**, 907-15.

Lee, C., Scherr, H. M. and Wallingford, J. B. (2007). Shroom family proteins regulate gamma-tubulin distribution and microtubule architecture during epithelial cell shape change. *Development* **134**, 1431-41.

Lee, J. Y. and Harland, R. M. (2010). Endocytosis is required for efficient apical constriction during Xenopus gastrulation. *Curr Biol* **20**, 253-8.

Poulain, F. E. and Sobel, A. (2010). The microtubule network and neuronal morphogenesis: Dynamic and coordinated orchestration through multiple players. *Mol Cell Neurosci* **43**, 15-32.

Samson, F., Donoso, J. A., Heller-Bettinger, I., Watson, D. and Himes, R. H. (1979). Nocodazole action on tubulin assembly, axonal ultrastructure and fast axoplasmic transport. *J Pharmacol Exp Ther* **208**, 411-7.

Solomon, F. (1980). Neuroblastoma cells recapitulate their detailed neurite morphologies after reversible microtubule disassembly. *Cell* **21**, 333-8.

Somsel Rodman, J. and Wandinger-Ness, A. (2000). Rab GTPases coordinate endocytosis. *J Cell Sci* **113 Pt 2**, 183-92.

Suzuki, M., Hara, Y., Takagi, C., Yamamoto, T. S. and Ueno, N. (2010). MID1 and MID2 are required for Xenopus neural tube closure through the regulation of microtubule organization. *Development* **137**, 2329-39.

Svoboda, K. K. and O'Shea, K. S. (1987). An analysis of cell shape and the neuroepithelial basal lamina during optic vesicle formation in the mouse embryo. *Development* **100**, 185-200.

Troutt, L. L. and Burnside, B. (1988). Microtubule polarity and distribution in teleost photoreceptors. *J Neurosci* **8**, 2371-80.

Urrutia, R., Henley, J. R., Cook, T. and McNiven, M. A. (1997). The dynamins: redundant or distinct functions for an expanding family of related GTPases? *Proc Natl Acad Sci U S A* **94**, 377-84.